UCSF
UC San Francisco Electronic Theses and Dissertations

Title
Regulation of synaptic vesicle endocytosis by synaptotagmin I

Permalink
https://escholarship.org/uc/item/24r967dp

Author
Poskanzer, Kira

Publication Date
2006

Peer reviewed|Thesis/dissertation

eScholarship.org Powered by the California Digital Library
University of California

Regulation of Synaptic Vesicle Endocytosis by Synaptotagmin I

by

Kira Poskanzer

DISSERTATION

Submitted in partial satisfaction of the requirements for the degree of

DOCTOR OF PHILOSOPHY

in

Neuroscience

in the

GRADUATE DIVISION

of the

UNIVERSITY OF CALIFORNIA, SAN FRANCISCO

Copyright (2006)

by

Kira E. Poskanzer

Acknowledgements

I am incredibly grateful for the people—family, friends, colleagues, and faculty—who have supported me during graduate school. Grae Davis was an enthusiastic, positive, and forward-thinking mentor who taught me to always look at a wider biological context and to embrace new technology when tackling questions. I thank Grae for his instant excitement whenever I wanted to discuss data, for his unstinting encouragement, for teaching me how to give a good scientific talk, and for understanding that time outside of the lab is important, too.

Most of my time in graduate school was spent in the company of members of the Davis lab. I've been fortunate to be around such open-minded, clever, good-natured, stimulating people during my days in the lab. Their challenging questions and thoughtful discussions helped me think much more broadly and clearly about biology. Special thanks go to Kurt Marek, with whom I worked on the photo-inactivation project, and who was especially incisive and talented at thinking many steps ahead. Sean Sweeney made the original transgenic animal that I worked on during my rotation project. I'm thankful that he let me take it on as my own, and that I was able to learn genetics from such an expert. I want to thank Rick Fetter for helping with all the electron microscopy, and doing experiments with enormous precision and care. In addition, Gama Ruiz has provided me with incredible technical support throughout my time in the lab.

I am grateful to the members of my orals and thesis committees for their advice and encouragement: Robert Edwards, Ulrike Heberlein, Ellen Lumpkin, Roger Nicoll, Stephen Smith, and Mark von Zastrow.

Most of all, I want to thank my caring family and friends for their endless support, and good humor, and genuine interest in my project. I am exceptionally lucky to have these people on my side.

Preface

Some of the material contained in this dissertation has been published elsewhere. Chapter 2, *Synaptotagmin I is Necessary for Compensatory Synaptic Vesicle Endocytosis* in vivo, was published in *Nature* (2003) 426, 559–563 (Poskanzer et al., 2003). Chapter 4, *Mobilization and Fusion of a Non-Recycling Pool of Synaptic Vesicles Under Conditions of Endocytic Blockade*, was published in *Neuropharmacology* (2004) 47, 714–723 (Poskanzer and Davis, 2004).

Involvement of Co-authors

Thesis Advisor's Statement

Chapter 2 of this dissertation contains experiments that Kira Poskanzer did in collaboration with other members of my laboratory. Chapter 3 contains experiments that Kira Poskanzer did in collaboration with Richard Fetter. Kira performed all of the imaging experiments, which established the basis for the major conclusions of these chapters.

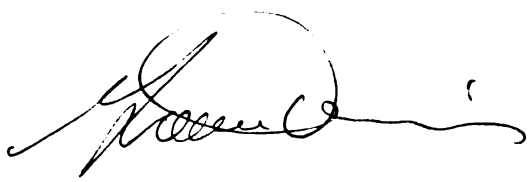

Graeme W. Davis, Ph.D.

Regulation of Synaptic Vesicle Endocytosis by Synaptotagmin I

by

Kira Poskanzer

Robert Edwards

Chair, Thesis Committee

Abstract

Synaptic vesicles are recycled and re-used after exocytosis, in a process termed compensatory synaptic vesicle endocytosis. Compensatory synaptic vesicle endocytosis ensures that the neuron can continue to signal during sustained neurotransmission and over the lifetime of the neuron. Since exocytosis and endocytosis are temporally and spatially coupled, it has been difficult to dissect the molecular mechanisms that control synaptic vesicle endocytosis. Describing the function of a protein that may be involved

in both processes is especially complicated, because disruption of an exocytic protein would likely obscure analysis of any endocytic function.

Experiments presented in this thesis examine the role of a protein known to be important for synaptic vesicle exocytosis, Synaptotagmin I (Syt I), in compensatory synaptic vesicle endocytosis. These studies were possible through use of a genetically encoded fluorescent reporter of real-time vesicle endocytosis, the synapto-pHluorins. In the first chapter, synapto-pHluorins have been combined with a technique to acutely and specifically photo-inactivate Syt I, FlAsH-FALI. Inactivating Syt I only during the endocytic phase of the vesicle cycle reveals that this protein is indeed necessary for compensatory synaptic vesicle endocytosis. Once it was shown that Syt I is involved in this process, a structure-function approach was taken to determine which domains and possible interaction partners are involved in endocytosis. Kinetic and ultrastructural data demonstrate that the C_2B domain of Syt I is necessary for endocytosis, and that the rate of synaptic vesicle endocytosis and the size of the vesicles formed are independently controlled through different residues of Syt I. These data indicate that Syt I may not only act to couple exocytosis and endocytosis, but also to coordinate different aspects of the endocytic process.

In the last section of this thesis, the synapto-pHluorins are used as a tool to measure the functional vesicle pools at the *Drosophila* NMJ. These results indicate that a large portion of synaptic vesicles cannot be released, except when endocytosis is inhibited. This data opens the door for determining what mechanisms control the partitioning of vesicles into pools and whether endocytosis may be a process that actively contributes to neural function and identity.

Table of Contents

ACKNOWLEDGEMENTS iii

PREFACE v

INVOLVEMENT OF CO-AUTHORS vi

ABSTRACT vii

TABLE OF CONTENTS ix

LIST OF FIGURES AND TABLES xi

CHAPTER ONE: GENERAL INTRODUCTION 1

Synaptic Vesicle Endocytosis: Initial Descriptions and Debates 3
Molecular Participants in Endocytosis 5
Coupling and Coordination of Exocytosis and Endocytosis 10
Kinetics of Synaptic Vesicle Endocytosis 12
Localization of Synaptic Vesicle Endocytosis 15
Endocytosis and Synaptic Vesicle Pools at the Drosophila *NMJ* 16

CHAPTER TWO: SYNAPTOTAGMIN I IS NECESSARY FOR COMPENSATORY SYNAPTIC VESICLE ENDOCYTOSIS *IN VIVO* 19

Summary 20
Results 21
Discussion 28
Figures 29

CHAPTER THREE: DISCRETE RESIDUES IN THE C_2B DOMAIN OF SYNAPTOTAGMIN I INDEPENDENTLY SPECIFY ENDOCYTIC RATE AND SYNAPTIC VESICLE SIZE 43

Summary 44
Introduction 45
Results 48
Discussion 65
Figures 72

CHAPTER FOUR: MOBILIZATION AND FUSION OF A NON-RECYCLING POOL OF SYNAPTIC VESICLES UNDER CONDITIONS OF ENDOCYTIC BLOCKADE 92

Summary 93
Introduction 94
Results 97

Discussion 107
Figures 110

CHAPTER FIVE: GENERAL CONCLUSIONS 122

Detection and Dissection of Endocytosis with Fluorescence 124
Linking Exocytosis and Endocytosis 128

EXPERIMENTAL PROCEDURES 131

APPENDIX: SYNAPTO-PHLUORIN IMAGING AT THE *DROSOPHILA* NMJ 143

REFERENCES 146

List of Figures and Tables

Figure 2-1. Neuronal expression of UAS-n-Syb-pH *does not affect function or morphology at the NMJ*.....29

Figure 2-2. Endocytosis is impaired at syt^{null} *synapses*.....31

Figure 2-3. Synapto-pHluorins exhibit pH-sensitivity at the Drosophila *NMJ*.....33

Figure 2-4. Photoinactivation of Syt 14C impairs endocytosis after normal vesicle fusion.....35

Figure 2-5. Images demonstrating n-Syb-pH intensity changes at the NMJ following the shift from the restrictive to the permissive temperature.....37

Figure 2-6. n-Syb-pH remains on the synaptic plasma membrane after FlAsH-FALI of Syt 14C......39

Figure 2-7. Photoinactivation of Syt 14C impairs stimulus-dependent FM4-64 loading at the NMJ.....41

Figure 3-1. Synaptic vesicle endocytosis is slowed in syt^{null} *animals*.....71

Table 3-1. Electrophysiological analysis of syt *mutations.*.....73

Figure 3-2. Perturbation of Syt I function affects synaptic vesicle size......75

Figure 3-3. Endocytosis rate is slowed in mutants that affect the entire C_2B *domain of Syt I*...78

Figure 3-4. Protein levels of Syt I and α*-adaptin at control and transgenic rescue synapses.*...80

Figure 3-5. Endocytosis rate is normal at UAS-syt-KQ *rescue synapses.*.....82

Figure 3-6. Synaptic vesicle size is increased following stimulation at UAS-syt-KQ *rescue synapses.*.....84

Figure 3-7. Endocytosis rate and synaptic vesicle size are unchanged at UAS-syt-D229N *rescue synapses.*.....86

Figure 3-8. Stimulation in the UAS-syt-D3,4N *rescue animal causes a slowed endocytosis rate without affecting synaptic vesicle size.*.....88

Figure 3-9. High extracellular Ca2+ rescues endocytic rate in the UAS-syt-D3,4N, *but not* syt^{null} *animals*.....90

Figure 4-1. Assaying SV release and recycling using n-Syb-pH at the Drosophila NMJ.....110

Figure 4-2. Stimulation in the presence of bafilomycin provides evidence for a non-recycling, resting pool of SVs.....113

Figure 4-3. The resting pool of SVs can be mobilized and released under conditions of endocytic blockade......115

Figure 4-4. Restricted localization of n-Syb-pH at the plasma membrane following endocytic blockade......118

Figure 4-5. Summary and model of synaptic vesicle pools......120

Chapter One:
General Introduction

Neurotransmission at a synapse occurs when individual synaptic vesicles filled with neurotransmitter fuse to the pre-synaptic plasma membrane and release their contents into the synaptic cleft, and onto receptors on the post-synaptic cell. This chemical signaling event forms the basis for cell-cell communication within entire networks of neurons in the nervous system. In order for an active nerve terminal to sustain neurotransmission while maintaining cellular integrity, the neuron must recycle previously released synaptic vesicles. This process is termed compensatory synaptic vesicle endocytosis. Without endocytosis, the neuron would quickly become depleted of its pool of vesicles, its size would greatly increase, and the pre-synaptic plasma membrane could swell out of alignment with the post-synapse specialization. Thus, the continued ability of neurons to release neurotransmitter and function over their lifetimes is dependent on their capacity to efficiently and precisely endocytose synaptic vesicles.

Many cells—including neurons, exocrine and endocrine cells, mast cells, neutrophils, and many egg cells—undergo compensatory endocytosis following stimulated exocytosis in order to regulate their surface area and composition (Jarousse and Kelly, 2001b). At the neuronal synapse, compensatory endocytosis contends with a number of particular challenges. The cell must precisely endocytose the amount of membrane released during exocytosis. Endocytosis must occur fast enough to replenish the vesicle pool and to allow continued exocytosis at sites of synaptic vesicle release. The resulting synaptic vesicles that are formed must be the correct size and composed of the correct number and types of synaptic vesicle proteins for further rounds of exocytosis. In addition, compensatory endocytosis must be dynamic enough to respond

to a wide range of exocytic events under highly variable stimulation conditions, and be ready to function even after long quiescent periods.

Although compensatory synaptic vesicle endocytosis clearly plays a critical housekeeping role at the synapse to enable continued vesicle exocytosis, endocytosis itself also may be important in shaping characteristics of synaptic function. After vesicle fusion, endocytosed material may be directed into one of various pathways that affect how immediately, and under what circumstances, synaptic vesicles are re-used. As such, endocytosis could act as a rate-limiting process to control the cell's exocytic response to certain types of stimulation. Thus, synaptic vesicle endocytosis may be an active process that helps determine the features of a particular synapse and its response to changes in neural activity.

Synaptic Vesicle Endocytosis: Initial Descriptions and Debates

Once the quantal nature of neurotransmission was established, it was hypothesized that synaptic vesicles were the elements that stored and released the quanta of neurotransmitter (Del Castillo and Katz, 1954). To follow these constituents of the synaptic terminal and observe their behavior during and after nerve stimulation, electron microscopic (EM) experiments at the large frog neuromuscular junction (NMJ) were carried out. Although it took many years to confirm the one vesicle-one quantum hypothesis (Heuser et al., 1979), other nerve stimulation/EM experiments provided the first descriptions of synaptic vesicle endocytosis at the synapse (Ceccarelli et al., 1973;

Heuser and Reese, 1973; Turner and Harris, 1973). Two of these seminal studies tracked membrane internalization (through use of the electro-dense markers horseradish peroxidase and dextran) at various post-stimulation time points, but observed different results and came to vastly different conclusions. One described clathrin-coated vesicles at sites away from the active zone, as well as large, membranous cisternal structures that could resolve into synaptic vesicle-sized compartments over time (Heuser and Reese, 1973). In contrast, the other observed clathrin-independent endocytosis at the sites of vesicular release in the synaptic terminal, and no large endosomal/cisternal membrane structures (Ceccarelli et al., 1973).

These two important early studies raised major questions about the phenomenology of synaptic vesicle endocytosis that are still contested today. First, it remains unclear to what extent clathrin-mediated endocytosis is responsible for the internalization of synaptic vesicles. While it has been demonstrated that the perturbation of proteins known to be important in clathrin-mediated endocytosis can disrupt synaptic vesicle endocytosis (Gonzalez-Gaitan and Jackle, 1997; Guichet et al., 2002; Shupliakov et al., 1997; Verstreken et al., 2002; Zhang et al., 1998) *and* that synaptic vesicles are often observed with clathrin coats (Gad et al., 2000; Kadota and Kaneseki, 1969; Smith and Smith, 1984; Teng and Wilkinson, 2000), there are also data that support the idea that some synaptic vesicles are normally internalized in the absence of clathrin (Ceccarelli et al., 1973; Daly et al., 2000; Jockusch et al., 2005; Meshul and Pappas, 1984). Secondly, the question of whether endocytosis occurs at the active zone or at specialized sites outside of it has not yet been resolved, although there is evidence it could occur at either, or both, places at the synaptic plasma membrane (Estes et al., 1996; Gaidarov et al.,

1999; Koenig and Ikeda, 1996; Roos and Kelly, 1998; Teng and Wilkinson, 2000). Third is the question of how fast endocytosis occurs and how dynamic this rate can be under differing conditions of neural activity. There is a wide variation in reported rates of endocytosis, often depending on the stimulus condition, the organism in which it was tested, and the experimental technique. Although many studies have shown that synaptic vesicle endocytosis can be best described with two different rate constants, some have found a best fit with only one rate constant (Wu, 2004).

All of these conflicting data suggest that synaptic vesicle endocytosis may occur differently under different conditions, and that there may be more than one type of synaptic vesicle endocytosis occurring at a given time. If this is indeed the case, it follows that different kinds of endocytosis may be shuttling recycled vesicles into distinct processing pathways, and further downstream, into different functional synaptic vesicle pools. Evidence from both the frog and *Drosophila* NMJ supports this hypothesis, and implicates the process of synaptic vesicle endocytosis in actively shaping pre-synaptic function (Koenig and Ikeda, 1996; Richards et al., 2000).

Molecular Participants in Endocytosis

Some early ultrastructural studies at the synapse implicated clathrin in synaptic vesicle endocytosis, but did not address the molecular mechanisms important in controlling internalization of synaptic vesicles any further. It is known from non-neuronal models that clathrin-mediated endocytosis involves a host of protein-protein interactions

necessary to form a clathrin lattice that can bend and pinch off a section of membrane and the proteins embedded in it (Schmid, 1997). Some of the proteins involved in clathrin coat formation, such as the adaptor proteins AP-2 and AP180, were subsequently shown to have a role in synaptic vesicle endocytosis (Gonzalez-Gaitan and Jackle, 1997; Zhang et al., 1998). These data not only implicated additional proteins in synaptic vesicle recycling, but also strengthened the argument that this process was, at least in part, dependent on clathrin.

Description of other molecular players in endocytosis was greatly advanced by the characterization of the temperature sensitive *shibire* mutant in *Drosophila.* Following stimulation, the *shibire*^{ts} mutant exhibits a reversible block in neurotransmission at the restrictive temperature, caused by a depletion of synaptic vesicles. This depletion is the result of a complete blockade of synaptic vesicle endocytosis (Koenig and Ikeda, 1989; Koenig et al., 1983; Kosaka and Ikeda, 1983). It was later demonstrated that the *shibire* gene encodes the GTPase dynamin, that dynamin is localized to the necks of pinching-off membrane, and that it is necessary in the fission of newly re-formed vesicles (Damke et al., 1994; Hinshaw, 2000; Marks et al., 2001). The discovery of a gene necessary for endocytosis opened the door for the identification of other important endocytosis molecules. Biochemical interaction assays led to the characterization of a host of endocytosis accessory proteins, including endophilin (Ringstad et al., 1999), amphiphysin (David et al., 1996), DAP160/intersectin (Roos and Kelly, 1998), synaptojanin (McPherson et al., 1996), epsin (Chen et al., 1998), and syndapin (Qualmann et al., 1999).

Now that these proteins and others have been shown to be involved in synaptic vesicle endocytosis, the challenge has been to pinpoint their action within this multi-step

process. Although the biophysical particulars are debated, it is generally believed that once a vesicle completely fuses with the plasma membrane, clathrin-mediated endocytosis begins by a demarcation of a stretch of membrane that will be endocytosed. Next, there is an initial curvature of the membrane, followed by more extensive curvature and a narrowing of the neck of the nascent vesicle. Lastly, the vesicle undergoes fission from the plasma membrane and uncoating of the clathrin coat (Brodin et al., 2000). Although much data supports this type of progression through clathrin-dependent steps, a form of non-clathrin-mediated endocytosis, termed kiss-and-run, has also been proposed (Aravanis et al., 2003; Fesce et al., 1994; Gandhi and Stevens, 2003; Stevens and Williams, 2000). In the kiss-and-run model, a vesicle does not fully fuse with the plasma membrane during exocytosis, but instead remains somewhat intact and releases its contents through a small fusion pore. Thus, when this vesicle is endocytosed, it will have already bypassed many of the initial steps delineated above. There is data to support the idea that dynamin would be involved in the retrieval of the vesicle in the kiss-and-run model (Verstreken et al., 2002), but it still remains unclear whether synapses undergo this type of fusion events and if they do, how the molecular mechanisms involved might differ from endocytosis following full vesicle fusion.

The analysis of genetic mutations, and other types of perturbations, in various endocytosis proteins has been critical in understanding what their function in synaptic vesicle endocytosis might be. Ultrastructural analyses, in particular, are important because they can give a picture of membrane configuration during a protein perturbation, and thereby point to a blockage at a specific endocytic step. However, because endocytosis following full vesicle fusion involves such dramatic changes—the

membrane is bent, then pinched, and turned outside in—and so many proteins are involved, it is unlikely that each of the proteins are only involved at one particular step. Therefore, determining at what stage endocytosis is blocked during a perturbation may relay only part of the function of that protein, because it is impossible to probe steps further downstream. It will be an interesting, but considerable, challenge to develop the tools necessary to precisely identify the function and timing of the interactions involved in retrieving a synaptic vesicle from the plasma membrane.

Almost all the proteins involved in synaptic vesicle endocytosis have been described to function exclusively in the endocytic phase of the synaptic vesicle cycle. Similarly, much evidence suggests that a toolbox of proteins is important in specifically regulating the exocytosis of synaptic vesicles. One exception is that of Synaptotagmin I (Syt I), an integral synaptic vesicle protein widely believed to be the primary calcium sensor for synaptic vesicle exocytosis (Fernandez-Chacon et al., 2001). Syt I also interacts biochemically with the clathrin adaptor protein complex, AP-2 (Chapman et al., 1998; Haucke and De Camilli, 1999; Haucke et al., 2000; Zhang et al., 1994). This biochemical interaction, as well as ultrastructural evidence showing increased vesicle size and decreased numbers in some Syt I mutants, has led to the hypothesis that Syt I functions in endocytosis. Until recently, however, this hypothesis hadn't been directly tested (Jorgensen et al., 1995; Reist et al., 1998). Investigating the role of Syt I in endocytosis *in vivo* is the subject of Chapters 2 and 3 of this thesis, as well as additional studies (Fukuda et al., 1995b; Littleton et al., 2001; Nicholson-Tomishima and Ryan, 2004).

It should be emphasized that the synaptic vesicle membrane contains many different types of proteins, both transmembrane and lipid-linked, most of which have been implicated in the regulated fusion of a synaptic vesicle in response to local calcium influx. In contrast, most of the proteins involved in endocytosis are cytosolic and are thought to be recruited to the plasma membrane or endocytosing synaptic vesicles in order to function in endocytosis. While synaptic vesicle proteins necessary for exocytosis must be correctly sorted into synaptic vesicles during retrieval, it is tempting to consider that they may also play active roles in endocytosis. Syt I, a known transmembrane synaptic vesicle exocytic protein, has also been shown to be important in endocytosis (Nicholson-Tomishima and Ryan, 2004; Poskanzer et al., 2003). In this vein, it was recently discovered that synaptobrevin, a v-SNARE necessary for vesicle exocytosis, may be important for certain kinds of endocytosis (Deak et al., 2004). The Syt I-binding protein, stoned/stonin, has also been implicated in both processes (Fergestad and Broadie, 2001; Martina et al., 2001). Because of their localization to these subcellular compartments, many other synaptic vesicle proteins have the potential to be directly involved in endocytosis. However, disruption of a protein involved in exocytosis would likely obscure analysis of a possible endocytic function of this protein. Thus, techniques that can specifically disrupt protein function during endocytosis will need to be employed to determine which synaptic vesicle proteins are involved in endocytosis and answer some of these outstanding questions.

Coupling and Coordination of Exocytosis and Endocytosis

Compensatory synaptic vesicle endocytosis is thought to precisely recycle the number of vesicles released during exocytosis (Heuser and Reese, 1973), while creating vesicles with a complete complement of synaptic vesicle proteins. Because the process is compensatory, there must exist coordination between exo- and endocytosis in order to couple the number of vesicles internalized to the number of released vesicles. Two general models could account for the coordination of endocytosis with exocytosis. In one model, endocytosis is directly triggered by a change caused by fusion of a vesicle to the plasma membrane, and is therefore completely dependent on exocytosis. For example, a synaptic vesicle protein, deposited in the plasma membrane during exocytosis, could subsequently direct or demarcate the amount of membrane that is endocytosed. Because it is inserted in the synaptic plasma membrane during vesicle fusion and can bind to a number of molecules implicated in endocytosis, such as AP-2 and PIP_2, Syt I has emerged as a possible candidate to link the two phases of the synaptic vesicle cycle.

In the second model, exo- and endocytosis are triggered somewhat independently by neural activity, such that conditions that cause exocytosis also allow endocytosis to occur. It is well accepted that calcium influx triggers synaptic vesicle exocytosis, and there are also some lines of research that implicate calcium in initiating endocytosis. First, a group of endocytic accessory proteins—dynamin, amphiphysin, AP180, epsin, eps15, and synaptojanin—are rapidly and coordinately dephosphorylated in response to nerve stimulation and calcium influx (Bauerfeind et al., 1997; Chen et al., 1999; Cousin et al., 2001; Liu et al., 1994; Slepnev et al., 1998). Calcineurin, a calcium-dependent phosphatase that is enriched at nerve terminals, has been proposed to act as a calcium

trigger for endocytosis by directly dephosphorylating these endocytic proteins (Marks and McMahon, 1998). Secondly, recent work has demonstrated a calcium-dependent interaction between endophilin and pre-synaptic calcium channels (Chen et al., 2003). In this scheme, both the start and the extent of exo- and endocytosis would be regulated by an increase in calcium level, although each would have different sensors and effectors. Although these data posit that synaptic vesicle endocytosis can be regulated by calcium concentration, it should be noted that the extent to which endocytosis is calcium-dependent remains highly controversial. Conflicting evidence has demonstrated that endocytosis can be facilitated (Sankaranarayanan and Ryan, 2001; Teng and Wilkinson, 2005), slowed (von Gersdorff and Matthews, 1994), or unchanged (Wu and Betz, 1996) by calcium concentration. In general, these two models for how synaptic vesicle endocytosis is coupled to exocytosis are not necessarily mutually exclusive. Different aspects of the endocytic process (such as initiation or extent) or different endocytic pathways may be controlled by different mechanisms.

Any model for the coordination of both phases of the vesicle cycle is complicated by the question of how much the synaptic vesicle membrane mixes with the plasma membrane, and how widely synaptic vesicle proteins diffuse in the plasma membrane after vesicle fusion. The problem of sorting synaptic vesicle proteins from plasma membrane proteins is vastly different depending on how much these membranes mix after vesicle fusion. Some evidence argues that there is little intermixing between the two membranous components (Torri-Tarelli et al., 1990), but the data are far from conclusive. Two different forms of endocytosis could be advantageous for the neuron in order to simplify this cell biological problem. In kiss-and-run fusion, the vesicle remains

mostly intact, so vesicle proteins wouldn't mix with those in the plasma membrane and the neuron would not have to sort different protein populations (Aravanis et al., 2003). In addition, a kind of bulk endocytosis or macropinocytosis, first suggested by one of the earliest ultrastructural studies, might act to internalize large amounts of membrane and protein into an intermediate cisternal/endosomal compartment (Di Paolo et al., 2004; Heuser and Reese, 1973; Paillart et al., 2003). Sorting of synaptic vesicle proteins into small, synaptic vesicle-sized structures would then take place at a later step, as budding events (perhaps clathrin-dependent) from this large, membranous structure. This type of endosomal intermediate may allow the neuron to take up membrane quickly during periods of intense exocytosis, and later sort synaptic vesicle proteins and membrane under fewer time constraints.

Kinetics of Synaptic Vesicle Endocytosis

In order to determine how exo- and endocytosis might be coordinated in time and space, it is first necessary to understand at what speed and in what place endocytosis occurs in the neuron. The first directly measured rates of compensatory synaptic vesicle endocytosis were obtained in cells with large terminals using capacitance techniques, which accurately track the changing size of the plasma membrane during vesicle recycling (Beutner et al., 2001; Neves and Lagnado, 1999; Sun et al., 2002; von Gersdorff and Matthews, 1994). These studies demonstrated that endocytosis seemed to be best described by two different rate constants: one fast (< 1s), and one much slower (≥ 10 s),

suggesting two different endocytic mechanisms. There is some data to support the idea that only the slower form of endocytosis is clathrin-dependent, while the faster is clathrin-independent (Jockusch et al., 2005). However, some of the neurons studied with capacitance (retinal bipolar cells and inner ear hair cells) release, and may retrieve, synaptic vesicles in a faster, more continuous fashion that most neurons, which are not accessible to capacitance measurements. Thus, these rates may not reflect endocytosis at most synapses.

FM dyes—fluorescent, styryl dyes that intercalate into lipid membranes—enable the examination of endocytosis in neurons that aren't amenable to capacitance assays (Betz et al., 1992). These dyes are taken up by internalizing membrane, and the extent and speed with which this happens in response to various stimulation conditions can be assayed by fluorescent microscopy. At vertebrate central synapses, FM1-43 was first used to describe vesicle recovery with a half time of tens of seconds (Ryan et al., 1993; Ryan et al., 1996). Since then, different FM dyes with different on-off kinetics have been applied to the problem to endocytosis (Klingauf et al., 1998; Pyle et al., 2000; Wu and Betz, 1996). However, there are drawbacks to using FM dyes: they measure only net membrane recycling, require a wait between dye loading and unloading, and rely on assumptions about the lifetime and diffusion of the dye (especially in the synaptic vesicle membrane, which has not been measured). Thus, perhaps the most quantitative application of FM dyes has been in estimating the size of vesicle recycling pools at the synapse, rather than in the kinetics of endocytosis, since bulk membrane uptake can be more accurately measured than endocytic rate.

The synapto-pHluorin (spH) imaging approach bypasses many of the problems of FM dyes. Genetically encoded monitors of pre-synaptic activity, the spH's are integral synaptic vesicle proteins with a pH-sensitive GFP fused to their luminal domain (Miesenbock et al., 1998). The acidic lumen of synaptic vesicles (pH~5.5) quenches the spH GFP fluorescence, and it is only when GFP encounters the neutral environment of the synaptic cleft upon vesicle exocytosis (pH~7.0) that the GFP fluoresces. Upon endocytosis and re-acidification of the vesicle, fluorescence is again quenched. Changes in fluorescence intensity therefore allow a temporal readout of the endocytosis of a synaptic vesicle protein for the first time. Because spH is encoded genetically, neurons do not need to have physical access to a dye; they must only be accessible to fluorescent imaging. Using spH, synaptic vesicle endocytosis measured *in vitro* and *in vivo* appears to occur on the order of seconds, begins during exocytosis, and can be described by a model in which the process is saturable (Poskanzer et al., 2003; Sankaranarayanan and Ryan, 2000; Sankaranarayanan and Ryan, 2001). Since spH is dependent on the pH environment, however, some caveats remain. First, it can be thorny to figure out which cellular compartment the spH is in. For example, a protein on the plasma membrane appears as the same fluorescence intensity as one in an un-acidified membrane compartment. In addition, the question of how the kinetics of the internalization of a synaptic vesicle protein relate to the formation of a new, properly sized synaptic vesicle remains unanswered.

No satisfactory unifying model for the timing of synaptic vesicle endocytosis has emerged. In some neurons, with certain approaches, two different rates appear to best describe endocytosis whereas in others, one rate best fits the data. It is unclear whether

two discrete molecular mechanisms underlie endocytosis in the systems described by two rates. Either way, the rate-limiting molecular step(s) for endocytosis is also unknown. Furthermore, it remains to be tested whether the endocytic differences observed at distinct neurons in different organisms have experimental or biological explanations. Apparent differences may be a result of different experimental approaches and conditions, or they may point to biological differences in neurons with distinct functions and demands.

Localization of Synaptic Vesicle Endocytosis

In considering the coordination of exo- and endocytosis, it is necessary to describe where both of these processes occur. It has been convincingly shown that synaptic vesicle exocytosis happens at specialized sites on the plasma membrane called active zones (Zenisek et al., 2000). There is also evidence to suggest that endocytosis occurs at dedicated sites that encompass the active zone, termed the peri-active zone. Endocytic proteins, such as dynamin, α-adaptin, endophilin, and the scaffolding molecule DAP160, are localized to this peri-active zone and excluded from the active zone (Estes et al., 1996; Gonzalez-Gaitan and Jackle, 1997; Koh et al., 2004; Marie et al., 2004; Roos and Kelly, 1998). Additionally, internalizing membrane has been observed, ultrastructurally, in many kinds of neurons outside of the active zone (Gad et al., 1998; Koenig and Ikeda, 1996; Shupliakov et al., 1997). Based on these data, one current model is that exocytosis occurs at the active zone, then synaptic vesicle proteins and membrane move into the

peri-active zone, where endocytic machinery is scaffolded to organize and direct synaptic vesicle retrieval. This model is attractive because it allows for the separation of exo- and endocytic machines at the synaptic plasma membrane. In addition, it describes the area devoted to endocytosis as larger than that of exocytosis, because the peri-active zone surrounds the entire active zone. Since endocytosis probably occurs at least an order of magnitude slower that exocytosis (seconds vs. milliseconds), it is appealing to consider that vesicles waiting to be endocytosed would have a large area to move into in order to make room for incoming exocytosing vesicles. Finally, the very movements of certain proteins or lipids themselves into the peri-active zone following exocytosis could be important in activating endocytic machinery and triggering endocytosis. This spatial separation at the synaptic plasma membrane might therefore be an important mechanistic tool with which the neuron links exo- and endocytosis.

Endocytosis and Synaptic Vesicle Pools at the *Drosophila* NMJ

There is a wide variety sizes of different type of synaptic terminals, and in the number of synaptic vesicles contained within them. Even so, it is interesting to note that all synaptic vesicles fall into roughly the same size range (~30 nm) and generally have similar mechanisms controlling their release. It has also been proposed that synaptic vesicles at all synapses are divided into functionally distinct pools that are accessed under different conditions. Current data support the idea that there are some vesicles primed for immediate exocytosis (readily releasable), some that are capable of release soon after

those first released (recycling), and others that are generally held back from exocytosis (reserve) (Rizzoli and Betz, 2005). This field is confusing, in part because terms and definitions of vesicle pools are not consistent across studies and organisms, although overall principles are generally similar. On the other hand, distinctions among neural types may be important, because partitioning of vesicles into functional pools might be distinct in neurons with different functions. This idea seems especially probable when considering vastly different synapses, such as the *Drosophila* NMJ with many thousands of vesicles over multiple active zones and central vertebrate synapses containing tens of vesicles at one active zone. If it is indeed true that different synapses partition vesicles differently, the assignment of vesicles into various pools could also be a read-out of functional synaptic changes. Thus, it is possible that compensatory synaptic vesicle endocytosis, which controls vesicle internalization after stimulated exocytosis, might participate in synaptic function by directing this vesicular traffic (Richards et al., 2000). For example, assigning a re-forming vesicle into a reserve pool, rather than a recycling one, would cause the synapse to have fewer recycling vesicles and could lead to synaptic depression over a long stimulus train, through depletion of an active vesicle pool. These adjustments could be monitored through unknown mechanisms in the pre-synaptic cell. However, post-synaptic signals may also have the potential to intercellularly regulate endocytosis and vesicle pool distributions (Micheva et al., 2003). Lastly, if vesicles in different pools are molecularly distinct, it is possible that these differences among different pool populations could be specified during the packaging of a vesicle for retrieval during endocytosis.

The study of compensatory synaptic vesicle endocytosis has been defined by the neuronal types often best suited for the experimental techniques. Very extensive NMJ terminals that have many vesicles and can be bathed in extracellular solutions (while remaining somewhat intact) were useful for early ultrastructural assays. Neurons with large surface areas were necessary for the type of kinetic data obtained with capacitance measurements, while genetic model organisms have greatly advanced the investigation of the molecular basis of synaptic vesicle endocytosis. The larval *Drosophila* NMJ offers many advantages as a system for studying this process. It allows the examination of a synapse that contains genetic mutations and/or transgenically expressed constructs. In addition, it is possible to carry out genetic screens at this synapse to identify still unknown genes in endocytosis. Electrophysiology, electron microscopy, and immunocytochemistry are all standard techniques at the *Drosophila* NMJ. Furthermore, the larvae are transparent, which is an advantage for applying novel fluorescent imaging and protein photoinactivation techniques to the question of endocytosis. In combination, all of these tools have the potential to greatly further our understanding of how synaptic vesicle endocytosis is molecularly controlled.

Chapter Two:

Synaptotagmin I is Necessary for Compensatory Synaptic Vesicle Endocytosis *in vivo*

Summary

Neurotransmission requires a balance of synaptic vesicle exocytosis and endocytosis (Jarousse and Kelly, 2001b). Synaptotagmin I (Syt I) is widely regarded as the primary calcium sensor for synaptic vesicle exocytosis (Brose et al., 1992; Fernandez-Chacon et al., 2001; Geppert et al., 1994; Littleton et al., 1993; Perin et al., 1990). Previous biochemical data suggest that Syt I may also function during synaptic vesicle endocytosis (Fergestad and Broadie, 2001; Fukuda et al., 1995b; Haucke and De Camilli, 1999; Haucke et al., 2000; Jarousse and Kelly, 2001a; Jorgensen et al., 1995; Littleton et al., 2001; Reist et al., 1998; von Poser et al., 2000; Zhang et al., 1994); however, ultrastructural analyses at synapses with impaired Syt I function have provided an indirect and conflicting view of the role of Syt I during synaptic vesicle endocytosis (Fukuda et al., 1995b; Geppert et al., 1994; Jorgensen et al., 1995; Littleton et al., 2001; Reist et al., 1998). Until now it has not been possible experimentally to separate the exocytic and endocytic functions of Syt I *in vivo*. Here, we test directly the role of Syt I during endocytosis *in vivo*. We use quantitative live imaging of a pH-sensitive green fluorescent protein (GFP) fused to a synaptic vesicle protein (synapto-pHluorin) to measure the kinetics of endocytosis in syt^{null} *Drosophila*. We then combine live imaging of the synapto-pHluorins with photoinactivation of Syt I, through fluorescein-assisted light inactivation, after normal Syt I-mediated vesicle exocytosis. By inactivating Syt I only during endocytosis, we demonstrate that Syt I is necessary for the endocytosis of synaptic vesicles that have undergone exocytosis using a functional Syt I protein.

Results

We tagged the synaptic vesicle protein n-Synaptobrevin (n-Syb) with superecliptic, pH-sensitive green fluorescent protein (GFP) (Gandhi and Stevens, 2003; Miesenbock et al., 1998; Sankaranarayanan and Ryan, 2000; Sankaranarayanan and Ryan, 2001). Expression of n-Syb-synapto-pHluorin (n-Syb-pH) in *Drosophila* neurons does not alter the functional or morphological development of the neuromuscular junction (NMJ). We show that spontaneous and evoked neurotransmitter release, the electrophysiological response to a stimulus train, FM4-64 recycling, and synaptic bouton number are normal in these animals (Figure 2-1). Quantitative imaging of n-Syb-pH demonstrates a stimulus-locked, reliable increase in fluorescence intensity that decays to baseline with an average time constant (τ = 12.6 ± 1.23 sec) similar to that observed at vertebrate central synapses (Figure 2-2A,B) (Gandhi and Stevens, 2003; Sankaranarayanan and Ryan, 2000).

Additional experiments demonstrate that n-Syb-pH functions as a reliable pH-sensitive monitor of synaptic vesicle recycling at the *Drosophila* NMJ. First, n-Syb-pH shows robust changes in fluorescence intensity in response to experimental manipulation of pH (2-3A,B). Second, bafilomycin, which blocks synaptic vesicle re-acidification, inhibits the fluorescence decay after nerve stimulation, consistent with a failure to re-acidify endocytosed vesicles (Figure 2-2C) (Sankaranarayanan and Ryan, 2001). Third, we generated transgenic animals harboring n-Syb-pH and a temperature sensitive mutation in dynamin (*shibire^{ts}*). At the permissive temperature, n-Syb-pH fluorescence exhibits a wild-type, stimulus-dependent increase and decay. However, at the restrictive

temperature the stimulus-dependent increase in n-Syb-pH fluorescence does not decay, consistent with the complete block of synaptic vesicle endocytosis that has been documented in *shibire*^{ts} (Figure 2-2D) (Koenig and Ikeda, 1996). This endocytic block is reversible after shifting to the permissive temperature (data not shown).

To test the function of Syt I during endocytosis, we first used n-Syb-pH to measure the kinetics of endocytosis at the NMJ of *syt*^{null} flies. In these experiments, the stimulus-dependent (50 Hz for 10 s) increase in n-Syb-pH fluorescence is significantly less in the *syt*^{null} synapses compared with controls, consistent with previous electrophysiological data (Figure 2-2E,F) (Fernandez-Chacon et al., 2001; Geppert et al., 1994; Loewen et al., 2001; Yoshihara and Littleton, 2002). Furthermore, n-Syb-pH fluorescence after stimulation at the *syt*^{null} NMJ does not decay, suggesting a severe impairment of vesicle endocytosis (Figure 2-2E,F). If endocytosis is impaired in the *syt*^{null} animals, then we also expect persistent, low frequency stimulation to cause a gradual accumulation of n-Syb-pH at the synaptic plasma membrane. Therefore, we stimulated wild type and *syt*^{null} synapses (1 Hz for 250 s) and imaged n-Syb-pH fluorescence before and after the stimulus train. We observe a statistically significant increase in n-Syb-pH fluorescence only at the *syt*^{null} synapses, indicating that n-Syb-pH has not been efficiently recycled in the *syt*^{null} animals (Figure 2-2G). Although these data are consistent with a role for Syt I during vesicle endocytosis, stimulus-evoked exocytosis is severely impaired in the *syt*^{null} animals and we do not know the nature of the Syt I-independent vesicular release that remains.

To test the function of Syt I during endocytosis without affecting Syt I-mediated exocytosis, we pursued experiments to photoinactivate Syt I rapidly following normal

stimulus-dependent exocytosis. We have previously shown that fluorescein-assisted light inactivation (FlAsH-FALI) is an efficient and specific method for the photoinactivation of Syt I (Marek and Davis, 2002). Briefly, Syt I is tagged with a 17 amino acid, tetracysteine motif (Syt I4C) that covalently binds the membrane-permeable fluorescein derivative 4',5'-bis(1,3,2-dithioarsolan-2-yl)fluorescein (FlAsH) (Gaietta et al., 2002; Griffin et al., 1998). Neuronal expression of Syt I4C rescues the *syt*^{null} mutation, even when bound to the FlAsH ligand (Marek and Davis, 2002). Epifluorescent illumination of FlAsH-bound Syt I4C decreases the evoked release in seconds, demonstrating efficient fluorophore-assisted light inactivation (FALI). FlAsH-FALI of Syt I4C does not alter sucrose-evoked release, demonstrating the specificity of Syt I4C photoinactivation (Marek and Davis, 2002). We have now combined FlAsH-FALI of Syt I4C with the n-Syb-pH technique. To ensure that endogenous Syt I does not affect our results, Syt I4C is always expressed in a *syt*^{null} mutant background. As both FlAsH and n-Syb-pH fluoresce in the green spectrum, we took advantage of the fact that epitope-bound FlAsH bleaches three orders of magnitude more rapidly than n-Syb-pH (Figure 2-3C). Epifluorescent illumination of FlAsH for 2 min decreases the FlAsH signal to near extinction, allowing us to quantitatively image n-Syb-pH.

In the first FlAsH-FALI experiment we used *shibire*^{ts} to conditionally block synaptic vesicle endocytosis and trap vesicles at the plasma membrane that have fused in the presence of functional Syt I4C during stimulation at the restrictive temperature. We then photoinactivated Syt I4C for 2 min, before shifting the preparation to the permissive temperature. If Syt I is necessary for endocytosis, we expect that n-Syb-pH will be retained at the plasma membrane following the shift to the permissive

temperature and the release of the *shibire^{ts}* endocytic block (Figure 2-4A). In these experiments n-Syb-pH fluorescence is quantified beginning at the time of the shift to the permissive temperature (t = 0). A previous ultrastructural study followed endocytosis at multiple time points in *shibire^{ts}* following a shift to the permissive temperature (Koenig and Ikeda, 1996). These previous data showed that endocytosis, after release from a dynamin block, occurs at the order of several minutes, which is slower than that observed following a short stimulus in a wild type flies (see Figure 2-2). The slow rate of endocytosis following release from a dynamin block may be caused by the abundance of membrane and vesicle protein that are trapped at the plasma membrane during the endocytic block.

In this experiment we used transgenic *Drosophila* flies that harbor the *shibire^{ts}* mutation as well as neuronally-driven Syt I4C and neuronally-driven n-Syb-pH in a *syt^{null}* background. These animals were raised at the permissive temperature, and show normal vesicle recycling at the permissive temperature (Figure 2-2D). In our control condition stimulation at the restrictive temperature in the absence of FlAsH induces a stable increase in n-Syb-pH fluorescence that decays upon shift to the permissive temperature, reflecting normal endocytosis (Figure 2-4B,C; see also Figure 2-5, Control). This control experiment includes a 2-min illumination before the shift to the permissive temperature to control for the effects of illumination. Our experimental condition includes the presence of FlAsH ligand and a 2-min illumination before the shift to the permissive temperature to induce photoinactivation of Syt I4C. In this experiment the n-Syb-pH signal does not decay on shifting to the permissive temperature, indicating that Syt I4C photoinactivation significantly impairs endocytosis (Figure 2-4B,C; see also Figure 2-5,

FlAsH). To determine whether FlAsH fluorescence confounds our assay of endocytosis, we quantified the total synaptic n-Syb-pH fluorescence by the addition of membrane-permeable, high pH NH_4Cl saline (pH 7.4) at the end of each experiment (Figure 2-3B). The total n-Syb-pH fluorescence is identical in control and experimental conditions, indicating that FlAsH bleaches to near extinction in these experiments (Figure 2-4C). Thus, the lack of n-Syb-pH fluorescence change after Syt I4C photoinactivation cannot be attributed to additional fluorescence contributed by the presence of the FlAsH ligand. These results demonstrate that photoinactivation of Syt I4C blocks the endocytosis of synaptic vesicles that have fused with the plasma membrane using a previously functional Syt I4C molecule.

In a second FlAsH-FALI experiment we tested whether Syt I4C photoinactivation blocks endocytosis without previously pausing the vesicle cycle using *shibire*^{ts}. Here, we assayed the retention of n-Syb-pH at the synaptic plasma membrane after Syt I4C photoinactivation. FlAsH-FALI of Syt I4C was initiated at the time of stimulation (50 Hz for 5 s) and lasted for 3 min (Figure 2-6A). If Syt I4C photoinactivation blocks endocytosis that normally occurs during and after the stimulus, then we expect to observe increased fluorescence at the end of the 3-min period due to unrecycled n-Syb-pH retained at the synaptic plasma membrane. We also expect to see a greater decrease in n-Syb-pH fluorescence after an acid wash, which should quench the surface n-Syb-pH fluorescence (Figure 2-3A) (Sankaranarayanan and Ryan, 2001). In this protocol, Syt I4C-dependent exocytosis will decline during the stimulation owing to photoinactivation of Syt I4C, so that the total amount of exocytosis will be less in the experimental animals compared with controls (Marek and Davis, 2002). However, this

will cause us to underestimate any potential difference in the accumulation of surface n-Syb-pH caused by Syt I4C photoinactivation compared with controls. As a control, we demonstrated that n-Syb-pH recycles normally in this genetic background (Figure 2-3D).

In these experiments, Syt I4C photoinactivation results in a statistically significant increase in surface n-Syb-pH fluorescence, consistent with impaired endocytosis. We quantified n-Syb-pH fluorescence 10 s before application of the acid wash (Figure 2-6A). At this time, n-Syb-pH intensity is significantly greater at synapses that have received both stimulation and Syt I4C photoinactivation compared with controls (Figure 2-6B, star). Subsequent acid wash reduced n-Syb-pH fluorescence to statistically similar levels in all conditions (Figure 2-6B). Therefore, the decrease in surface fluorescence after acid wash is significantly greater at experimental synapses compared with controls (Figure 2-6C). These data are consistent with a requirement of Syt I during compensatory endocytosis. Furthermore, these data argue against the possibility that Syt I functions exclusively during vesicle re-acidification, as we have assayed the plasma membrane retention of n-Syb-pH.

Finally, we measured FM4-64 uptake as an alternative assay of vesicle endocytosis. We first demonstrated normal FM4-64 loading and unloading at the *Drosophila* NMJ (Figure 2-7B) (Kuromi and Kidokoro, 1998). We then took advantage of the fact that endocytosis is slow compared with exocytosis, allowing temporal separation of these processes. First, we stimulated (30 Hz for 1 min) synapses in the presence of FM4-64, causing similar exo- and endocytosis in all conditions. After the stimulus, vesicles will cease exocytosis, but will continue to endocytose, compensating for the large amount of release that occurred during the stimulation. We continued to bathe the

synapses in FM4-64 while illuminating for 2 min. This allowed the nerve terminal to endocytose the dye during Syt I4C photoinactivation. After washing the FM4-64 away, we measured the amount of FM-64 taken up during this endocytic phase of the experiment (Figure 2-7A). If Syt I is necessary for compensatory endocytosis then we expect to observe less loading of the nerve terminal in Syt I4C-photoinactivated synapses. FlAsH-FALI of Syt I4C results in statistically lower mean fluorescence values of FM4-64 compared with controls, indicating that Syt I4C photoinactivation impairs endocytosis (Figure 2-7C). We observed control levels of FM4-64 loading in the presence of FlAsH-bound Syt I4C without any illumination, demonstrating that the ligand-bound Syt I4C itself does not impair endocytosis.

Discussion

By temporally uncoupling exo- and endocytosis, we have found an essential role for a known exocytic protein (Syt I) during endocytosis. Although different modes of endocytosis with different time courses may exist (Aravanis et al., 2003; Gandhi and Stevens, 2003; Verstreken et al., 2002), a specialized form of clathrin-mediated endocytosis, termed compensatory endocytosis, participates in the maintenance of the synaptic vesicle pool (Gandhi and Stevens, 2003; Jarousse and Kelly, 2001b). Compensatory endocytosis involves the formation of synaptic vesicles that are surrounded by clathrin and the AP-2 adaptor complex, as well as associated adaptor proteins (Jarousse and Kelly, 2001b). Our data are consistent with a model based on previous biochemical data suggesting that Syt I nucleates the formation of clathrin coated vesicles by serving as a synaptic plasma membrane docking site for the AP-2 complex (Fergestad and Broadie, 2001; Haucke and De Camilli, 1999; Haucke et al., 2000; Jarousse and Kelly, 2001a; von Poser et al., 2000; Zhang et al., 1994). This model provides a means to link the extent of synaptic vesicle exocytosis and endocytosis. Finally, it has been demonstrated that multiple Syt proteins can bind AP-2 (Li et al., 1995). However, since we have acutely disrupted Syt I, there should not be an opportunity for other Syt proteins to bind AP-2 and nucleate endocytosis in our experiments.

Figures

Figure 2-1. Neuronal expression of UAS-n-Syb-pH does not affect function or morphology at the NMJ.

(A) Excitatory postsynaptic potentials (EPSP) recorded at muscle 6 in segment A3 in wild type (wt) and animals expressing *UAS-n-Syb-pH* (n-Syb-pH) under the control of a neuronal GAL4 driver (*elaV$^{3L:1}$-GAL4*). There is no difference in the average EPSP amplitude or the spontaneous miniature EPSP (mEPSP) amplitudes between these genotypes. (B) A representative train of EPSPs recorded from an n-Syb-pH expressing synapse (10 Hz for 3 min, 2.0 mM Ca^{2+}). EPSP amplitudes are constant throughout the stimulus train, consistent with normal vesicle recycling (n = 5). Inset: representative EPSPs at two different times during the stimulus train. (C) Endocytosis is normal in n-Syb-pH animals. Synapses at muscle 6/7 in wild type (n = 5) and n-Syb-pH (n = 5) animals were bathed in 10 μM FM4-64 and stimulated for 1 min at 30 Hz in HL3 + 0.5 mM Ca^{2+}, then washed in HL3 + 0 mM Ca^{2+} for 5 minutes, and imaged (load). Synapses were stimulated again (30 Hz, 1 min in HL3 + 0.5 mM Ca^{2+}) and re-imaged (unload). Mean FM4-64 fluorescence was measured for each condition. There is no significant difference in FM4-64 fluorescence intensity between genotypes. (D) Morphological analysis at n-Syb-pH expressing synapses. Synaptic bouton number was counted at muscles 6 and 7 in segments A2–A5 in wild type (n = 14) and n-Syb-pH (n = 19) animals. There is no significant difference in bouton numbers.

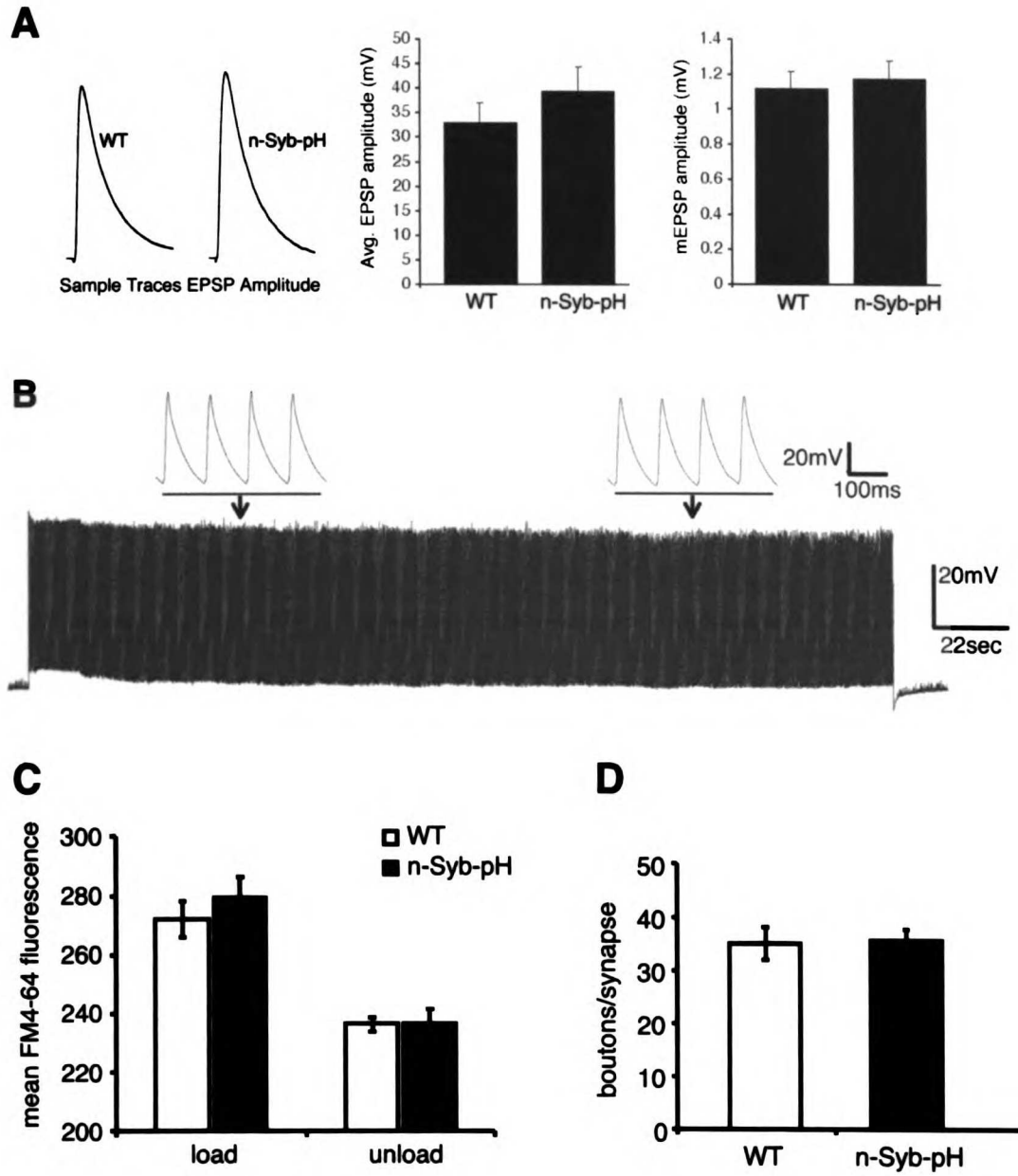
A
WT
n-Syb-pH
Sample Traces EPSP Amplitude
Avg. EPSP amplitude (mV)
50
45
40
35
30
25
20
15
10
5
0
WT
n-Syb-pH
mEPSP amplitude (mV)
1.4
1.2
1
0.8
0.6
0.4
0.2
0
WT
n-Syb-pH
B
20mV
100ms
20mV
22sec
C
mean FM4-64 fluorescence
300
280
260
240
220
200
WT
n-Syb-pH
load
unload
D
boutons/synapse
50
40
30
20
10
0
WT
n-Syb-pH

Figure 2-2. Endocytosis is impaired at *syt*^{null} synapses.

(A) n-Syb-pH fluorescence intensity changes at the NMJ before (1 s, 4 s), during (7 s) and after (10 s–20 s) nerve stimulation. Scale represents arbitrary fluorescence units throughout all panels. (B) Average n-Syb-pH fluorescence values for the synapse in (a) (n = 7 trials.) (C) Representative traces of n-Syb-pH intensity before (open circles) and after (filled circles) addition of bafilomycin (5 μM, 5 min incubation). (D) n-Syb-pH intensity in a *shibire*^{ts} mutant at permissive (open circles) and restrictive temperatures (closed circles). (E) n-Syb-pH intensity at wild type (open circles; n = 4) and *syt*^{null} (filled circles; n = 7) synapses. (F) n-Syb-pH intensity data at *syt*^{null} synapses replotted from (e). (G) n-Syb-pH fluorescence change in wild type (white bar, n = 6) and *syt*^{null} (filled bar, n = 5) synapses following a 250-s, 1-Hz stimulus. Fluorescence change is calculated as the difference between pre- and post-stimulus intensities, normalized to pre-stimulus values. No images were taken during the stimulus to minimize photobleaching. *syt*^{null} synapses show a significant increase in n-Syb-pH intensity ($p < 0.003$).

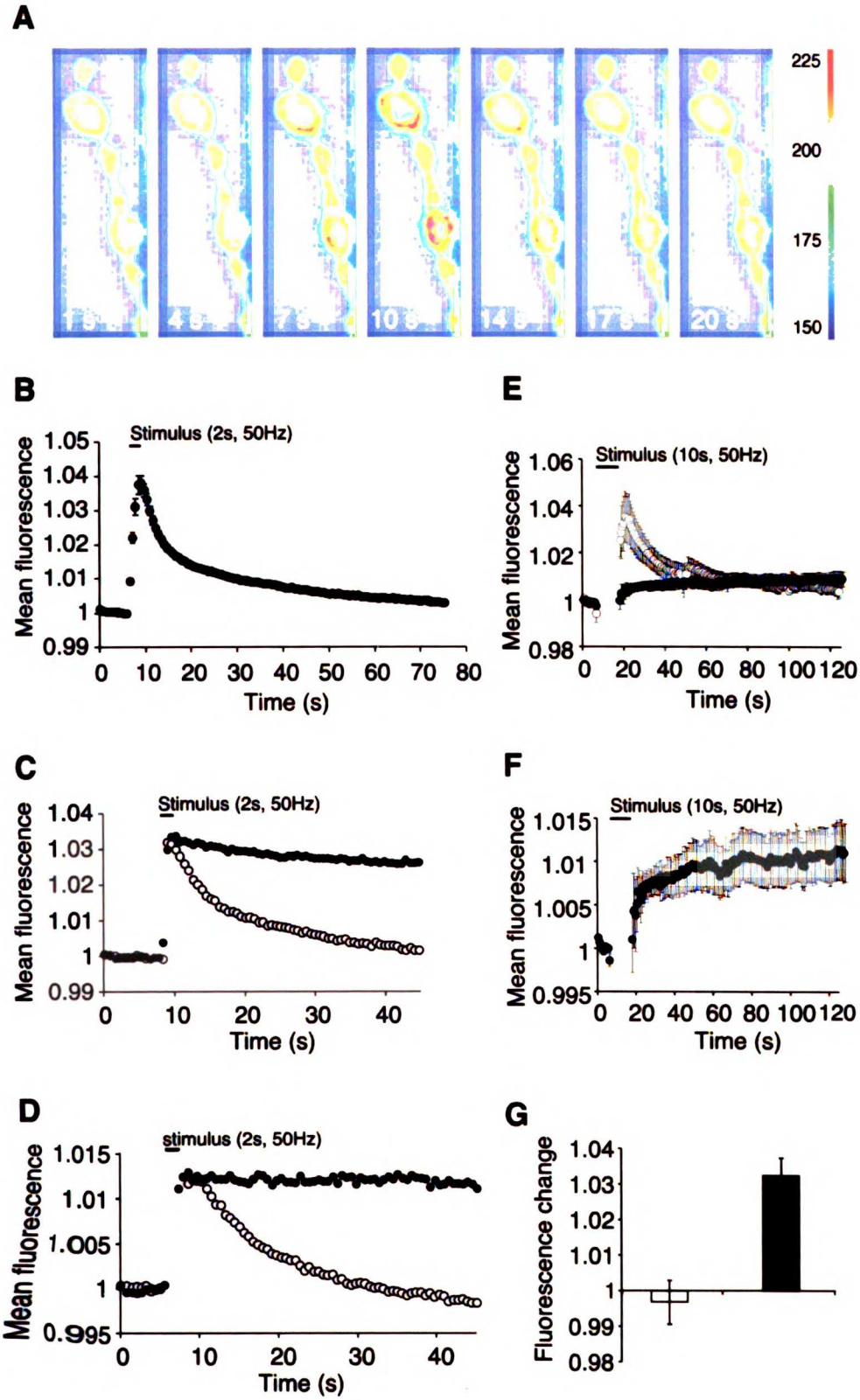
A
225
200
175
150
B
Stimulus (2s, 50Hz)
Mean fluorescence
Time (s)
E
Stimulus (10s, 50Hz)
Mean fluorescence
Time (s)
C
Stimulus (2s, 50Hz)
Mean fluorescence
Time (s)
F
Stimulus (10s, 50Hz)
Mean fluorescence
Time (s)
D
stimulus (2s, 50Hz)
Mean fluorescence
Time (s)
G
Fluorescence change

Figure 2-3. Synapto-pHluorins exhibit pH-sensitivity at the Drosophila NMJ.

(A) Acidic saline (black bar) quenches the fluorescence of surface n-Syb-pH expression. (B) Membrane-permeable NH_4Cl (black bar) increases fluorescence intensity of n-Syb-pH in the presynaptic terminal, revealing previously quenched n-Syb-pH at synaptic vesicles. Representative trials of individual synapses are shown. (C) Syt I4C-bound FlAsH bleaches more rapidly than n-Syb-pH. Values are calculated as the change in fluorescence relative to background ($\Delta F/F$) and normalized to the first data point. Syt I4C expressing synapses (closed circles) were labeled with FlAsH and illuminated for 120 seconds. FlAsH fluorescence bleaches to near background levels during this time. N-Syb-pH expressing synapses (open circles) were imaged identically for 120 seconds in the absence of stimulation. This fluorescence represents the basal surface expression of n-Syb-pH that has been observed in other systems (Gandhi and Stevens, 2003; Sankaranarayanan and Ryan, 2000; Sankaranarayanan and Ryan, 2001). During the 120 seconds of illumination, the surface n-Syb-pH fluorescence bleaches by less than 1%. (D) All genetic backgrounds used throughout this study show the indistinguishable n-Syb-pH recycling. Genotypes shown: genotype 1 = *UAS-n-Syb-pH,elaV*^{3E1}, genotype 2 = *UAS-Syt4C,syt*^{AD4}/*syt*^{D27};*UAS-n-Syb-pH/elaV*^{3E1}, genotype 3 = *w,shi*^{ts2};*UAS-Syt4C,syt*^{AD4}/*syt*^{D27};*UAS-n-Syb-pH/elaV*^{3E1}.

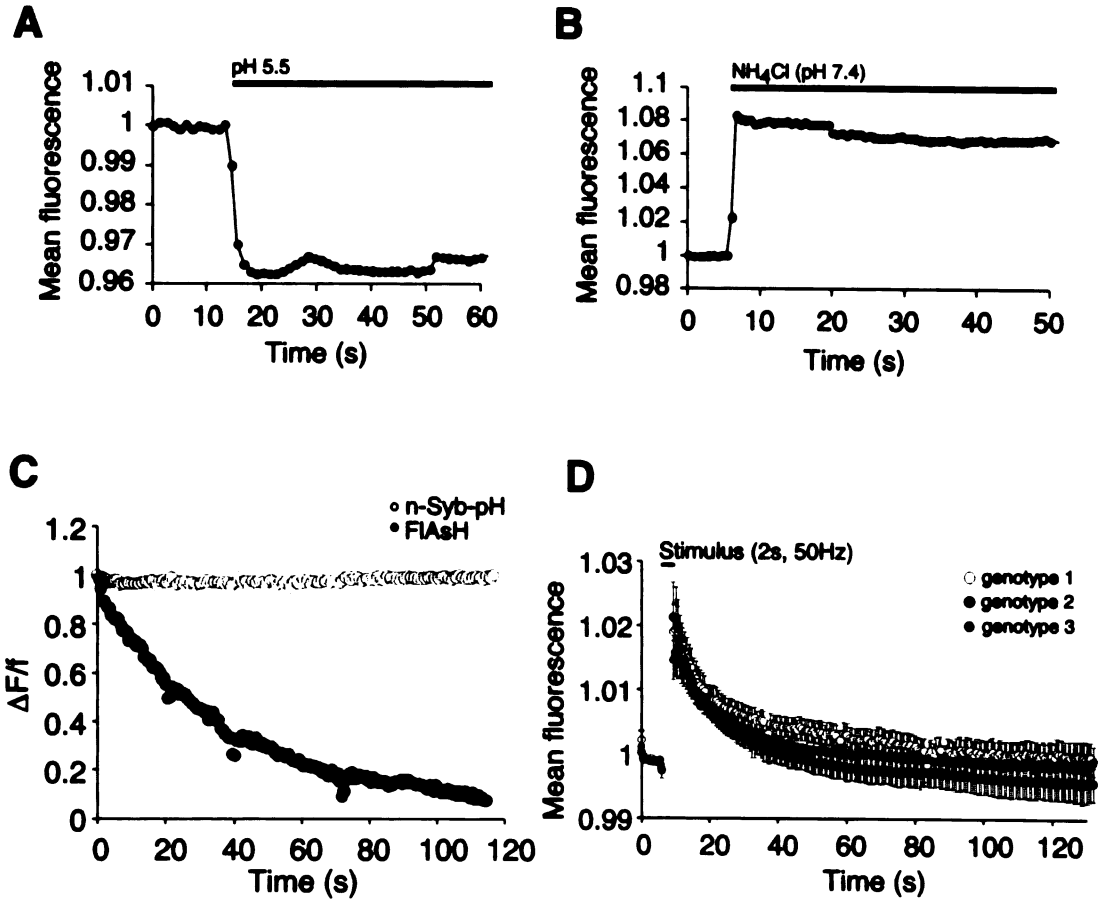
A
pH 5.5
Mean fluorescence
1.01
1
0.99
0.98
0.97
0.96
0 10 20 30 40 50 60
Time (s)
B
NH4Cl (pH 7.4)
Mean fluorescence
1.1
1.08
1.06
1.04
1.02
1
0.98
0 10 20 30 40 50
Time (s)
C
n-Syb-pH
FlAsH
ΔF/f
1.2
1
0.8
0.6
0.4
0.2
0
0 20 40 60 80 100 120
Time (s)
D
Stimulus (2s, 50Hz)
genotype 1
genotype 2
genotype 3
Mean fluorescence
1.03
1.02
1.01
1
0.99
0 20 40 60 80 100 120
Time (s)

Figure 2-4. Photoinactivation of Syt I4C impairs endocytosis after normal vesicle fusion.

(A) Schematic of the experimental protocol and results. (B) Quantification of the n-Syb-pH intensity changes after shift from restrictive to permissive temperatures. Each line represents a single trial from a different animal. Values are normalized to the first time-point after shift to the permissive temperature. (C) Mean values for data in (b). Data are binned in 2-min intervals. The last point (NH_4Cl) is the intensity after addition of NH_4Cl saline at the conclusion of each trial.

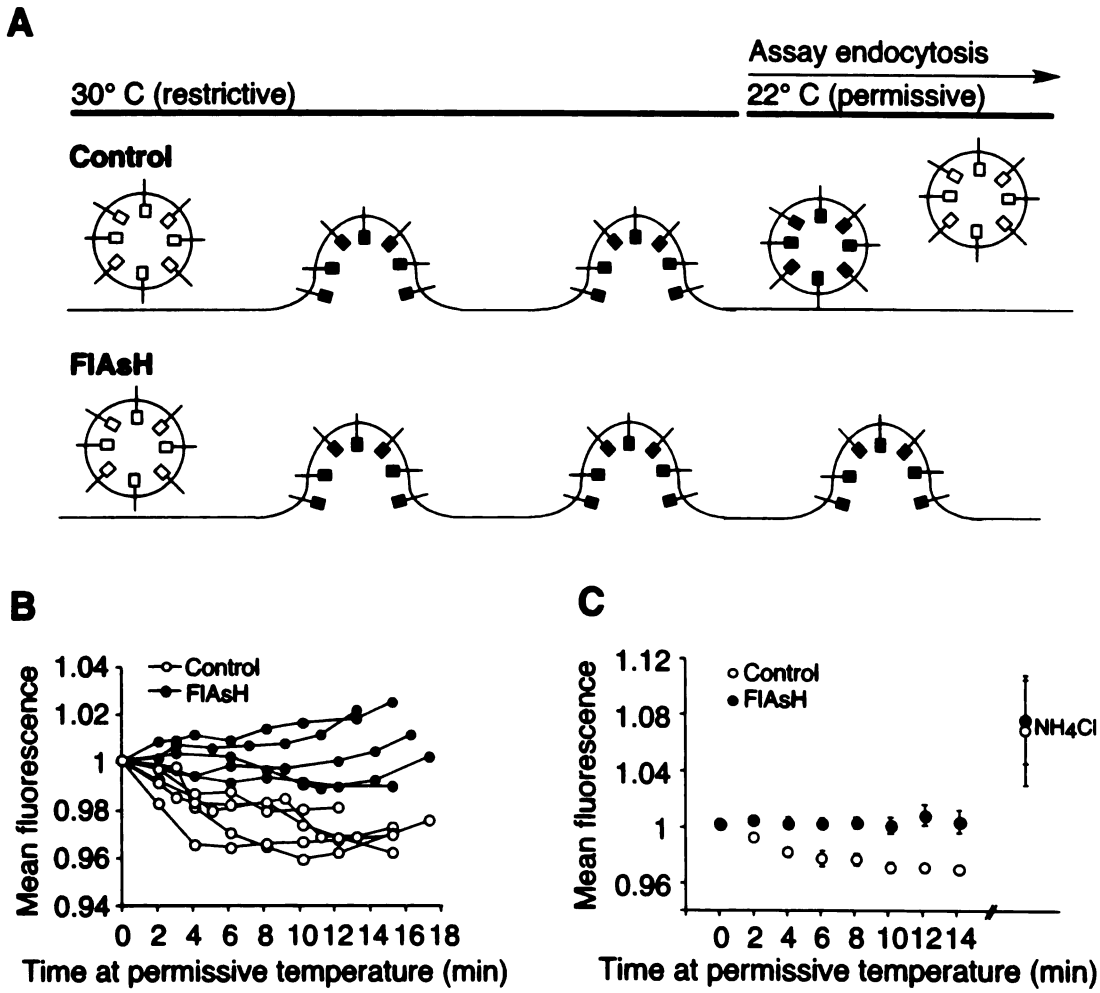
A
Assay endocytosis
30° C (restrictive)
22° C (permissive)
Control
FlAsH
B
Control
FlAsH
Mean fluorescence
1.04
1.02
1
0.98
0.96
0.94
0 2 4 6 8 10 12 14 16 18
Time at permissive temperature (min)
C
Control
FlAsH
NH4Cl
Mean fluorescence
1.12
1.08
1.04
1
0.96
0 2 4 6 8 10 12 14
Time at permissive temperature (min)

Figure 2-5. Images demonstrating n-Syb-pH intensity changes at the NMJ following the shift from the restrictive to the permissive temperature

(A) Synapses are from the same gentoype in the top panels (control, without FlAsH ligand) and bottom panels (FlAsH, with FlAsH ligand). Scale represents arbitrary fluorescence units.

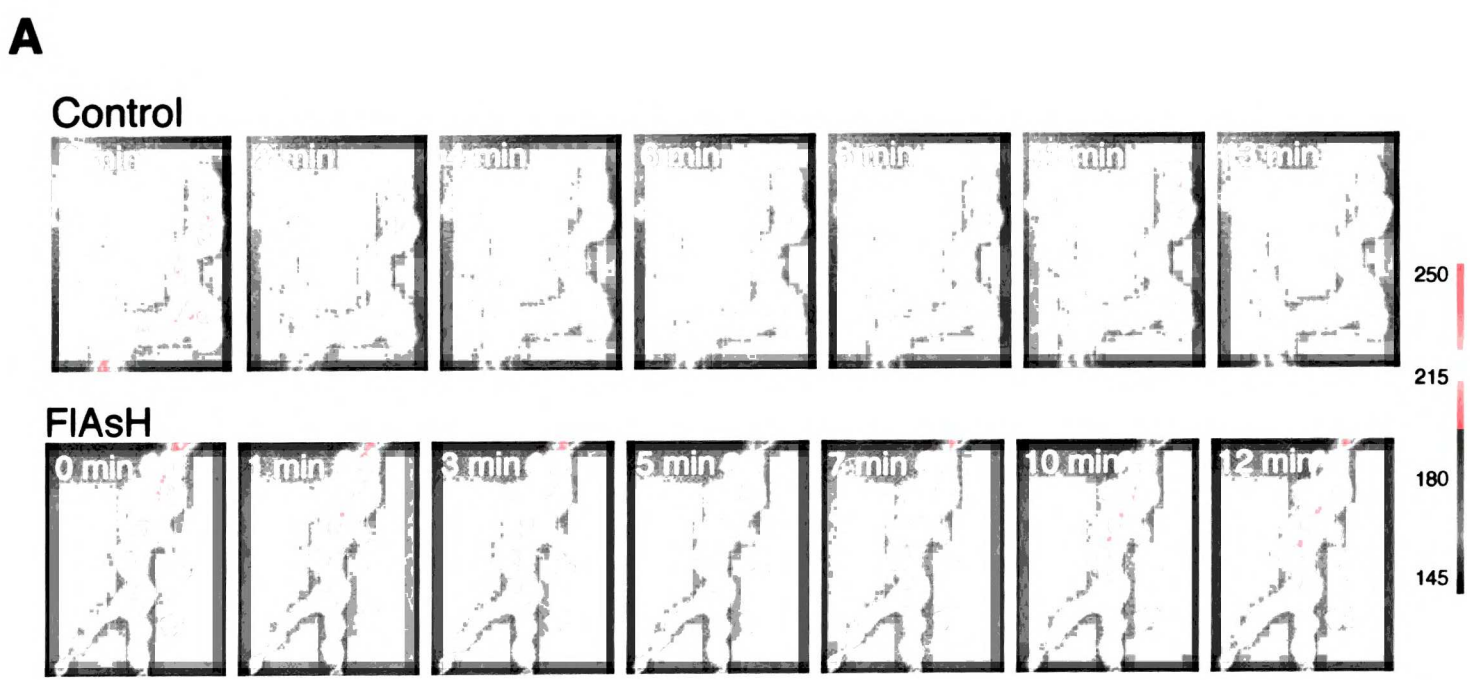
A
Control
FlAsH
0 min
1 min
3 min
5 min
7 min
10 min
12 min
250
215
180
145

Figure 2-6. n-Syb-pH remains on the synaptic plasma membrane after FlAsH-FALI of Syt I4C.

(A) Protocol for acid wash experiments. (B) Data shown include the ten time points before addition of the acid wash, and the subsequent 50 time points. (C) Change in intensity from the mean of the first ten points to the mean of the last ten in (b). Conditions include the presence (+) or absence (-) of FlAsH ligand and presence or absence of stimulation (5 s, 50 Hz). Synapses with Syt I4C photoinactivation and stimulation (n = 11) show a significantly greater change in fluorescence intensity than FlAsH alone (n = 9, $p < 0.01$) or stimulation alone (n = 12, $p < 0.01$, t-test). Controls are not significantly different from each other. The genotype used is *syt^{AD4},UAS-syt4C/syt^{D27};UAS-n-Syb-pH/elaV^{3E1}*.

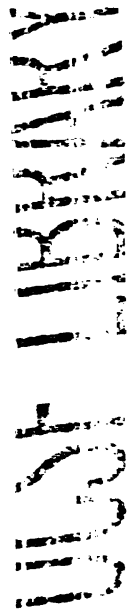

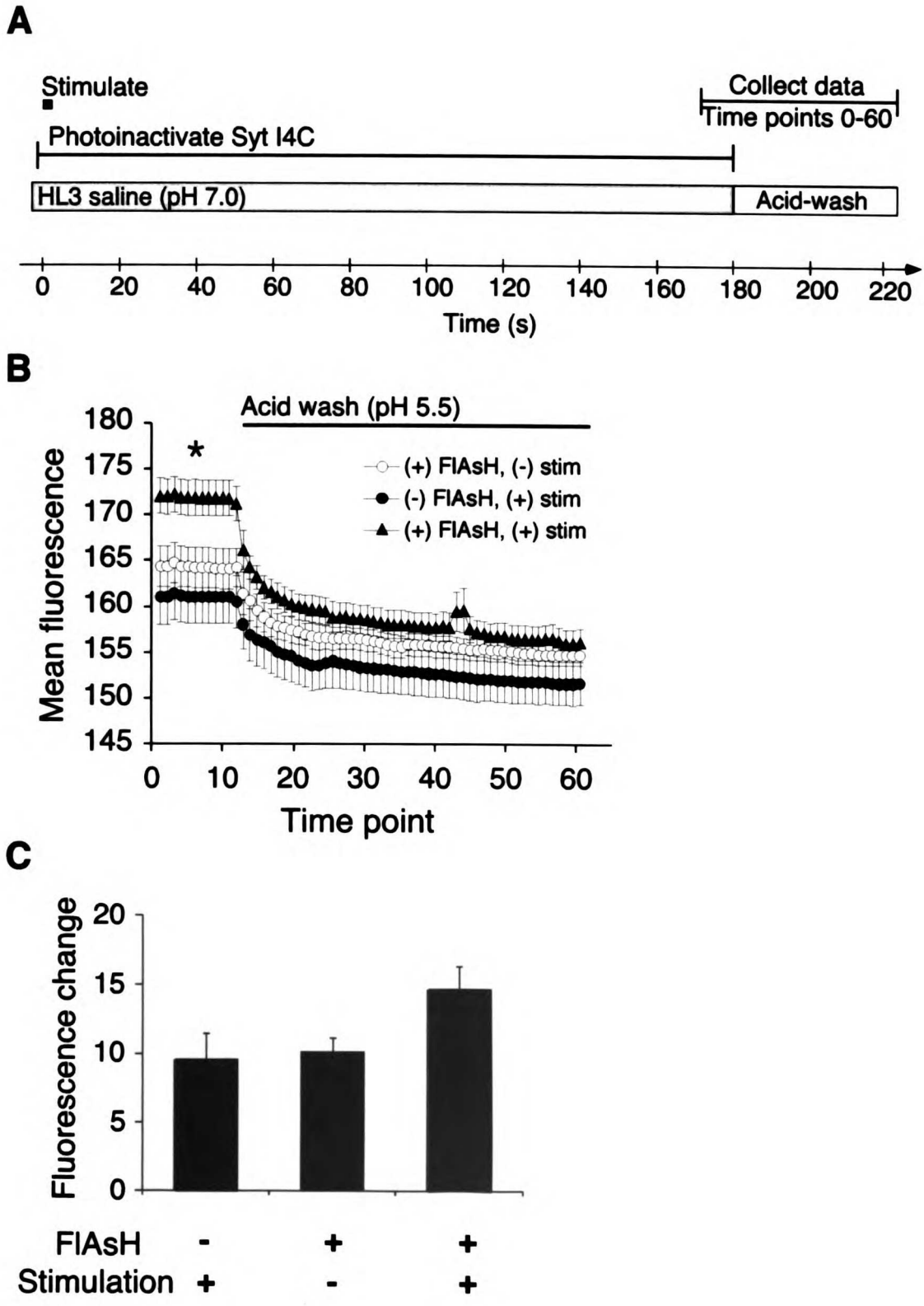
A
Stimulate
Collect data
Time points 0-60
Photoinactivate Syt I4C
HL3 saline (pH 7.0)
Acid-wash
0 20 40 60 80 100 120 140 160 180 200 220
Time (s)
B
Acid wash (pH 5.5)
*
(+) FlAsH, (-) stim
(-) FlAsH, (+) stim
(+) FlAsH, (+) stim
Mean fluorescence
180 175 170 165 160 155 150 145
0 10 20 30 40 50 60
Time point
C
Fluorescence change
20 15 10 5 0
FlAsH - + +
Stimulation + - +

Figure 2-7. Photoinactivation of Syt I4C impairs stimulus-dependent FM4-64 loading at the NMJ.

(A) Protocol for FM4-64 experiments. (B) Images demonstrating efficient loading (left) and unloading (right) of FM4-64. (C) Quantification of FM4-64 loading at synapses in the presence (+) or absence (-) of FlAsH ligand, and the presence or absence of illumination. Loading of FM4-64 is significantly less ($p < 0.02$) at synapses that have undergone photoinactivation of Syt I4C (+ FlAsH, + illumination; n = 6) compared with controls (- FlAsH, + illumination; n = 7), (+ FlAsH, - illumination; n = 8).

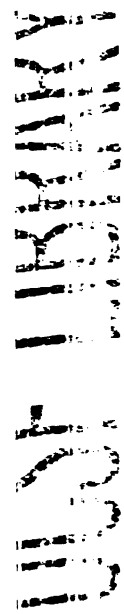

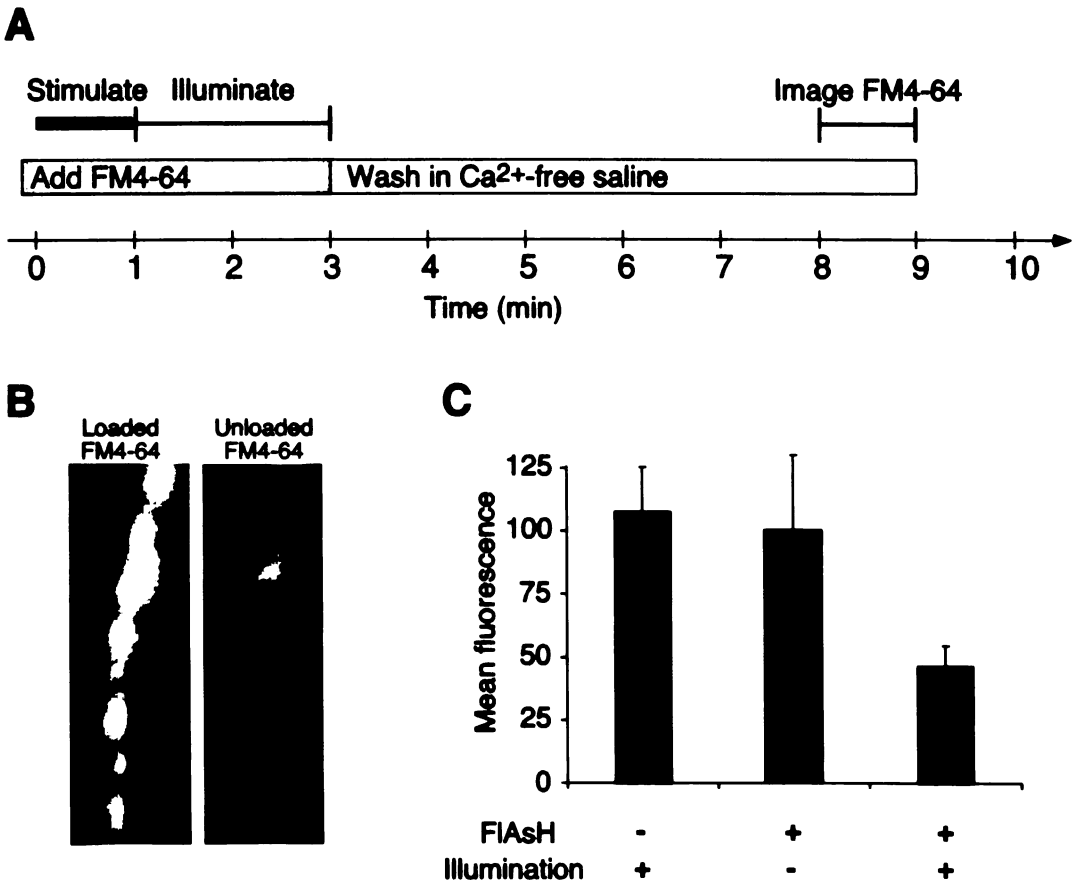
A
Stimulate
Illuminate
Image FM4-64
Add FM4-64
Wash in Ca2+-free saline
0
1
2
3
4
5
6
7
8
9
10
Time (min)
B
Loaded FM4-64
Unloaded FM4-64
C
Mean fluorescence
125
100
75
50
25
0
FlAsH
Illumination
-
+
+
+
-
+

Chapter Three:

Discrete Residues in the C_2B Domain of Synaptotagmin I Independently Specify Endocytic Rate and Synaptic Vesicle Size

Summary

It has been demonstrated that synapses lacking functional Synaptotagmin I (Syt I) have a decreased rate of synaptic vesicle endocytosis. Beyond this, the function of Syt I during endocytosis remains undefined. Here, we demonstrate that a decreased rate of endocytosis in *syt^{null}* mutants correlates with a stimulus-dependent perturbation of membrane internalization, assayed ultrastructurally. We then separate the mechanisms that control endocytic rate and vesicle size by mapping these processes to discrete residues in the Syt I C_2B domain. Mutation of a poly-lysine motif alters vesicle size but not endocytic rate, whereas the mutation of calcium-coordinating aspartate residues (*syt-D3,4N*) alters endocytic rate but not vesicle size. Finally, slowed endocytic rate in the *syt-D3,4N* animals, but not *syt^{null}* animals, can be rescued by elevating extracellular calcium concentration, supporting the conclusion that calcium coordination within the C_2B domain contributes to the calcium dependence of endocytic rate..

Introduction

Various experimental approaches have been used to dissect and describe the process of synaptic vesicle endocytosis. Ultrastructural experiments have followed vesicle reformation and have provided a descriptive view of membrane trafficking during this process (Ceccarelli et al., 1973; Gad et al., 1998; Heuser and Reese, 1973; Koenig and Ikeda, 1989). Several different pathways for vesicle endocytosis have been proposed based on this work: one in which clathrin-coated vesicles of the appropriate size are formed directly at the plasma membrane following full fusion of the synaptic vesicle, a second in which large cisternae are first pinched off from the plasma membrane before giving rise to appropriately sized vesicles, and a third in which vesicles are retrieved prior to full fusion with the plasma membrane by a dynamin-dependent, clathrin-independent mechanism (termed kiss-and-run). In parallel to this ultrastructural work, biochemical and forward genetic approaches have identified many, if not the majority, of proteins directly involved in the process of synaptic vesicle endocytosis (David et al., 1996; Di Paolo et al., 2004; Kosaka and Ikeda, 1983; McPherson et al., 1996; Ringstad et al., 1999; Roos and Kelly, 1998; Zhang et al., 1998; Zhang et al., 1994). Finally, kinetic approaches using capacitance or live imaging (FM dyes, synapto-pHluorins) have measured rates that describe how fast the process of endocytosis proceeds from initiation to the formation of fully internalized membrane (Klingauf et al., 1998; Neves and Lagnado, 1999; Ryan et al., 1996; Sankaranarayanan and Ryan, 2000; von Gersdorff and Matthews, 1994).

A remaining challenge is to unify our molecular understanding with the ultrastructural and biophysical descriptions of synaptic vesicle endocytosis. The ultimate goal is to define how a macro-molecular machine is assembled, modified, and then resolved to control high fidelity compensatory endocytosis of synaptic vesicle membrane and protein. As a step toward this goal, the function of individual proteins and specific protein-protein interactions needs to be characterized during endocytosis. This will not only refine our molecular understanding of endocytosis, but may clarify our understanding of the diverse potential pathways by which synaptic vesicles are formed. Here we focus on the function of Syt I during synaptic vesicle endocytosis.

Syt I, while widely considered to be the primary Ca^{2+} sensor for synaptic vesicle exocytosis, has also recently been shown to be necessary for endocytosis, since synapses lacking a functional Syt I protein show severely impaired rates of endocytosis (Nicholson-Tomishima and Ryan, 2004; Poskanzer et al., 2003). Syt I can interact biochemically and genetically with a host of molecules at the pre-synaptic active zone, including syntaxin (Kee and Scheller, 1996), N-type Ca^{2+} channels (Sheng et al., 1997), the clathrin adaptor complex AP-2 (Chapman et al., 1998; Zhang et al., 1994), phosphoinositides (Fernandez et al., 2001; Fukuda et al., 1995a; Schiavo et al., 1996), and stoned (Phillips et al., 2000). Syt I, therefore, has the potential to regulate more than one stage of vesicle reformation through these diverse molecular interactions.

Here, we have undertaken a structure-function analysis of Syt I to define how this protein participates in the process of synaptic vesicle endocytosis *in vivo*. We have applied ultrastructural and kinetic assays of endocytosis to a range of molecular perturbations that affect the function of the Syt I protein. We demonstrate that Syt I

regulates both the rate and the size of synaptic vesicles formed during endocytosis and we are able to assign control of these two processes to discrete regions of the Syt I protein. Mutation of a poly-lysine motif within the C_2B domain does not affect the rate of endocytosis, but disrupts vesicle size. Conversely, Ca^{2+}-coordination within the C_2B domain is required for the normal rate of vesicle endocytosis, but is not necessary for the formation of appropriately sized vesicles. To our knowledge, this is the first time that these different aspects of the vesicle cycle have been separated. Based on our new data, we discuss models for how Syt I may participate in synaptic vesicle endocytosis.

Results

In order to characterize the role of Syt I during endocytosis, we established an experimental protocol to measure the altered kinetics of vesicle recycling in Syt I mutants, including syt^{null} and domain-specific mutant combinations. We then used ultrastructural analysis, following the same stimulus protocol, to correlate changes in the kinetics of vesicle endocytosis with stimulus-dependent changes in vesicle membrane retrieval.

Syt I null mutations perturb both endocytic rate and vesicle size

We first examined the kinetics of endocytosis at synapses in two heteroallelic syt^{null} combinations, $syt^{\Delta D4/D27}$ and $syt^{\Delta D4/N13}$ at the *Drosophila* NMJ. We assayed the kinetics of endocytosis with a pre-synaptically expressed synapto-pHluorin (n-Syb-pH) transgene, which consists of a synaptic vesicle protein (n-Synaptobrevin) tagged with a pH-sensitive GFP molecule (Gandhi and Stevens, 2003; Li et al., 2005; Miesenbock et al., 1998; Poskanzer and Davis, 2004; Sankaranarayanan and Ryan, 2000). In Figure 3-1A, we show the n-Syb-pH response to a 50 Hz, 10 s stimulus, normalized to baseline fluorescence levels. As predicted from prior electrophysiological studies (Geppert et al., 1994; Littleton et al., 1993), the syt^{null} synapses (light and dark blue) show a decrease in evoked neurotransmitter release compared to wild type controls (black), as demonstrated by a decrease in EPSP amplitude (Table 3-1) and a smaller $\Delta F/F$ peak value (Figure 3-1A). When we compare rates among genotypes (Figure 3-1B), it is clear that both syt^{null}

genotypes show a significantly slowed endocytosis rate (τ = 29.8 ± 6.6 s and 22.8 ± 8.7 s for $syt^{AD4/D27}$ and $syt^{AD4/N13}$, respectively when fit to a single exponential function) compared to controls (τ = 13.7 ± 1.1 s; $p < 0.03$). In all n-Syb-pH experiments, tau values are identical when fit to normalized or non-normalized curves.

At vertebrate central synapses, the rate of endocytosis slows as stimulus number is increased, suggesting that the rate of endocytosis is sensitive to the extent of exocytosis (Fernandez-Alfonso and Ryan, 2004; Sankaranarayanan and Ryan, 2000). Since syt^{null} animals release fewer vesicles, a change in exocytosis could be the cause of slowed endocytic rate in these animals. Therefore, we determined whether the rate of endocytosis is influenced by the amount of exocytosis at the Drosophila NMJ. We measured endocytic rates in wild type animals over a range of extracellular Ca^{2+} concentrations and stimulus durations. Increasing Ca^{2+} concentration (from 0.2–2.0 mM during a 10 s stimulus) and stimulus duration (from 1–10 s in 2.0 mM Ca^{2+}) both cause an increase in transmitter release as demonstrated by larger peak $\Delta F/F$ values (Figure 3-1C,D). However, rates of endocytosis remain unchanged over the range of Ca^{2+} concentration and stimulus duration tested (Figure 3-1E,F, $p > 0.2$). Thus, the decrease in endocytic rate in syt^{null} animals is not a simple consequence of impaired exocytosis. Together, these kinetic results demonstrate that synapses lacking Syt I are capable of endocytosis, but that the rate of endocytosis is significantly slower than wild type. These data are in agreement with kinetic measurements recently made at vertebrate central synapses, which demonstrate an approximately two-fold slower rate of endocytosis at synapses in syt^{null} neuronal cultures (Nicholson-Tomishima and Ryan, 2004).

In order to describe how Syt I controls membrane internalization during endocytosis, we examined vesicle reformation ultrastructurally in syt^{null} synapses. Prior ultrastructural studies of synapses lacking Syt I only described resting-state synapses (Geppert et al., 1994; Jorgensen et al., 1995; Reist et al., 1998). However, EM studies which have successfully probed the time-course and form of membrane retrieval have examined synaptic terminals following an experimental stimulus (Ceccarelli et al., 1973; Di Paolo et al., 2004; Gad et al., 1998; Heuser and Reese, 1973; Koenig and Ikeda, 1989; Koenig and Ikeda, 1996; Llinas et al., 2004). In the current experiments, we compare control and syt^{null} synapses in two conditions: at rest and following stimulation with the same protocol used in our n-Syb-pH kinetic analysis.

We fixed the NMJ prior to and one minute after the cessation of a 50 Hz, 10 s stimulus. At the latter time-point, the majority of n-Syb-pH has been quenched in wild type animals, indicating that the vesicles released during the stimulus should be newly re-formed (Figure 3-1A). We reasoned that defects in membrane recycling in the mutants might be clearly revealed at this time-point. Control synapses expressing n-Syb-pH in a wild type background looked similar at rest and after stimulation (Figure 3-2A,B). We find no evidence of vesicular intermediates at the plasma membrane or elsewhere in the synaptic bouton. We observe a small, but statistically significant, decrease in vesicle diameter in the post-stimulation condition (mean = 26.3 nm ± 0.44) compared to at rest (30.1 ± 0.44 nm, $p < 0.01$, Figure 3-2C). This decrease in vesicle size is observed throughout the vesicle distribution (Figure 3-2C). One explanation for this curious result is that our physiological saline is not identical to the larval haemolymph. Therefore, our post-stimulus condition differs from the resting condition in that a large number of

vesicles recycle in physiological saline, as opposed to the natural larval haemolymph. Subtle differences in osmolarity or tonicity between the saline and haemolymph might affect vesicle size. As such, this small decrease in vesicle diameter compared to rest should affect all of our post-stimulus experiments identically and we find evidence that this is the case (see below). Importantly, this effect will cause an underestimation of the experimentally observed increases in vesicles size that we report below. In conclusion, wild type synapses efficiently endocytose the vesicles released in a 50 Hz, 10 s stimulus within one minute. These data correlate well with n-Syb-pH decay kinetics following the same stimulus protocol.

It has previously been observed that, at the Drosophila NMJ, synapses that lack Syt I contain vesicles with a modest increase in diameter (Reist et al., 1998). We have confirmed this phenotype at syt^{null} synapses expressing n-Syb-pH at rest (mean = 38.4 ± 1.23 nm compared to 30.1 ± 0.44 nm at rest in wild type, $p < 0.01$; Figure 3-2C,F). However, when we examine syt^{null} synapses after stimulation, we observe a dramatic further increase in average vesicle diameter (46.6 ± 1.56 nm, Figure 3-2D–F, $p < 0.005$). Inspection of individual active zones demonstrates that vesicular structures with diameters greater than 100 nm can be observed throughout the vesicle cluster, both at the active zone and at the peri-active zone region (Figure 3-2E). In some instances, we observe structures that are clearly still continuous with the peri-active zone plasma membrane, suggesting that these aberrantly large vesicles represent newly internalized membrane (Figure 3-2E, arrow). These data also indicate that the retrieval of abnormally large vesicles from the plasma membrane at syt^{null} synapses is ongoing at a time when most endocytosis has been completed in the controls. These large vesicles are

reminiscent of large cisternae documented in prior ultrastructural studies of vesicle reformation following stimulation (Heuser and Reese, 1973; Koenig and Ikeda, 1989).

It remains a formal possibility that the large vesicles formed in these experiments are a consequence of abnormal vesicle fusion, either the fusion of vesicles with each other or aberrant fusion events at the plasma membrane that cannot be properly recovered. To rule out these possibilities, we stimulated vesicle fusion in the presence of a functional Syt I protein and then photo-inactivated Syt I prior to vesicle endocytosis, testing for defects by fixing for EM during the endocytic phase of the vesicle cycle. To photo-inactivate Syt I, we utilize a tetracysteine-tagged Syt I that binds the membrane permeable fluorescein derivative, FlAsH (Gaietta et al., 2002; Marek and Davis, 2002; Tour et al., 2003). Pre-synaptic FlAsH-bound Syt I rescues the *syt*^{null} mutation, and can be photo-inactivated (FALI) in seconds in a background with no endogenous Syt I expression (Marek and Davis, 2002). The experiments reported here require the use of the temperature-sensitive mutation in dynamin, *shibire*^{ts2} (*shi*^{ts}). In brief, vesicle fusion is stimulated while the synapse is held at the restrictive temperature for *shi*^{ts} (30°C), which strongly inhibits endocytosis (Koenig et al., 1983). While vesicular membrane and proteins are trapped at the plasma membrane, Syt I is photo-inactivated for two minutes (this represents the time necessary to bleach FlAsH to extinction to ensure complete photoinactivation [Poskanzer et al., 2003]). The synapse is then returned to the permissive temperature (22°C) for five minutes before being fixed and processed for EM. At control synapses, endocytosis, as measured by n-Syb-pH fluorescence decay, proceeds to near completion within five minutes (Poskanzer et al., 2003). In contrast,

synapses that have undergone Syt I photoinactivation show impaired n-Syb-pH decay, suggesting that endocytosis is severely perturbed (Poskanzer et al., 2003).

In experiments where we photo-inactivate Syt I specifically during endocytosis, control EM's underwent identical temperature changes, incubation in FlAsH ligand, and stimulation, but did not experience the illumination that causes FlAsH photoinactivation of Syt I. Control synapses (Figure 3-2G) appear similar to wild type in every respect and there is no change in the average vesicle diameter (31.1 ± 0.93 nm, compared to 30.1 ± 0.44 nm for wild type, $p > 0.3$, Figure 3-2J). In contrast, vesicles in synapses at which Syt I was specifically photo-inactivated in the endocytic phase of the vesicle cycle are significantly larger than controls (46.2 ± 1.28 nm, $p < 0.001$), with an average diameter and frequency distribution nearly identical to that observed at the stimulated *syt*^{null} synapses (Figure 3-2H–J). As with the *syt*^{null} synapses, dramatically enlarged vesicular structures that often exceed 100 nm are observed throughout the pool of synaptic vesicles.

When we compare the EM results from *syt*^{null} and Syt I photo-inactivated synapses to the n-Syb-pH kinetic data following identical stimulation conditions, several conclusions can be made. First, our data argue against the possibility that altered rates of n-Syb-pH internalization are simply caused by impaired vesicle re-acidification, since there are clearly additional problems with the endocytic process in both of these experimental paradigms. Second, the slower endocytosis kinetics correlate with a prolonged period of membrane internalization, since membrane invaginations connected to the plasma membrane can still be observed one minute after the cessation of stimulation at *syt*^{null} synapses. Thus, Syt I mutations slow the rate of membrane

internalization. Finally, Syt I is required to specify the size of newly formed vesicles. A remaining question is whether the loss of Syt I generally cripples the process of endocytosis, or whether Syt I has specific, separable functions that can determine both the rate and the size of synaptic vesicles. To distinguish between these possibilities, we undertook a structure-function analysis of Syt I during endocytosis.

The C_2B domain is necessary for vesicle endocytosis

Syt I contains one transmembrane domain and two Ca^{2+}-binding C_2 domains, termed C_2A and C_2B (Perin et al., 1991). The C_2A domain is thought to mediate Ca^{2+}-induced phospholipid and syntaxin binding (Fernandez et al., 2001; Kee and Scheller, 1996; Ubach et al., 1998). The C_2B domain has been shown to be important for Ca^{2+}-dependent Syt I oligomerization (Chapman et al., 1996; Sugita et al., 1996), as well as phospholipid (Fernandez et al., 2001; Schiavo et al., 1996), Ca^{2+}-channel (Sheng et al., 1997), and clathrin adaptor complex AP-2 (Chapman et al., 1998; Haucke and De Camilli, 1999; Zhang et al., 1994) binding. We began by looking at n-Syb-pH dynamics in animals with the syt^{AD1} mutation, an early stop codon that leads to deletion of the entire C_2B domain (DiAntonio and Schwarz, 1994; Littleton et al., 2001). As homozygotes, or *in trans* to a null mutation, syt^{AD1} animals are not viable at the third instar larval stage (Littleton et al., 1994; Yoshihara and Littleton, 2002). However, it has previously been shown that the syt^{AD1} allele, in combination with the strong hypomorphic syt^{T7} allele, causes a decrease in evoked neurotransmitter release (Littleton et al., 1994). Therefore, we examined the $syt^{AD1/T7}$ combination in the n-Syb-pH

background and tracked n-Syb-pH fluorescence intensity in response to a 50 Hz, 10 s stimulus.

We find that syt^{4D1}/+ control synapses show the same fluorescence decay rate after the stimulus (τ = 10.0 ± 1.2 s) as wild type (τ = 10.3 ± 1.0 s) (Figure 3-3A, B). In contrast, the $syt^{4D1/T7}$ synapses exhibit two main differences compared to the controls: a smaller peak $\Delta F/F$ value and a slower rate of endocytosis (τ = 29.8 ± 9.7s; $p < 0.04$) (Figure 3-3A,B). By these measures, the $syt^{4D1/T7}$ synapses are similar to syt^{null} synapses, indicating that the C_2B domain is important for synaptic vesicle endocytosis, as well as exocytosis. Although we were unable to evaluate homozygous syt^{4D1} mutants, this conclusion is further supported by analysis of point mutations that disrupt specific sequences within the C_2B domain (see below).

Residues implicated in Syt I oligomerization alter exocytosis, but do not affect the rate of endocytosis

The syt^{4D3} allele contains a Y to N substitution at residue 364, which lies in the C_2B domain and is highly conserved from *C.elegans* to humans (DiAntonio and Schwarz, 1994; Littleton et al., 2001). This mutation is thought to disrupt conformational changes in the C_2B domain of Syt I that are important for homo-oligomerization (Fukuda et al., 2000; Littleton et al., 2001). Prior data indicate that the syt^{4D3} mutation causes a reduction in evoked release and, as with syt^{4D1}, this mutation acts dominantly when placed in *trans* to the hypomorphic alleles syt^{T7} or syt^{T41} (Littleton et al., 2001). Consistent with this data, we find a decrease in peak n-Syb-pH fluorescence during the stimulus train in both the $syt^{4D3/T7}$ and $syt^{4D3/T41}$ mutant combinations compared to controls when

expressed in the n-Syb-pH background (Figure 3-3C,D). When we quantify endocytic rates, we find that heterozygous $syt^{AD3}/+$ synapses have a rate of endocytosis (τ = 10.3 ± 0.7 s) that is not statistically different from wild type controls performed in parallel (τ = 12.9 ± 1.2 s; $p > 0.08$; data not shown on graph for clarity). When we compare endocytic rates in $syt^{AD3/T7}$ and $syt^{AD3/T41}$ to wild type and heterozygous controls, we find that the mutant synapses are not significantly different compared to wild type (τ = 14.2 ± 2.0 s and 15.7 ± 1.7 s for $syt^{AD3/T7}$ and $syt^{AD3/T41}$, $p > 0.1$). There is a slight, statistically significant difference when these mutants are compared to the heterozygous $syt^{AD3}/+$ synapses ($p < 0.04$). However, since $syt^{AD3}/+$ is not different than wild type and since the magnitude of the difference in endocytic rates comparing $syt^{AD3}/+$ with $syt^{AD3/T7}$ or $syt^{AD3/T41}$ is small, we conclude that the residues implicated in Syt I oligomerization do not play a significant role in synaptic vesicle endocytosis and cannot account for the slowed rated of endocytosis observed in the syt^{null} animals.

The poly-lysine motif in the C_2B domain controls vesicle size but does not affect endocytic rate

We next tested the function of a conserved poly-lysine motif located within the Syt I C_2B domain. These residues have been shown to interact biochemically with the α-adaptin and μ2 regions of the heterotetrameric protein complex AP-2, raising the possibility that endocytic clathrin machinery is recruited to sites where Syt I is inserted in the plasma membrane via these residues (Haucke and De Camilli, 1999; Haucke et al., 2000; Zhang et al., 1994). These residues have also been implicated in biochemical

interactions with inositol polyphosphates (Fukuda et al., 1995a). It remains unknown whether these residues are necessary for compensatory synaptic vesicle endocytosis *in vivo*. To test this possibility, we rescue the *syt^{null}* mutation with a Syt I transgene in which three lysines (K379,380,384) important for AP-2 binding and interaction with acidic phospholipids have been mutated to glutamines (Chapman et al., 1998; Mackler and Reist, 2001). We use a neural-specific GAL4 driver, *elaV^{3E1}-GAL4*, to drive both the *UAS-syt-KQ* and *UAS-n-Syb-pH* transgenes pre-synaptically in a *syt^{null}* (*syt$^{AD4/N13}$*) mutant background. As a control, we rescue the *syt^{null}* animal with a wild type version of Syt I (*UAS-syt-wt*) expressed pre-synaptically with the same *GAL4* driver.

We first perform immunostaining to confirm that both of these genotypes express and correctly localize Syt I. We observe similar levels and localization of Syt I protein at *UAS-syt-wt* and *UAS-syt-KQ* synapses, both of which show slightly less Syt I compared to wild type (Figure 3-4A,C–D). Because the Syt-KQ protein could compromised AP-2 binding, we also controlled for AP-2 levels at these synapses. Immunostaining for the α-adaptin subunit of AP-2 reveals similar levels and localization in all genotypes tested, including *UAS-syt-KQ* (Figure 3-4G–L). Synaptic boutons are consistently smaller in all transgenic genotypes but this does not correlate with the stimulus-dependent differences among genotypes observed for endocytic rate or vesicle size. Finally, we recorded electrophysiologically from both *UAS-syt-wt* and *UAS-syt-KQ* rescue synapses that also express n-Syb-pH. We observe mEPSP and EPSP amplitudes (Table 3-1) that are similar to those previously published for these genotypes in the absence of n-Syb-pH expression (Mackler and Reist, 2001).

In all of the following experiments, we compare the experimental rescue animals with the *UAS-syt-wt* rescue animal to control for genetic background and Syt I expression levels. In response to a 50 Hz, 10 s stimulus, we observe no difference in n-Syb-pH endocytic rate in the *UAS-syt-wt* (τ = 15.9 ± 3.7s) rescue animals when we compare them to wild type ($p > 0.1$, data not shown). At the *UAS-syt-KQ* rescue synapse, we observe a very slight increase in peak $\Delta F/F$ compared to the *UAS-syt-wt* synapse (Figure 3-5A). However, when we compare endocytic rates, we find that the rate of endocytosis in the *UAS-syt-KQ* animals (τ = 19.6 ± 2.2 s) is no different than in the *UAS-syt-wt* animals ($p > 0.4$, Figure 3-5B). This rate is significantly different than wild type ($p < 0.005$), but the appropriate comparison is with the *UAS-syt-wt* rescue animals, which establish the normal baseline for wild type *syt* transgene expression in the syt^{null} mutant background. Similar results are obtained when we express these transgenes in the other syt^{null} background ($syt^{AD4/D27}$, data not shown). To further test whether the poly-lysine residues mutated in the *UAS-syt-KQ* transgene affect endocytosis rate, we quantified endocytic rate in the *UAS-syt-KQ* rescue animals over a range of stimulus durations. At all of the stimuli tested (from 1–10 s), the *UAS-syt-KQ* rescue synapses exhibit peak $\Delta F/F$ values and endocytosis rates similar to *UAS-syt-wt* rescue animals (Figure 3-5C,D). These data indicate that the Syt I interactions via this poly-lysine motif are not required for the rate of synaptic vesicle endocytosis.

We next examined membrane internalization, ultrastructurally, at the *UAS-syt-KQ* rescue synapse and compared these data to *UAS-syt-wt* rescue synapses as controls. As a baseline, we find that the control *UAS-syt-wt* rescue synapses show a statistically significant increase in mean vesicle diameter (38.4 ± 0.83 nm) at rest compared to wild

type animals ($p < 0.001$, Figure 3-6C; compare with Figure 3-2C). However, when these control synapses are stimulated, there is a small decrease in mean vesicle diameter (35.8 ± 0.94 nm, $p < 0.04$) compared to the rest condition, similar to that observed at wild type synapses. These data, and the n-Syb-pH quenching data described above, indicate that the rescue of the *syt^{null}* by *UAS-syt-wt* is adequate but not complete, and emphasize the importance of using this genotype to compare with other experimental transgenic rescue animals.

The *UAS-syt-KQ* rescue synapse at rest has an mean vesicle diameter (38.7 ± 0.77 nm, Figure 3-6D) equivalent to that observed in the *UAS-syt-wt* controls at rest ($p > 0.7$). However, following stimulation, the *UAS-syt-KQ* rescue synapse shows a significant further increase in mean vesicle diameter (43.8 ± 0.90 nm, $p < 0.005$, Figure 3-6D) not seen in the *UAS-syt-wt* controls, but similar to that observed in the *syt^{null}* synapses following stimulation. Vesicles with diameters in excess of 80 nm can be observed throughout the vesicle pool. Importantly, the increase in vesicle diameter is observed throughout the distribution of vesicle sizes and, therefore, the increase in mean diameter cannot be attributed to a small number of very large vesicles (Figure 3-6D). Thus, the poly-lysine motif in the C_2B domain of Syt I is one of the important determinants that controls the formation of normally sized synaptic vesicles. Since endocytosis proceeds at a rate that is equivalent to transgenic controls, these data dissociate, for the first time, the molecular mechanisms that control endocytic rate from those that govern synaptic vesicle size.

Ca^{2+}-coordinating residue in the C_2A domain does not affect endocytosis

Syt I is capable of binding five Ca^{2+} molecules, three in the C_2A domain (Ubach et al., 1998) and two in the C_2B domain (Fernandez et al., 2001). At vertebrate central synapses, Ca^{2+}-coordinating residues in both the C_2A and C_2B domains are necessary for normal neurotransmitter release (Fernandez-Chacon et al., 2001; Stevens and Sullivan, 2003). In *Drosophila,* mutation of the highly conserved Ca^{2+}-binding residues in the C_2B domain, but not the C_2A domain, impair neurotransmitter release (Mackler et al., 2002; Robinson et al., 2002). To test the function of the Ca^{2+}-coordinating residues in vesicle endocytosis, we expressed n-Syb-pH in flies harboring mutations that selectively disrupt the Ca^{2+}-coordinating aspartate residues in the C_2A or the C_2B domain.

We first examine flies that express a form of Syt I with the second Ca^{2+}-binding aspartate residue in the C_2A domain mutated to asparagine. It has been demonstrated that this transgene can inhibit Ca^{2+}-binding, but does not affect neurotransmitter release in a syt^{null} background (Robinson et al., 2002). We again perform the same n-Syb-pH and EM experiments in flies expressing *UAS-syt-D229N* in a syt^{null}, *UAS-n-Syb-pH* background. The only Syt I protein in this rescue animal (*UAS-syt-D229N*) is that with the disrupted C_2A Ca^{2+}-binding site and this protein localizes normally (Figure 3-4F). In our endocytic assays, the *UAS-syt-D229N* animals show no significant difference from *UAS-syt-wt* controls in endocytic rate ($p > 0.3$). There is also no change in mean vesicle diameter comparing rest (35.9 ± 0.33 nm) and post-stimulation conditions (36.7 ± 0.73) (Figure 3-7A–C; $p > 0.3$). Although the distributions are not identical (the KS statistic reveals a significant difference), we do not observe a shift in the entire vesicle distribution toward larger vesicle diameters as we observe in the syt^{null} and *UAS-syt-KQ*

animals. These data demonstrate that this Ca^{2+}-coordinating residue in the C_2A domain is not necessary for the rate or form of vesicle endocytosis.

Ca^{2+}-coordinating aspartate residues in the C_2B domain control endocytic rate

We next examine flies that express a form of Syt I with the third and fourth Ca^{2+}-binding aspartate residues in the C_2B domain mutated to asparagines. These flies, *UAS-syt-D3,4N*, were previously shown to exhibit greatly reduced evoked neurotransmitter release in response to a single action potential, and show a large reduction in Ca^{2+}-dependent phospholipid binding (Mackler et al., 2002). We observe that expression of the *UAS-syt-D3,4N* transgene in the *syt^{null};n-Syb-pH* background shows a similar electrophysiological phenotype to that observed in the absence of n-Syb-pH expression, with dramatically decreased EPSP amplitudes (Table 3-1).

In our experiments, we express the *UAS-syt-D3,4N* transgene pre-synaptically in a *syt^{null}*; *UAS-n-Syb-pH* background, so that *UAS-syt-D3,4N* is the only form of Syt I in the terminal. Importantly, this mutant form of Syt I localizes normally (Figure 3-4E). Following a 50 Hz, 10 s stimulus, the peak n-Syb-pH fluorescence change in these animals is reduced compared to the *UAS-syt-wt* animals (Figure 3-8A), which agrees with prior electrophysiological demonstration of a decrease in evoked release (Mackler et al., 2002). We also observe a striking slowing in endocytosis rate at *UAS-syt-D3,4N* rescue synapses, with an average endocytic rate (τ = 33.4 ± 8.3 s) that is more than two-fold slower than that observed in the *UAS-syt-wt* control (15.9 ± 3.7 s, Figure 3-8B; $p < 0.04$). This slowed endocytic rate in the *UAS-syt-D3,4N* rescue animals is comparable to that

bserved in *syt*^{null} animals, indicating that the Ca^{2+}-coordinating function of C_2B domain f Syt I can account for the extent of the defect in n-Syb-pH recycling in the *syt*^{null} imals.

Mutations in Syt I Ca^{2+}-coordinating residues may also disrupt synchronized eurotransmitter release. Therefore, it is possible that large amounts of asynchronous lease after the stimulus train could lead to an apparent decrease in the rate of ndocytosis, as measured by n-Syb-pH internalization. To address this possibility, we corded electrophysiologically from the *UAS-syt-D3,4N* synapses and assayed ynchronous release following a 50 Hz, 10 s stimulus train. As previously emonstrated, EPSP amplitudes in response to single stimuli are dramatically reduced ompared to genetic controls [(Mackler et al., 2002), Table 3-1]. However, during a 50 z, 10 s stimulus train, transmitter release facilitates dramatically and then decays to aseline following the end of the stimulus train (Figure 3-8F). The large increase in lease during the stimulus train likely includes a large component of asynchronous lease, given the small size of individual EPSPs that are observed throughout the imulus train (Figure 3-8F). Most important for our n-Syb-pH analysis, however, is that ere is no evidence that asynchronous release persists for prolonged periods after the nd of the stimulus train. EPSP amplitudes decay to baseline in less than 500 ms in both e *UAS-syt-wt* and *UAS-syt-D3,4N* synapses (n = 7 synapses). In comparison, our easurements of n-Syb-pH decay have a time constant that is more than an order of agnitude slower. Thus, we can rule out the possibility that persistent asynchronous lease following the stimulus train causes the slowed rate of n-Syb-pH decay at the *AS-syt-D3,4N* rescue synapses.

We next addressed whether the *UAS-syt-D3,4N* mutation also affects the size of newly re-formed synaptic vesicles, as seen at the syt^{null} synapse. When we compare synapses at rest from *UAS-syt-wt* and *UAS-syt-D3,4N* rescue animals, we observe no difference in average vesicle diameter ($p > 0.5$, Figure 3-5C,8C–E). There is also no difference in mean vesicle diameter between these genotypes in the stimulated condition ($p > 0.8$, Figure 3-5C,8C–E), or when we compare the *UAS-syt-D3,4N* synapses at rest (37.7 ± 0.88 nm) and after stimulation (36.0 ± 0.48 nm, $p > 0.8$, Figure 3-8C–E). Although the distributions are not identical (a statistical difference is revealed using the KS statistic), there is no evidence for the emergence of large diameter vesicles that exceed those observed in wild type.

Two lines of evidence suggest that the lack of change in vesicle diameter is not caused by a severe decrease in vesicle fusion. First, our electrophysiological recordings demonstrate that there is substantial neurotransmitter release in the *UAS-syt-D3,4N* animals during the 50 Hz, 10 s stimulus train (Figure 3-8F). Second, there is a quantitatively greater increase in peak fluorescence intensity ($\Delta F/F$) during the stimulus train in the *UAS-syt-D3,4N* synapses compared to the syt^{null} synapses (Figure 1A and Figure 8A). Thus, there is as much or greater vesicle fusion at *UAS-syt-D3,4N* than at syt^{null} synapses, and yet the change in vesicle size is only observed at the syt^{null} synapses. These data indicate that vesicle reformation post-stimulus occurs normally at the *UAS-syt-D3,4N* rescue synapses, but at a slower rate, and that this slowed rate does not cause misregulation of membrane internalization.

These data suggest that Ca^{2+} coordination by the Syt I C_2B domain confers Ca^{2+}-dependence to the rate of endocytosis. To further test this possibility, we asked whether

e rate of endocytosis can be restored by assaying synaptic vesicle recycling in *UAS-syt-3,4N* animals at elevated (5 mM) Ca^{2+}. At 5 mM extracellular Ca^{2+} we find that there is statically significant speeding of the rate of vesicle endocytosis at the *UAS-syt-D3,4N* scue synapse (15.6 ± 2.0 s) compared to the rate observed at 2 mM Ca^{2+} (33.4 ± 8.3 s, <0.05, Figure 3-9A). This rate approaches, but remains slower than, the rate observed *UAS-syt-wt* controls analyzed at the same Ca^{2+} concentration (10.2 ± 0.93 s, $p < 0.02$, gure 3-9A). At 5mM Ca^{2+}, we observe increased vesicle exocytosis as assessed by both ak n-Syb-pH ΔF/F and electrophysiological analysis of 50 Hz, 10 s nerve stimulation igure 3-9D and data not shown). Importantly, the change in endocytic rate cannot be ributed to a change in synchronous release because the defect in synchronous release, sessed by EPSP amplitude in response to a single action potential, is not improved by cording at 5mM Ca^{2+} (Figure 3-9C). These data demonstrate a selective improvement the rate of endocytosis at 5 mM Ca^{2+} in the *UAS-syt-D3,4N* animals. One possibility that this effect is mediated by an unidentified Ca^{2+} sensor involved in endocytosis. If , we would predict that the rate of endocytosis would speed in the syt^{null} animals. owever, there is no significant change in the rate of endocytosis in the syt^{null} animals nen Ca^{2+} levels are increased to 5mM (29.8 ± 6.6 s at 2 mM and 25.1 ± 4.6 s at 5 mM, p 0.4, Figure 3-9B). Thus, the speeding of endocytosis in the *UAS-syt-D3,4N* animals pends on the presence of the mutant Syt I protein. The increased rate of endocytosis high Ca^{2+} could either be mediated by residual Ca^{2+} binding in the mutant C_2B domain by Ca^{2+} binding in the C_2A domain. Since we demonstrate that mutations in the C_2A main do not alter endocytosis, we favor the idea that residual Ca^{2+} binding in the C_2B main mediates this effect.

Discussion

In this study we examine the rate and form of synaptic vesicle endocytosis under identical stimulation conditions. Using this approach, we demonstrate that discrete residues in the C_2B domain of Syt I independently specify the rate of synaptic vesicle endocytosis and the size of newly internalized vesicles. We demonstrate that the rate of endocytosis can proceed normally while vesicles of inappropriate size are generated. Conversely, we show that the rate of endocytosis can be slowed without perturbing the mechanisms that control vesicle size. Thus, the mechanisms that govern the rate and size of synaptic vesicle reformation can be broken down into independent processes that are normally coordinated by Syt I.

Two important comparisons should be made with our prior work in which we demonstrated a function for Syt I during vesicle endocytosis (Poskanzer et al., 2003). In our previous n-Syb-pH experiments examining syt^{null} animals, muscle contraction occluded a portion of our data during and shortly after nerve stimulation that prevented an accurate calculation of endocytic rate. By including a postsynaptic receptor antagonist in our saline, we now prevent muscle contraction, which allows uninterrupted visualization of fluorescence change over time (see Experimental Procedures). Our current data now agree with a report examining vesicle recycling at syt^{null} central neurons in which endocytosis is significantly slowed but not blocked (Nicholson-Tomishima and Ryan, 2004). We also previously reported that FlAsH photoinactivation of Syt I prevented subsequent quenching of n-Syb-pH following the release of a temperature-sensitive blockade of endocytosis (Poskanzer et al., 2003). Our data now demonstrate

that, in this protocol, membrane *is* internalized in the form of unusually large vesicles. Why was there no evidence of quenched n-Syb-pH signal in our previous study? We previously showed by FM4-64 staining that membrane internalization was impaired, following FlAsH photoinactivation, and that a significant fraction of the n-Syb-pH remains at the cell surface. If reacidification is also impaired within the large vesicle structures, then the combined effect of these three deficits may prevent significant n-Syb-pH quenching during this protocol.

Syt I-dependent mechanisms controlling synaptic vesicle size

Mutation of a poly-lysine motif in the C_2B domain of Syt I, previously shown to be important for Syt I-AP-2 binding (Chapman et al., 1998; Zhang et al., 1994), causes a defect in synaptic vesicle size. The defect in vesicle size observed in these animals is less severe than that observed in the *syt*^{null} animal, indicating that these residues contribute to this role of Syt I, but may not be the only residues important for this process. It is remarkable, however, that the mutation of the C_2B poly-lysine motif causes a selective defect in synaptic vesicle size without altering the rate of endocytosis. The specificity of this endocytic defect is surprising, considering that altered rate and altered membrane retrieval generally go hand in hand in genetic studies of synaptic vesicle recycling *in vivo*.

How can the specific defect in the size of recovered synaptic vesicles be explained? Previous studies have described endosomal cisternae that may represent normal intermediates in a vesicle recovery pathway, similar to those observed in non-neuronal cells (Gad et al., 1998; Heuser and Reese, 1973; Koenig and Ikeda, 1989; Stoorvogel et al., 1996; Whitney et al., 1995). One possibility, based on our data, is that

perturbing the Syt I-AP-2 interaction slows the progression through an acidified endosomal intermediate stage (perhaps before a clathrin-dependent budding step) that is normally rapidly resolved. Syt I-inositol polyphosphate interactions mediated by these residues could also be important for this process (Fukuda et al., 1995a). However, we do not observe budding events from the large vesicular structures in our micrographs, whereas budding from larger endosomal/cisternal membranous structures has been described at other synapses following stimulation (Gad et al., 1998; Heuser and Reese, 1973; Koenig and Ikeda, 1989). An alternate possibility is that Syt I controls the size of synaptic vesicle membrane retrieval at the plasma membrane. Syt I could demarcate the boundaries of new vesicles, and thereby control the amount, but not the speed, of membrane internalization. Finally, another alternative is that Syt I could control the integrity of the clathrin lattice, which could help to confine the proper extent and curvature of newly internalized membrane.

Ca^{2+}-coordinating residues control endocytic rate

We have shown that the mutation of Ca^{2+}-coordinating residues in the C_2B domain of Syt I slows the rate of endocytosis, without obviously altering any other aspect of endocytosis. It should be emphasized that when Ca^{2+}-coordinating residues in the C_2B domain are mutated, the rate of endocytosis slows to the same extent as that observed in *syt*^{null} mutations, demonstrating that these residues are sufficient to account for the function of Syt I in specifying endocytic rate. These data are in contrast to most other genetic studies of endocytosis molecules where a slower endocytic rate is accompanied by other effects, such as altered membrane internalization or vesicle size

(Di Paolo et al., 2004; Guichet et al., 2002; Koh et al., 2004; Marie et al., 2004; Verstreken et al., 2002; Zhang et al., 1998). Therefore, our data suggest that Ca^{2+}-coordinating residues in the C_2B domain of Syt I are involved in a step of the endocytic process directly related to the endocytic rate.

We provide several lines of evidence that Ca^{2+} binding in the C_2B domain may indeed establish the Ca^{2+}-dependence of endocytic rate. In vertebrate neurons, endocytic rate speeds with increasing extracellular Ca^{2+} concentration (Sankaranarayanan and Ryan, 2001). At the Drosophila NMJ, we find that endocytic rate remains unchanged over a wide range of extracellular Ca^{2+} concentrations, though it does speed somewhat at very high extracellular Ca^{2+} (compare Figure 3-1E and 3-9B). These data do not mean that endocytic rate is insensitive to Ca^{2+} at the Drosophila NMJ. Indeed, we demonstrate that the slowed endocytic rate in the *UAS-syt-D3,4N* animals can be significantly improved by raising extracellular Ca^{2+}. Importantly, no change in endocytic rate is observed in the syt^{null} animals, demonstrating that this is a Syt I-dependent effect, likely mediated by the binding of Ca^{2+} to either the C_2A or C_2B domains of Syt I. Since raising extracellular Ca^{2+} does not increase synchronous release, we argue that this effect is specific to the mechanisms of endocytosis. Because the C_2A domain does not appear to play a significant role in the rate of endocytosis (Figure 7), we favor the conclusion that Ca^{2+}-coordination in the C_2B domain of Syt I establishes a Ca^{2+}-dependent component of endocytic rate.

There are several possibilities for how Syt I could participate in the control of endocytic rate. First, it is possible that these Ca^{2+}-coordinating residues are involved in an interaction controlling the uncoating of synaptic vesicles prior to vesicle re-

acidification. Disrupting this process would slow the rate of n-Syb-pH decay, even though vesicles would be endocytosed correctly. We do not see an obvious accumulation of clathrin-coated vesicles in our EM images, although it is difficult to resolve clathrin coats on vesicles at this synapse. Another possible explanation is that the Ca^{2+}-coordinating residues are involved in the sorting of synaptic vesicle proteins to newly internalized vesicles. In this case, some n-Syb-pH molecules may be deposited in the plasma membrane during stimulation, but not reinternalized. If this were true, we might expect that n-Syb-pH molecules would accumulate on the plasma membrane over time. We see no evidence that baseline n-Syb-pH fluorescence levels are higher in the *UAS-D3,4N* rescue animals than controls, suggesting that this possibility is unlikely (data not shown). A third possibility is that Ca^{2+}-coordinating residues within the C_2B domain are specifically involved in a rate-limiting process that normally governs how fast vesicles are retrieved from the synaptic plasma membrane. If the initiation of endocytosis were delayed or became variable in these animals, the n-Syb-pH decay rate would appear slower because our n-Syb-pH measurements reflect the state of an entire a population of vesicles. Support for the idea that the initiation of endocytosis is delayed comes from the observation that endocytic intermediates attached to the plasma membrane are not found at the *UAS-D3,4N* rescue synapses. This hypothesis is attractive because it has long been hypothesized that Syt I functions to couple exo- and endocytosis at the neuronal synapse.

If Syt I does indeed function at such an early stage in the endocytic process, two models may explain its role. In one model, Syt I could establish new protein interactions—or take on a new conformation—following vesicle fusion that are required

to initiate endocytosis. In a second model, Syt I could assume a conformation or a participate in a binding interaction during exocytosis that is required for subsequent vesicle endocytosis. In other words, Syt I would be primed to initiate rapid endocytosis via molecular interactions established during exocytosis. This function of Syt I would be specifically disrupted by mutation of the Ca^{2+}-coordinating residues in the C_2B domain. Therefore, candidate molecular interactions include Ca^{2+}-channel binding, phospholipid binding, and Syt I homo-oligomerization (Chapman et al., 1996; Fernandez et al., 2001; Sheng et al., 1997; Sugita et al., 1996). Since we demonstrate that mutating residues implicated in Syt I oligomerization does not alter endocytic rate even though exocytosis is perturbed, our data argue against oligomerization of Syt I as being the essential interaction for control of endocytic rate. On the other hand, the importance of phospholipid regulation during endocytosis has been suggested by recent work showing altered endocytic rate in a $PI(4,5)P_2$ kinase null mutation, making this option an attractive possibility (Di Paolo et al., 2004).

Conclusion

Syt I has been proposed to couple exo- and endocytosis because it is required for both processes. Here, we have identified mutations in Syt I that uncouple exo- and endocytosis, for example, perturbing exocytosis but not endocytosis in the *syt*^{4D3} mutations. We have also identified mutations in Syt I that separate two properties of compensatory synaptic vesicle endocytosis that are normally coordinated: the rate of endocytosis and the size of internalized membrane. Thus, different regions of Syt I may

normally couple exo- and endocytosis as well as distinct aspects of the endocytic process. These data argue that Syt I is a molecular linchpin that enables rapid, high-fidelity endocytosis at the neuronal synapse.

Figures

Figure 3-1. Synaptic vesicle endocytosis is slowed in *syt*^{null} animals.

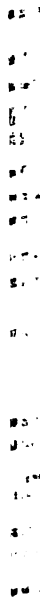

(A) n-Syb-pH response to a 50 Hz, 10 s stimulus train in 2.0 mM Ca^{2+} in wild type (black, n = 11) and two *syt*^{null} mutant backgrounds: *syt*$^{AD4/D27}$ (light blue, n = 18) and *syt*$^{AD4/N13}$ (dark blue, n = 10). The duration of the stimulus train is indicated (white horizontal bar). n-Syb-pH fluorescence intensity is normalized to the mean of the first ten time-points, before the onset of the stimulus. Less release in observed in the two *syt*^{null} mutants, as demonstrated by the smaller peak ΔF/F values compared to wild type. Error bars throughout the paper represent ± SEM. (B) Same data as shown in (a), with values normalized to the peak ΔF/F intensity, for visual comparison of endocytosis rate after the stimulus train. Both *syt*^{null} mutants show a slower rate of endocytosis than controls ($p < 0.03$, Student's t-test throughout). (C–D) Peak n-Syb-pH ΔF/F intensity at wild type synapses when varying Ca^{2+} concentration (with a 10 s stimulus duration) and stimulus duration (in 2.0 mM Ca^{2+}). Data points within a graph are collected under identical imaging conditions. (E–F) Endocytosis rates, fit to a single exponential function, at the Ca^{2+} concentrations and stimulus durations shown in (c) and (d).

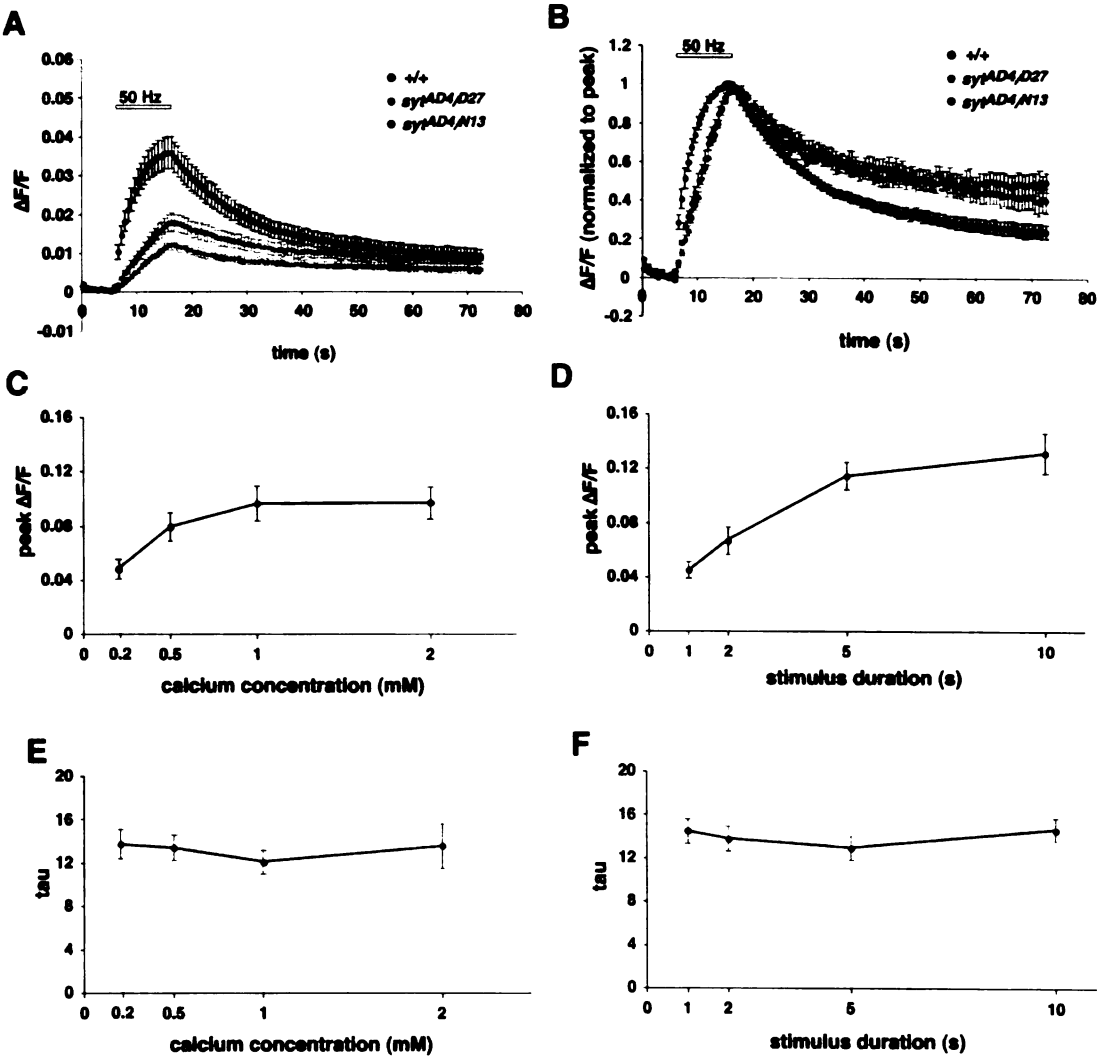
A
50 Hz
+/+
sytAD4/D27
sytAD4/N13
ΔF/F
time (s)
B
50 Hz
+/+
sytAD4/D27
sytAD4/N13
ΔF/F (normalized to peak)
time (s)
C
peak ΔF/F
calcium concentration (mM)
D
peak ΔF/F
stimulus duration (s)
E
tau
calcium concentration (mM)
F
tau
stimulus duration (s)

Table 3-1. Electrophysiological analysis of *syt* mutations.

Genotype[a]	mEPSP (mV) ± SEM	EPSP (mV) ± SEM	Train[b] (mV) ± SEM
wild type	1.08 ± 0.05	58 ± 3.2	64 ± 3.2
syt^{null};UAS-syt-wt	0.96 ± 0.08	52 ± 2.6[c]	54 ± 3.1
syt^{null}	1.10 ± 0.06	2 ± 0.6	25 ± 2.1*
syt^{null};UAS-syt-D229N	0.95 ± 0.05	55 ± 2.3	58 ± 2.8
syt^{null};UAS-syt-D3,4N	1.10 ± 0.07	2 ± 0.4	45 ± 4.0[d]
syt^{null};UAS-syt-KQ	1.10 ± 0.15	34 ± 1.8*	56 ± 3.4

[a] *syt^{null}* animals are *$syt^{AD4/D27}$*

[b] This measurement represents the average EPSP amplitude measured between 5 and 7 seconds during a 50 Hz, 10 s stimulus train.

[c] There is no difference compared to wild type (student's t-test, $p > 0.2$).

[d] There is no difference compared *syt^{null}; UAS-syt-wt* (student's t-test, $p > 0.1$).

* Significantly different from wild type and *syt^{null}; UAS-syt-wt* (student's t-test, $p < 0.01$).

Figure 3-2. Perturbation of Syt I function affects synaptic vesicle size.

(A–B) Representative EM micrographs taken from active zones at wild type synapses expressing n-Syb-pH. Synapses were either fixed immediately after dissection (wild type rest, a) or one minute after the cessation of a 50 Hz, 10 s stimulus (wild type stimulated, b). Vesicles within 200 nm of the pre-synaptic active zone (determined by the stereotypical T-bar structure and electro-dense material) were quantified. Note the consistency of vesicle diameter under both conditions. Scale bars = 200 nm for all panels. (C) Cumulative frequency distributions of vesicle diameter for wild type synapses at rest (gray, n = 215 vesicles, 12 active zones) and following the stimulus (blue, n = 257 vesicles, 8 active zones). Both the mean vesicle diameter ($p < 0.01$, Student's t-test (t-test) and these diameter distributions are statistically significantly different ($p < 0.001$, Kolmogorov-Smirnov (KS) test). (D–E) Representative active zones at syt^{null} synapses at rest (d) and after stimulation (e) demonstrate the increase in large vesicles throughout the vesicle cluster following stimulation. A large membrane internalization event still associated with the synaptic plasma membrane is indicated (arrow in e) (F) Cumulative frequency distributions of vesicle diameter for syt^{null} synapses at rest (gray, n = 218 vesicles, 12 active zones) and after the stimulus (blue, n = 375 vesicles, 20 active zones). There is a significant increase in mean vesicle diameter ($p < 0.005$, t-test) and a significant change in the vesicle distribution ($p < 0.001$, KS test). (G–H) EM images from active zones at synapses from the Syt I FlAsH photoinactivation experiment. In (g), synapses have been stimulated at the shi^{ts} restrictive temperature (30°C) and allowed to recover for five minutes at the permissive temperature (22°C) without

photoinactivation. In (h), Syt I was photo-inactivated following stimulation at the restrictive temperature before the preparation was brought back down to the permissive temperature for five minutes before fixation. Large vesicles are observed at active zones following photoinactivation of Syt I (h) (I) Cumulative frequency distribution of vesicle diameter for control synapses (gray, n = 335 vesicles, 11 active zones) and Syt I-photo-inactivated synapses (blue, n = 423 vesicles, 21 active zones) demonstrate a dramatic shift toward larger diameters ($p < 0.001$, KS test) and a significant increase in mean vesicle diameter ($p < 0.001$, t-test). The cumulative frequency distribution of post-stimulus syt^{null} synapses are re-plotted in red for comparison.

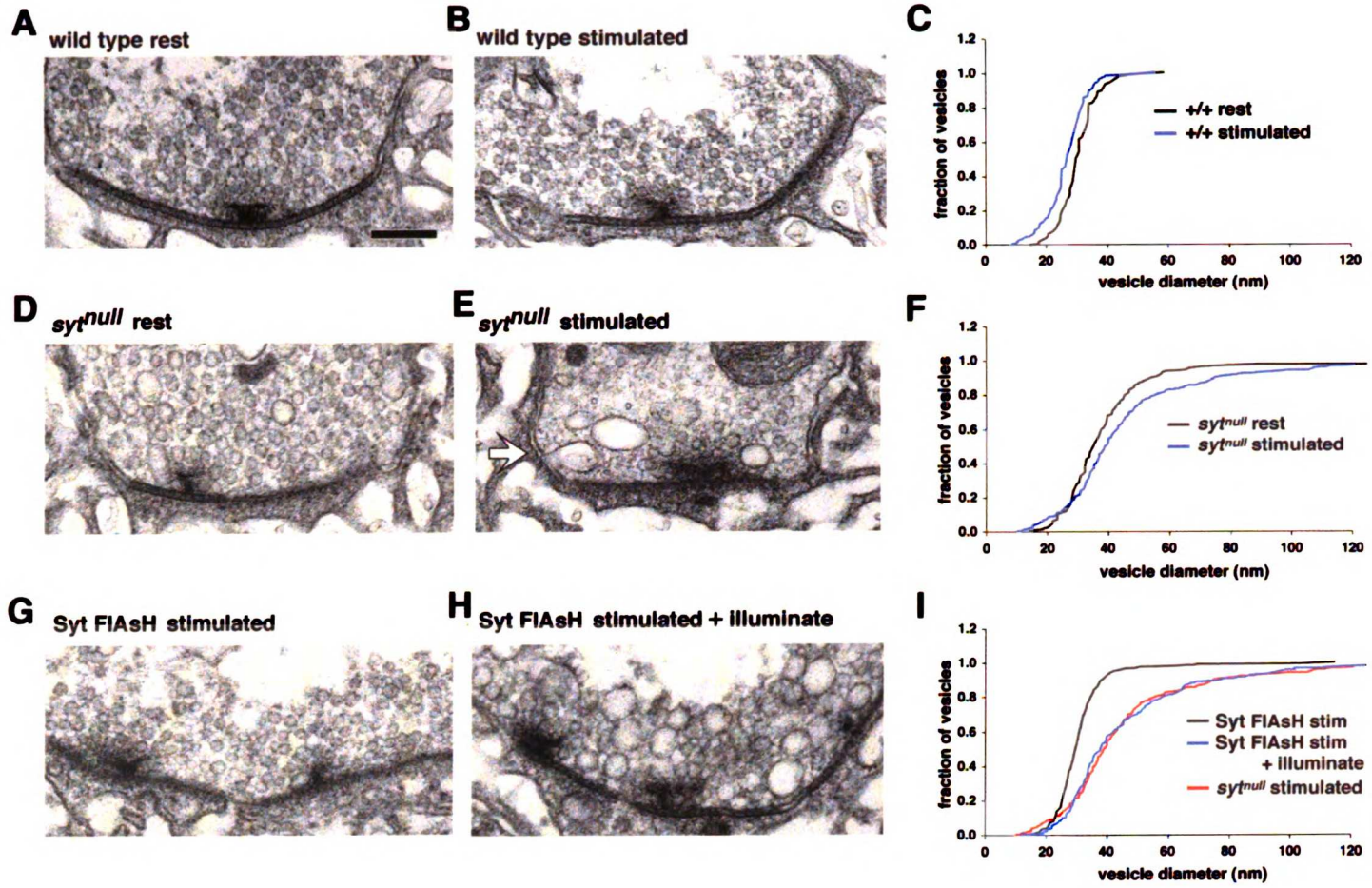
A
wild type rest
B
wild type stimulated
C
fraction of vesicles
vesicle diameter (nm)
+/+ rest
+/+ stimulated
D
syt^null rest
E
syt^null stimulated
F
fraction of vesicles
vesicle diameter (nm)
syt^null rest
syt^null stimulated
G
Syt FIAsH stimulated
H
Syt FIAsH stimulated + illuminate
I
fraction of vesicles
vesicle diameter (nm)
Syt FIAsH stim
Syt FIAsH stim
+ illuminate
syt^null stimulated

Figure 3-3. Endocytosis rate is slowed in mutants that affect the entire C_2B domain of Syt I.

(A) n-Syb-pH fluorescence dynamics in response to a 50 Hz, 10 s stimulus train in 2.0 mM Ca^{2+} at wild type (black, n = 10), syt^{AD1}/+ control (gray, n = 12), and $syt^{AD1/17}$ (blue, n = 11) synapses. (B) When n-Syb-pH fluorescence intensity is normalized to the peak $\Delta F/F$ intensity for all genotypes, a slower endocytosis rate is observed in the $syt^{AD1/17}$ animals compared to controls ($p < 0.04$). (C) n-Syb-pH fluorescence intensity changes in syt^{AD3} mutants. Heterozygous syt^{AD3}/+ synapses (gray, n = 12; $p > 0.08$) show no difference in endocytosis rate compared to wild type controls (not shown for clarity). $syt^{AD3/17}$ (light blue, n = 13) and $syt^{AD3/17}$ (dark blue, n = 13) synapses both show a decrease in vesicle release, as has been previously observed electrophysiologically. (D) When these n-Syb-pH data are normalized to the peak $\Delta F/F$ intensity, endocytosis rates are not different compared to wild type ($p > 0.1$).

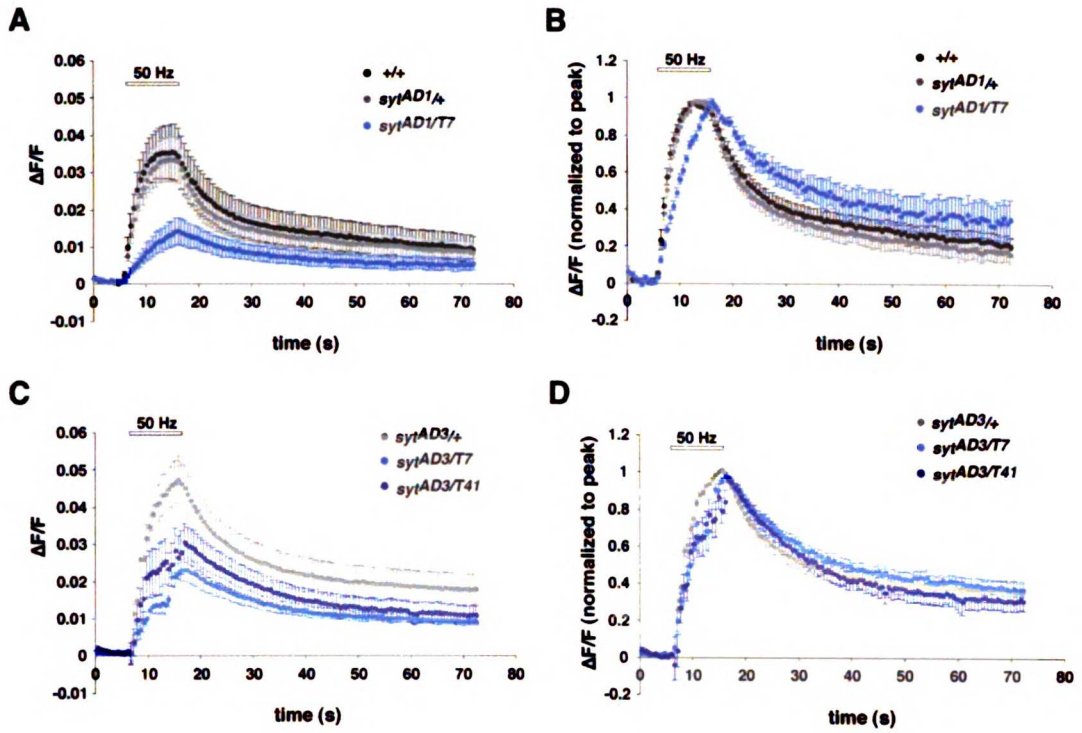
A
50 Hz
+/+
sytAD1/+
sytAD1/T7
ΔF/F
time (s)
B
50 Hz
+/+
sytAD1/+
sytAD1/T7
ΔF/F (normalized to peak)
time (s)
C
50 Hz
sytAD3/+
sytAD3/T7
sytAD3/T41
ΔF/F
time (s)
D
50 Hz
sytAD3/+
sytAD3/T7
sytAD3/T41
ΔF/F (normalized to peak)
time (s)

Figure 3-4. Protein levels of Syt I and α-adaptin at control and transgenic rescue synapses.

(A–F) Representative immunofluorescence staining for the Syt I protein. No staining is observed at the *syt*^{null} synapses (b). In all of the transgenic rescue animals (c–f), equivalent levels of Syt I are observed in the pre-synaptic terminal, slightly decreased compared to wild type. Subcellular localization appears normal. (G–L) Immunostaining for α-adaptin, part of the heterotetrameric AP-2 complex. All genotypes exhibit similar levels of α-adaptin protein, including the *UAS-syt-KQ* rescue animal. Synaptic boutons are consistently smaller in all transgenic genotypes and do not correlate with the stimulus-dependent differences among genotypes observed for endocytic rate or vesicle size.

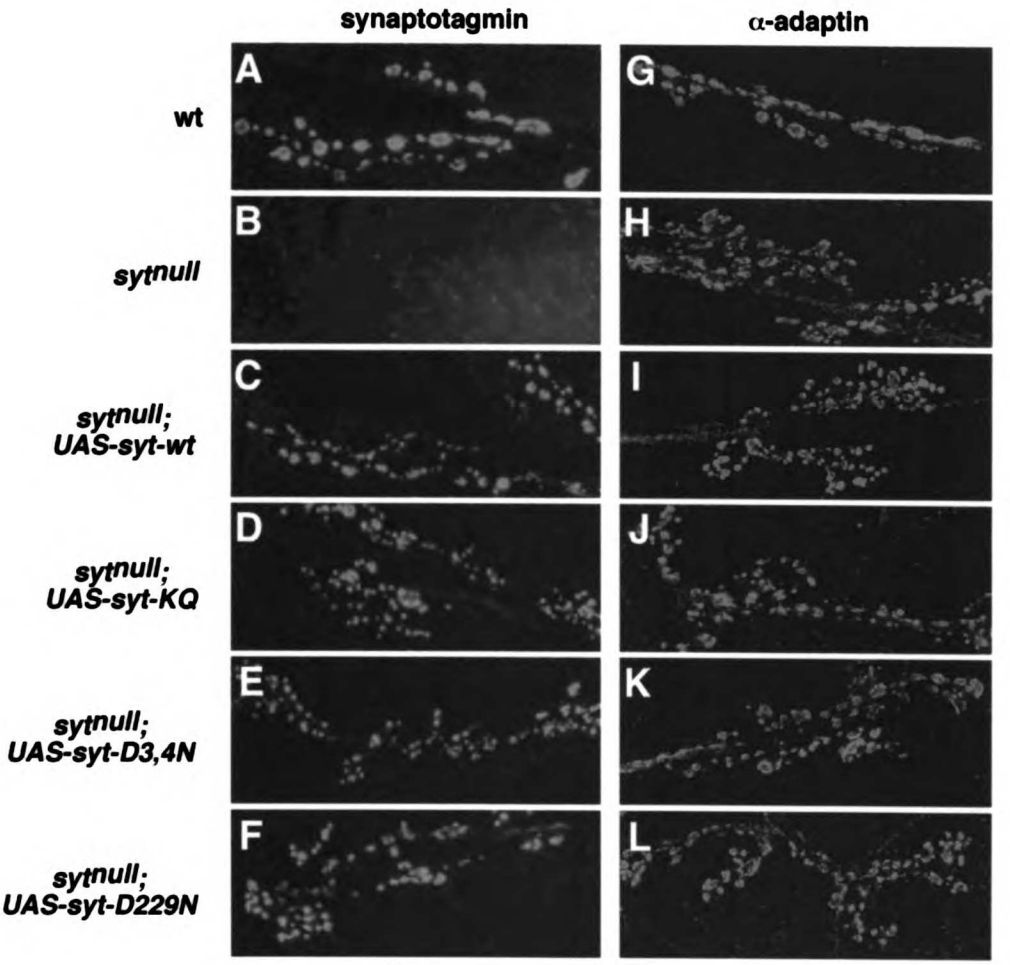
synaptotagmin
α-adaptin
wt
sytnull
sytnull; UAS-syt-wt
sytnull; UAS-syt-KQ
sytnull; UAS-syt-D3,4N
sytnull; UAS-syt-D229N
A
B
C
D
E
F
G
H
I
J
K
L

Figure 3-5. Endocytosis rate is normal at *UAS-syt-KQ* rescue synapses.

(A) n-Syb-pH fluorescence dynamics in response to a 50 Hz, 10 s stimulus train in 2.0 mM Ca^{2+} at *UAS-syt-wt* rescue (gray, n = 15) and *UAS-syt-KQ* rescue (red, n = 19) synapses. The *UAS-syt-KQ* transgene contains a disruption in the poly-lysine motif in the C_2B domain of Syt I. (B) When n-Syb-pH fluorescence intensity is normalized to the peak ΔF/F intensity for visual comparison, the same rate of endocytosis rate is observed in both genotypes ($p > 0.4$). (C) Peak n-Syb-pH ΔF/F intensity at *UAS-syt-wt* (gray) and *UAS-syt-KQ* (red) synapses at different stimulus durations (in 2.0 mM Ca^{2+}). Data within graphs are collected under identical imaging conditions. (D) Corresponding endocytosis rates, fit to a single exponential function, at the stimulus durations shown in (c) demonstrate that endocytosis rate does not change with stimulus duration in either of the transgenic genotypes.

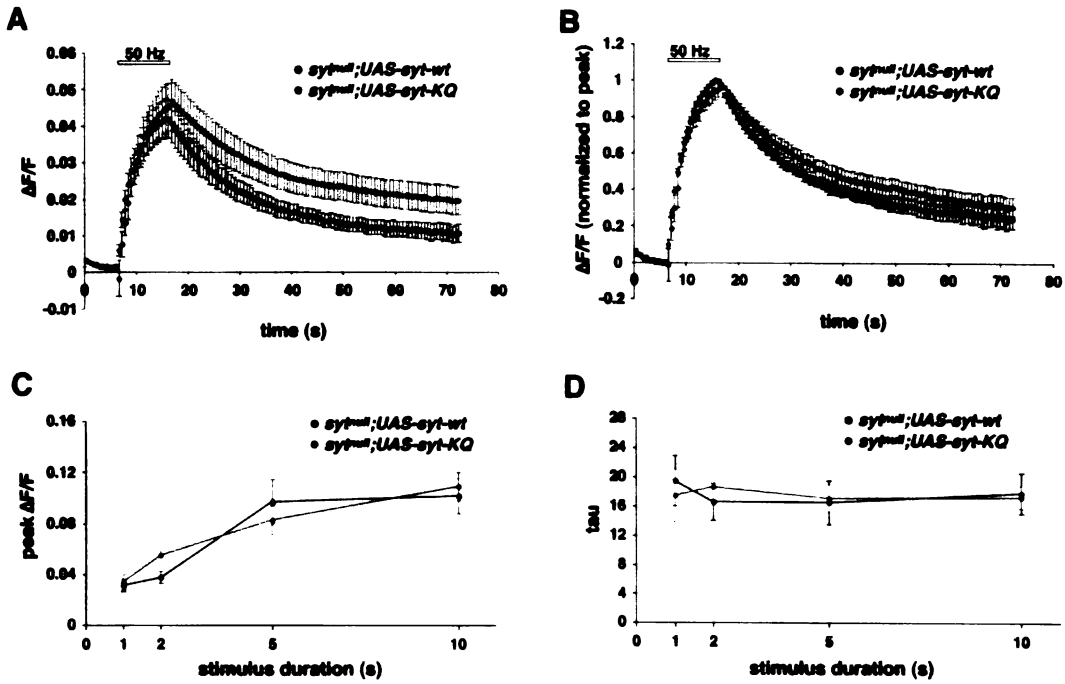
A
50 Hz
• syt^null;UAS-syt-wt
• syt^null;UAS-syt-KQ
ΔF/F
time (s)
B
50 Hz
• syt^null;UAS-syt-wt
• syt^null;UAS-syt-KQ
ΔF/F (normalized to peak)
time (s)
C
• syt^null;UAS-syt-wt
• syt^null;UAS-syt-KQ
peak ΔF/F
stimulus duration (s)
D
• syt^null;UAS-syt-wt
• syt^null;UAS-syt-KQ
tau
stimulus duration (s)

Figure 3-6. Synaptic vesicle size is increased following stimulation at *UAS-syt-KQ* rescue synapses.

(A–B) Representative active zones at *UAS-syt-KQ* rescue synapses. Synapses were either fixed immediately after dissection (rest, a) or one minute after the cessation of a 50 Hz, 10 s stimulus in 2.0 mM Ca^{2+} (stimulated, b). Scale = 200 nm. (C) Cumulative frequency distribution of vesicle diameter for *UAS-syt-wt* rescue synapses at rest (gray, n = 340 vesicles, 14 active zones) and following the stimulus (red, n = 394 vesicles, 18 active zones.) There is a small decrease in mean vesicle diameter ($p < 0.04$, t-test) and a change in the distribution of diameters ($p < 0.014$, KS test). (D) Cumulative frequency distribution of vesicle diameter for *UAS-syt-KQ* rescue synapses at rest (gray, n = 423 vesicles, 17 active zones) and following the stimulus (red, n = 302 vesicles, 13 active zones). *UAS-syt-KQ* stimulated synapses show an increase in mean vesicle diameter ($p < 0.005$, t-test) and shift in the distribution toward larger vesicle diameters ($p < 0.0005$, KS test).

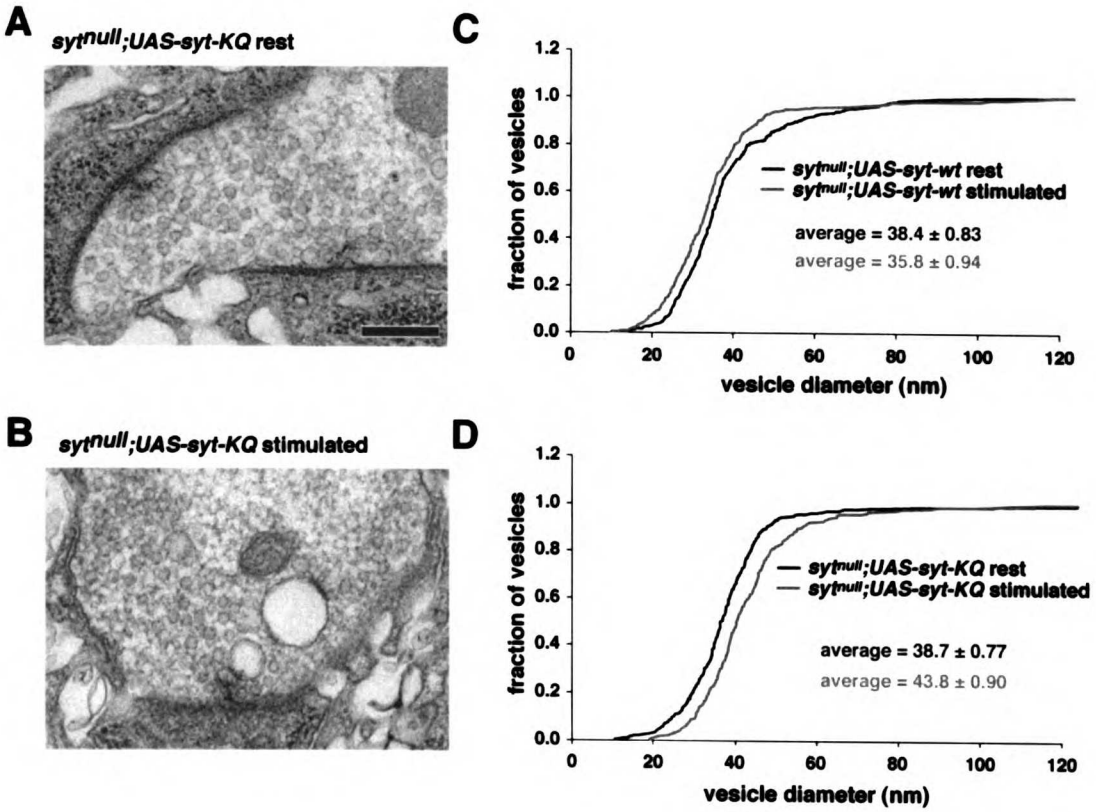
A
syt^null;UAS-syt-KQ rest
B
syt^null;UAS-syt-KQ stimulated
C
fraction of vesicles
1.2
1.0
0.8
0.6
0.4
0.2
0.0
0
20
40
60
80
100
120
vesicle diameter (nm)
syt^null;UAS-syt-wt rest
syt^null;UAS-syt-wt stimulated
average = 38.4 ± 0.83
average = 35.8 ± 0.94
D
fraction of vesicles
vesicle diameter (nm)
syt^null;UAS-syt-KQ rest
syt^null;UAS-syt-KQ stimulated
average = 38.7 ± 0.77
average = 43.8 ± 0.90

Figure 3-7. Endocytosis rate and synaptic vesicle size are unchanged at *UAS-syt-D229N* rescue synapses.

(A–B) n-Syb-pH fluorescence intensity in response to a 50 Hz, 10 s stimulus train in 2.0 mM Ca^{2+} at *UAS-syt-wt* rescue (gray, n = 15) and *UAS-syt-D229N* rescue (red, n = 18) synapses. The *UAS-syt-D229N* transgene contains a disuption in a Ca^{2+}-coordinating residue in the C_2A domain of Syt I. All aspects of n-Syb-pH dynamics in the *UAS-syt-D229N* rescue animal are not significantly different than controls ($p > 0.3$). (C) Cumulative frequency distribution of vesicle diameter for *UAS-syt-D229N* rescue synapses at rest (gray, n = 409 vesicles, 16 active zones) and following the stimulus (red, n = 463 vesicles, 20 active zones). There is no change in mean vesicle diameter ($p > 0.3$, t-test) but there is a change in the vesicle distribution ($p < 0.001$, KS test).

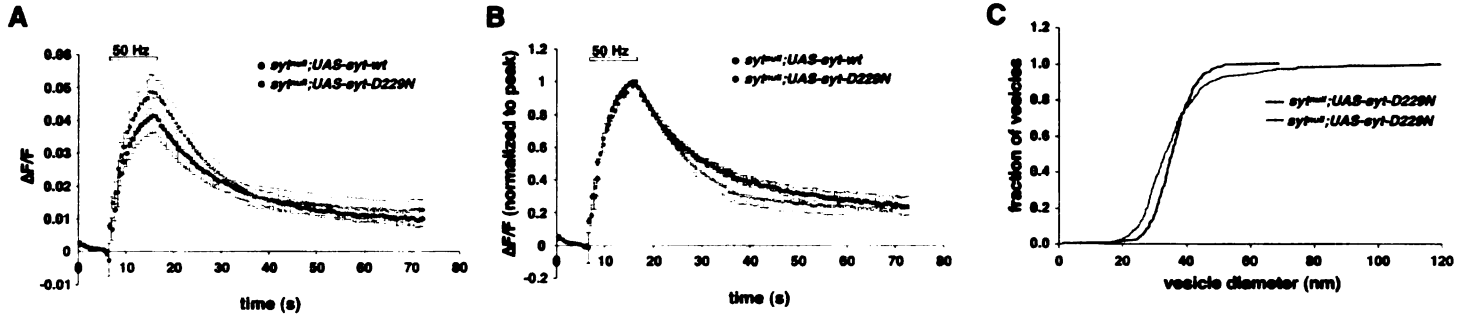
A
50 Hz
syt^null;UAS-syt-wt
syt^null;UAS-syt-D229N
ΔF/F
time (s)
B
50 Hz
syt^null;UAS-syt-wt
syt^null;UAS-syt-D229N
ΔF/F (normalized to peak)
time (s)
C
syt^null;UAS-syt-D229N
syt^null;UAS-syt-D229N
fraction of vesicles
vesicle diameter (nm)

Figure 3-8. Stimulation in the *UAS-syt-D3,4N* rescue animal causes a slowed endocytosis rate without affecting synaptic vesicle size.

(A) n-Syb-pH fluorescence intensity in response to a 50 Hz, 10 s stimulus train in 2.0 mM Ca^{2+} at *UAS-syt-wt* rescue (gray, n = 15) and *UAS-syt-D3,4N* rescue (red, n = 19) synapses. The *UAS-syt-D3,4N* transgene contains two mutations in the C_2B domain of Syt I which disrupt Ca^{2+}-coordination. Compared to *UAS-syt-wt* control synapses, the *UAS-syt-D3,4N* synapses show a decrease in peak n-Syb-pH fluorescence in response to the stimulus. (B) When n-Syb-pH fluorescence intensity is normalized to the peak $\Delta F/F$ intensity for visual comparison, the *UAS-syt-D3,4N* synapses exhibit a slower endocytosis rate ($p < 0.04$). (C–D) Representative active zones at *UAS-syt-D3,4N* rescue synapses at rest (c) and after stimulation (d). Scale = 200 nm. (E) Cumulative frequency distribution of vesicle diameters for *UAS-syt-D3,4N* rescue synapses at rest (gray, n = 373 vesicles, 20 active zones) and following the stimulus (red, n = 403 vesicles, 15 active zones). These synapses show no significant difference in mean vesicle diameter ($p > 0.09$, t-test), but the distributions are significantly different ($p < 0.02$, KS). (F) Recordings from muscle 6 during a 50 Hz, 10 s stimulus train in 2 mM Ca^{2+} saline. Representative recordings are shown for *UAS-syt-wt* control (top) and *UAS-syt-D3,4N* (bottom) rescue synapses. The rate of EPSP amplitude decay to baseline is rapid and equivalent in both genotypes (arrows). Scale: 10 mV, 2.5 s.

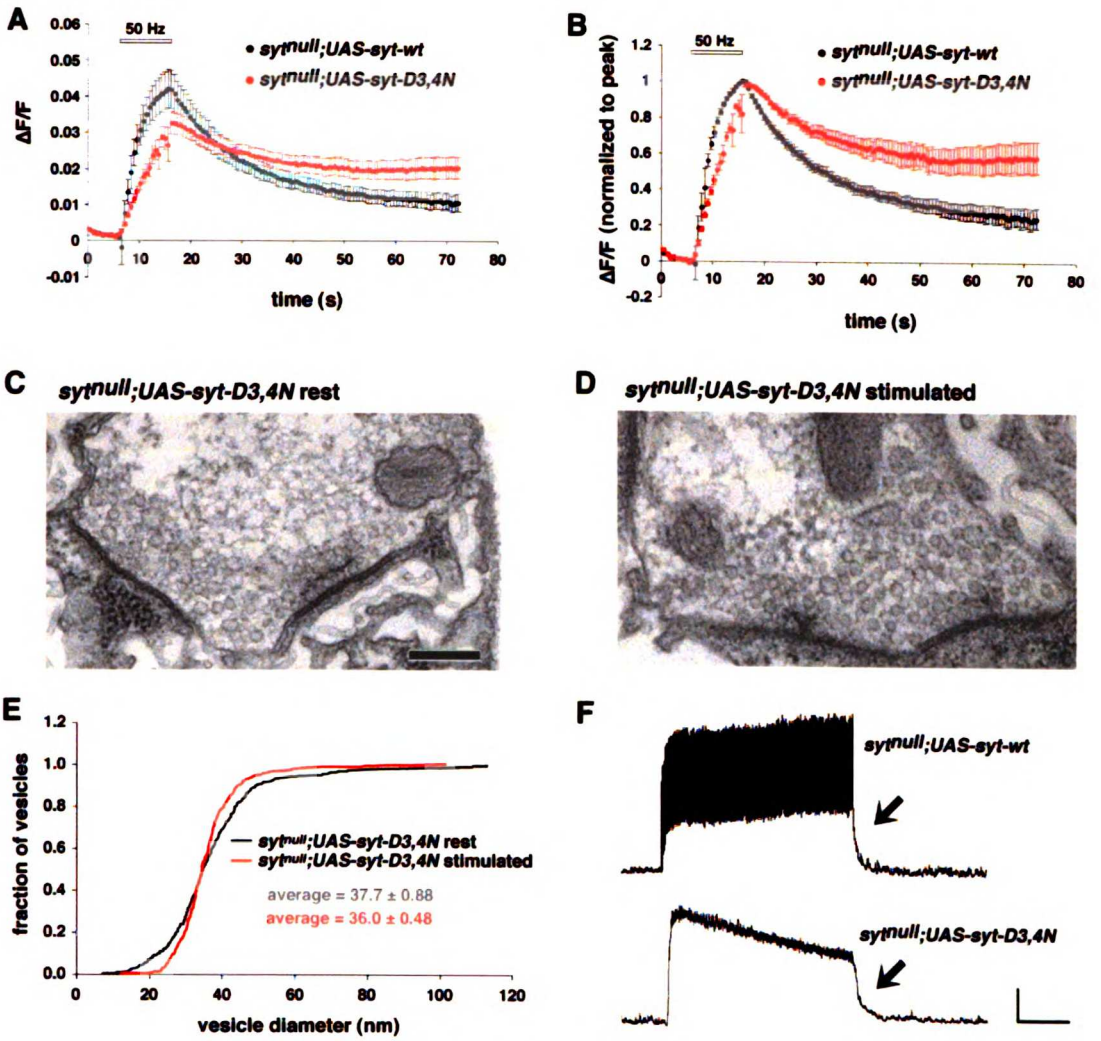
A
50 Hz
sytnull;UAS-syt-wt
sytnull;UAS-syt-D3,4N
ΔF/F
time (s)
B
50 Hz
sytnull;UAS-syt-wt
sytnull;UAS-syt-D3,4N
ΔF/F (normalized to peak)
time (s)
C
sytnull;UAS-syt-D3,4N rest
D
sytnull;UAS-syt-D3,4N stimulated
E
fraction of vesicles
sytnull;UAS-syt-D3,4N rest
sytnull;UAS-syt-D3,4N stimulated
average = 37.7 ± 0.88
average = 36.0 ± 0.48
vesicle diameter (nm)
F
sytnull;UAS-syt-wt
sytnull;UAS-syt-D3,4N

Figure 3-9. High extracellular Ca^{2+} rescues endocytic rate in the *UAS-syt-D3,4N*, but not syt^{null} animals.

(A) Endocytic rate calculated from n-Syb-pH decay following a 50 Hz, 10 s stimulus in either 2 or 5 mM Ca^{2+} in *UAS-syt-wt* (gray) and *UAS-syt-D3,4N* (red) rescue animals. Endocytic rate in *UAS-syt-D3,4N* rescue animals is significantly faster at the higher Ca^{2+} concentration ($p < 0.025$), whereas there is no significant change in the *UAS-syt-wt* rescue animals ($p > 0.15$). (B) n-Syb-pH endocytosis rates following a 50 Hz, 10s stimulus in wild type (gray) and syt^{null} (blue) animals in either 2.0 or 5.0 mM extracellular Ca^{2+}. Wild type animals show a slight, but significant speeding in rate at the higher Ca^{2+} concentration ($\tau = 13.7 \pm 1.0$ s in 2.0 mM, 9.5 ± 0.9 s in 5.0 mM, $p < 0.01$), but syt^{null} animals do not show a change in endocytosis rate ($p > 0.4$). (C) EPSP amplitude in response to a single action potential recorded in either 2.0 or 5.0 mM extracellular Ca^{2+} as indicated. Genotypes are listed in the box below the graph. (D) The depolarization achieved during a train of action potentials (50 Hz, 10 s) is shown for the two Ca^{2+} concentrations indicated. Train amplitude represents the average EPSP measured for the interval between 5 and 7 s during the 10 s train. Genotypes are listed in the box above the graph and are the same as in (c). (E) Representative traces show the response to a 50 Hz, 10 s stimulus train for the genotypes indicated recorded in 5.0 mM extracellular Ca^{2+}.

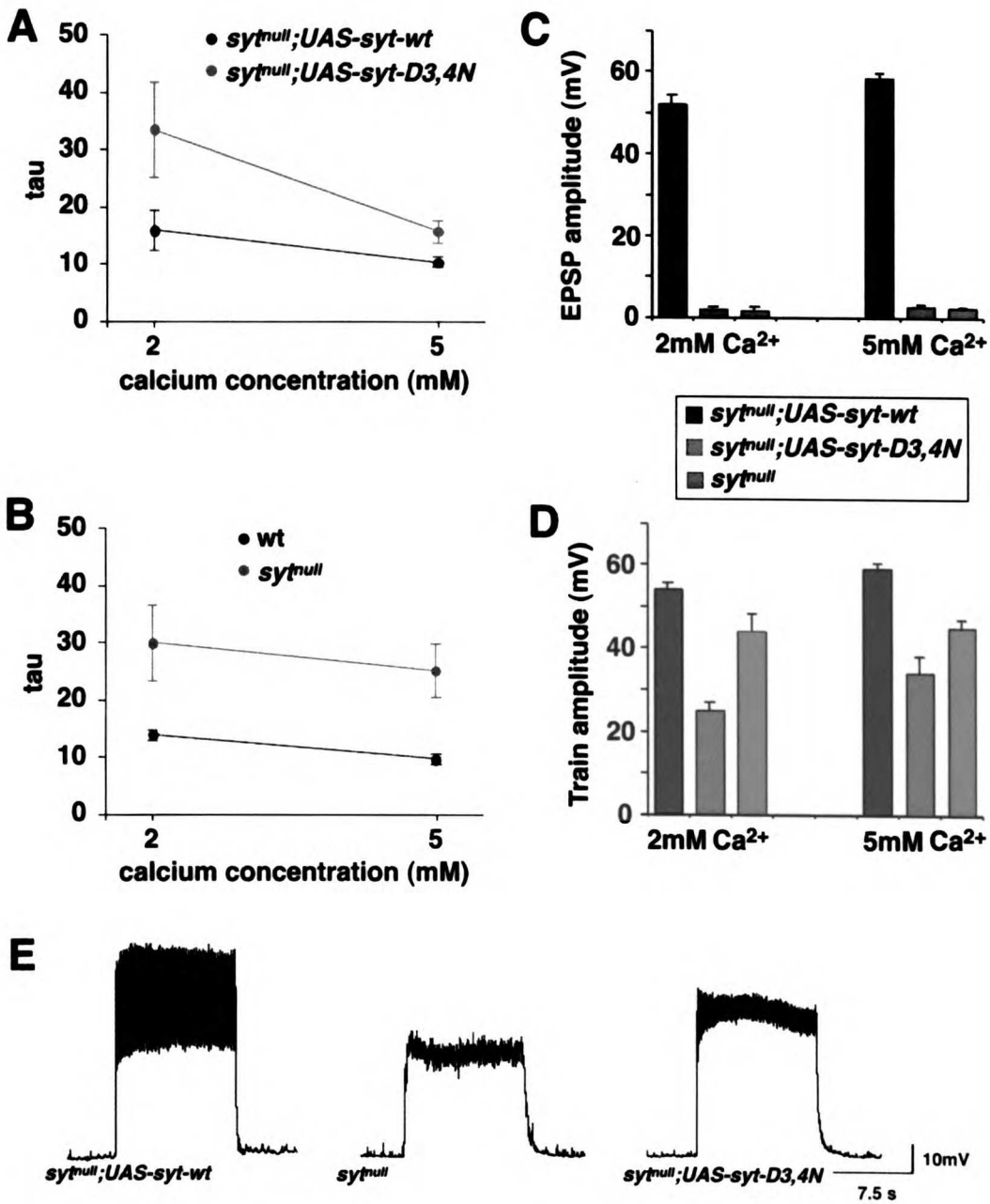
A
50
40
30
20
10
0
tau
2
5
calcium concentration (mM)
• syt^null;UAS-syt-wt
• syt^null;UAS-syt-D3,4N
B
50
40
30
20
10
0
tau
2
5
calcium concentration (mM)
• wt
• syt^null
C
EPSP amplitude (mV)
60
40
20
0
2mM Ca2+
5mM Ca2+
syt^null;UAS-syt-wt
syt^null;UAS-syt-D3,4N
syt^null
D
Train amplitude (mV)
60
40
20
0
2mM Ca2+
5mM Ca2+
E
syt^null;UAS-syt-wt
syt^null
syt^null;UAS-syt-D3,4N
10mV
7.5 s

Chapter Four:

Mobilization and Fusion of a Non-Recycling Pool of Synaptic Vesicles Under Conditions of Endocytic Blockade

Summary

At vertebrate central synapses, it has been demonstrated that a resting pool of synaptic vesicles (SVs) exists that normally does not participate in SV release and recycling. It remains unclear whether SVs within the resting pool are capable of mobilization and fusion. Here we combine live imaging of SV exo- and endocytosis using pH-sensitive GFP (synapto-pHluorins) with pharmacological and genetic manipulations of the SV cycle at the Drosophila NMJ. We demonstrate that a resting pool of SVs exists at this synapse that encompasses 30–41% of the total SV pool. Under conditions of endocytic blockade, using a temperature-sensitive dynamin mutation, the resting pool of SVs can be mobilized and released. We present a model for the presence of a resting pool of SVs that does require molecular specification of a subpopulation of SVs.

Introduction

Release of neurotransmitter from synaptic vesicles (SVs) and activation of neurotransmitter receptors account for the transmission of information from the presynaptic to the postsynaptic cell. There are a finite number of these SVs at any synapse, and it is through the recycling of these SVs that continued neurotransmission through multiple rounds of release is possible. However, it has been shown that there are different pools of SVs at the synapse and that these groups are released, and reused, under differing conditions (Sudhof, 2000). The "readily releasable pool" is thought to define a subset of SVs that are immediately released upon influx of calcium ions through voltage-gated calcium channels during nerve stimulation at mammalian synapses (Murthy and Stevens, 1999; Pyle et al., 2000; Rizzoli and Betz, 2004; Rosenmund and Stevens, 1996; Sara et al., 2002; Schikorski and Stevens, 2001). At mammalian synapses, the SVs that are not in the readily releasable pool, but can be released upon further stimulation are termed "reserve pool" SVs. (Sudhof, 2000). Together, the SVs in the readily releasable pool and the reserve pool make up the group called the "recycling pool," which is comprised of all the SVs capable of release. At central synapses, it has been estimated that this recycling pool comprises only a small amount of the entire pool of SVs, with most of the SVs residing in an un-releasable, "resting pool" (Harata et al., 2001; Murthy and Stevens, 1999; Sudhof, 2000).

At the Drosophila neuromuscular junction (NMJ), different terminology has been used to describe SV pools, with studies describing a "readily releasable pool", an

"exo/endo cycling pool," and a "reserve pool" (Delgado et al., 2000; Kuromi and Kidokoro, 1998; Kuromi and Kidokoro, 1999). As at central synapses, these pools describe groups of SVs that are mobilized at different rates and under different conditions. In short, the readily releasable and the exo/endo cycling pools seem to contain SVs that are more actively released than those in the reserve pool. However, it has never been determined whether there exists a non-recycling "resting pool" of SVs at this synapse. In this study, we adopt the terminology generally used to describe SV pools at mammalian synapses discussed above.

Much of the work characterizing SV pools at central and peripheral synapses has been carried out using the styryl dye FM1-43 and its analogues (Kuromi and Kidokoro, 1998; Pyle et al., 2000; Richards et al., 2003; Rizzoli et al., 2003; Sara et al., 2002; Schikorski and Stevens, 2001). These lipophilic dyes intercalate into the plasma membrane of cells and become trapped within cells when membrane exposed to the dye is endocytosed, such as when SVs are recycled. These FM experiments have been effective, but they rely on loading and unloading phases (with washes in between), which are temporally separated. They do not allow both exocytosis and endocytosis of SVs to be assayed directly in real time. In some recent experiments the recycling SV pool has been defined using pH-sensitive GFP molecules, termed the synapto-pHluorins (Fernandez-Alfonso and Ryan, 2004). However, this technique has not been used to directly measure the relative sizes of the recycling versus resting SV pools.

In this study, we use the genetically encoded synapto-pHluorins to examine the functional properties of the SV pools at the Drosophila NMJ. The synapto-pHluorins are pH-sensitive GFP molecules that have been fused to a SV protein, in this case, n-

Synaptobrevin (n-Syb-pH). Synapto-pHluorins are reliable monitors of SV exocytosis and endocytosis (Miesenbock et al., 1998). In the low pH (5.5) of the SV lumen, n-Syb-pH fluorescence is quenched. Upon exocytosis of SVs, the n-Syb-pH molecules experience the higher pH environment of the synaptic cleft and fluoresce at a higher intensity. By measuring n-Syb-pH fluorescence intensity over time following stimulation, the kinetics of SV recycling can be directly measured (Poskanzer et al., 2003; Sankaranarayanan and Ryan, 2000).

We have combined use of the synapto-pHluorins with a temperature-sensitive endocytosis mutant, *shibire*^{ts}, and a blocker of the V-type ATPase pump that is required for SV re-acidification, bafilomycin. These tools have allowed us to define the functional properties of SV pools at the Drosophila NMJ by directly imaging SV proteins as SVs are released and recycled in real time. We demonstrate the presence of a non-recycling, resting pool of SVs at this synapse for the first time and quantify the size of the resting pool compared to the recycling pool of SVs. We further demonstrate that the SVs within this resting pool are capable of mobilization and fusion under conditions of endocytic blockade. Based on these data, we present a model for SV mobilization and recycling during synaptic activation.

Results

In order to assay SV recycling, we expressed synapto-pHluorins in Drosophila motoneurons using the UAS/GAL4 system, and observed their dynamics at the presynaptic side of the Drosophila NMJ. During a 50 Hz, 2 s stimulus given to the pre-synaptic motor nerve, the n-Syb-pH fluorescence intensity rapidly increases, and then slowly decreases [Figure 4-1A, (Poskanzer et al., 2003)]. The fluorescence decay can be fit with a single exponential with a time constant of 12.6 seconds (Poskanzer et al., 2003). In these experiments, average n-Syb-pH fluorescence is measured over the entire presynaptic nerve terminal, which includes non-active zone areas where neither neurotransmitter release nor recycling occurs. This is done because each synaptic bouton contains multiple active zones and we do not have an independent, live marker for individual active zones in order to define regions of interest for analysis. Therefore, changes in average fluorescence intensity that we observe are small, but they are robust across synapses and animals (Poskanzer et al., 2003). We have previously shown that expression of n-Syb-pH does not affect normal synaptic morphology or function (assayed electrophysiologically) at this synapse (Poskanzer et al., 2003).

Stimulus-dependent changes in n-Syb-pH fluorescence could reflect a balance of SV exocytosis and endocytosis as has been previously demonstrated (Sankaranarayanan and Ryan, 2000). In order to use n-Syb-pH as a quantitative measure of SV exocytosis, it is necessary, therefore, to determine how much endocytosis contributes to the change in n-Syb-pH fluorescence that we observe during our stimulus paradigm (50Hz, 2s). To do

so, we examined SV recycling with the synapto-pHluorins in *shibire^{ts}* mutant flies. The *shibire^{ts}* flies have a mutation in the protein Dynamin, which causes a complete inhibition of endocytosis at the restrictive temperature (30°C) while allowing normal endocytosis to proceed at the permissive temperature (22°C) (Koenig and Ikeda, 1989; Koenig et al., 1983). Following stimulation in a *shibire^{ts}* animal at the permissive temperature, n-Syb-pH fluorescence decays to baseline indicating normal SV endocytosis. However, when the *shibire^{ts}* animals are shifted to the restrictive temperature, n-Syb-pH fluorescence does not decay, consistent with a complete block of endocytosis (Figure 4-1B). Furthermore, the peak fluorescence change during stimulation (50Hz, 2s) at the permissive temperature is not statistically different from that measured following the shift to the restrictive temperature (Figure 4-1B, C). Since endocytosis is blocked at the restrictive temperature, and the change in peak fluorescence is equal to that observed at the permissive temperature, this demonstrates that there is not a significant contribution of SV endocytosis to the change in n-Syb-pH fluorescence that we observe during a 50Hz, 2s stimulation. Therefore the change in n-Syb-pH fluorescence accurately reflects the amount of SV exocytosis during a 50Hz, 2s stimulus at this synapse.

In the experiments that we present in this study, we use repeated trials of 50Hz, 2s stimulation (30 second inter-trial interval) to assess the size of SV pools present at this synapse. We first stimulate the synapse and measure the consistency of SV exocytosis across trials. We find that the change in n-Syb-pH fluorescence does not change over the course of 15 trials (Figure 4-1D). This suggests that the synapse reliably releases the same amount of neurotransmitter each time it is stimulated, in this protocol. When we examine the time-course of n-Syb-pH fluorescence decay following each trial (reflecting

the rate of endocytosis), we find that this parameter also does not change (data not shown). This demonstrates that SV endocytosis reliably compensates for SV exocytosis during this stimulus regimen.

Next, we use n-Syb-pH in combination with bafilomycin (Baf) to quantify the size of the releasable pool of SVs. Baf is a cell-permeant pharmacological blocker of the V-type ATPase, which re-acidifies SVs after endocytosis and participates in the process by which SVs are filled with neurotransmitter. Baf has been used previously in hippocampal neurons to estimate the size of the SV releasable pool (Fernandez-Alfonso and Ryan, 2004). Since Baf blocks only SV re-acidification, nerve stimulation in the presence of Baf causes an increase in n-Syb-pH that does not decay following the stimulation [Figure 4-2A, (Poskanzer et al., 2003)]. Importantly for the present set of experiments, Baf has been shown not to affect SV exocytosis and SVs have been shown to recycle normally after Baf treatment, even when they are no longer completely filled with neurotransmitter (Cousin and Nicholls, 1997; Sankaranarayanan and Ryan, 2001; Zhou et al., 2000).

We first stimulate (50Hz, 2s) in the absence of Baf to confirm that n-Syb-pH dynamics are normal. We then continue with our repetitive stimulation protocol (50Hz, 2s stimuli, 30s inter-trial interval, 12 trials) in the presence of Baf (Figure 4-2B, trials 1–12). The peak fluorescence values for each trial that are plotted in Figure 2B indicate exocytosis-dependent increases in fluorescence intensity over and above the fluorescence levels achieved in the previous trial. The first stimulus trial following the addition of Baf shows no change in peak fluorescence compared to previous trials in the absence of Baf. On trials 2–5, we observe an increase in n-Syb-pH fluorescence, but the peak increase on

each trial is less than that observed on the previous trial. This indicates that each successive trial includes a larger fraction of recently recycled SVs. The fifth stimulus trial is the last trial in which we see any further stimulus-dependent increase in fluorescence intensity (Figure 4-2B). This indicates that no new (previously un-recycled) SVs are released following the fifth stimulus trial. Thus, five stimulus trials are sufficient to release the entire pool of recycling SVs.

At both central and peripheral synapses in the vertebrate nervous system, evidence suggests that there is a pool of SVs that does not undergo release and recycling under normal stimulus conditions (Harata et al., 2001; Murthy and Stevens, 1999). This pool of non-recycling SVs has been termed the "resting pool" or "cryptic pool" of SVs. Previous experiments at the Drosophila NMJ provide evidence for spatially separable pools of SVs that can be differentially accessed depending on stimulus frequency and duration (Kuromi and Kidokoro, 1998; Kuromi and Kidokoro, 2000; Kuromi and Kidokoro, 2002). However, it has yet to be determined whether a resting pool of non-recycling SVs is present at this genetically tractable synapse.

To determine whether a resting pool of SVs exists at the Drosophila NMJ, we continued our stimulus trials in the presence of Baf for 12 trials during which no increase in n-Syb-pH was observed. We then applied ammonium chloride (NH_4Cl) to the preparation and observe a large increase in n-Syb-pH fluorescence (Figure 4-2B'), which reaches a level that was not statistically different than that observed in control synapses assayed in parallel (Figure 4-1D'). NH_4Cl is a membrane-permeant solution that can change the pH in all cellular compartments (Sankaranarayanan and Ryan, 2000). When applied to a synapse expressing the synapto-pHluorins, NH_4Cl adjusts the pH in SVs

from pH 5.5 to pH 7.4. N-Syb-pH molecules on intact SVs no longer have their GFP fluorescence quenched by the low pH lumen of the SV, and their fluorescence intensity increases. Therefore, application of NH_4Cl reveals all of the n-Syb-pH molecules at the synapse, even those that would normally be quenched, providing a measure of the total number of SVs at a given synapse. Because we observe an increase in n-Syb-pH fluorescence upon NH_4Cl addition, our data indicate that a significant fraction of SVs was never released during our stimulus regimen in the presence of Baf.

One possible source of error in this experiment could result from difference in the pH of NH_4Cl (7.4) compared to the synaptic cleft. SVs that are released and recycled in the presence of Baf will assume the pH of the synaptic cleft and not be re-acidified. Therefore, the change in pH to 7.4 upon application of NH_4Cl could cause an increase in n-Syb-pH fluorescence even at previously released and recycled SVs. However, we can rule out this complication because n-Syb-pH trapped at the plasma membrane in the *shibire*^{ts} animal, held at the restrictive temperature, does not show a change in fluorescence intensity after application of NH_4Cl (see data below in Figure 4-3C', 4B). Thus, the difference in pH between the synaptic cleft and NH_4Cl is not enough to cause a resolvable change in n-Syb-pH fluorescence.

The results of our experiments to this point indicate that there is a population of SVs that is not released during repeated stimulation in the presence of Baf. The results do not imply, however, that no SVs were released upon stimulation. It has previously been shown that SVs can recycle normally after Baf treatment, even when they are no longer completely filled with neurotransmitter (Cousin and Nicholls, 1997; Zhou et al.,

2000). Thus, we conclude that a resting pool of SVs is present at the Drosophila NMJ, as has been observed at other synapses in the central and peripheral nervous systems. Application of NH_4Cl has been used to define a total pool of SVs at vertebrate central synapses, *in vitro* (Sankaranarayanan and Ryan, 2000). However, because this pool of SVs can not be recruited during stimulation, it has yet to be determined whether the fluorescence associated with NH_4Cl application represents a pool of SVs that are capable of mobility and fusion, yet normally do not participate in SV recycling. Indeed, it remains formally possible that NH_4Cl application, which is used to define the resting pool, could actually be revealing the presence of n-Syb-pH molecules within an acidic, non-SV compartment. Another alternative is that SVs within the resting pool are different in some way from other SVs and are not capable of mobilization and fusion. In Drosophila, we are able to test our hypothesis that the NH_4Cl identifies a resting pool of SVs that can be mobilized and fuse at the active zone, but which normally do not do so. Our experiments take advantage of the temperature-sensitive dynamin mutation, *shibire^{ts}*, at the Drosophila NMJ. It has been established that persistent stimulation at the restrictive temperature in the *shibire^{ts}* mutation can deplete all SVs from the synapse, assayed ultrastructurally (Koenig and Ikeda, 1989; Koenig et al., 1983). Therefore, we have expressed n-Syb-pH in the *shibire^{ts}* genetic background. We can now assay whether prolonged stimulation can eliminate the NH_4Cl fluorescence increase at the end of stimulation and therefore determine whether NH_4Cl defines a pool of SVs that are capable of mobilization and fusion with the plasma membrane.

When n-Syb-pH is expressed in the *shibire^{ts}* mutant background, exocytosis and endocytosis, as measured by n-Syb-pH fluorescence dynamics, is normal at the

permissive temperature (22°C) (Figure 4-1B). At the restrictive temperature (30°C), however, n-Syb-pH fluorescence intensity increases upon nerve stimulation, but does not decrease after the stimulus, confirming that endocytosis is blocked [Figure 4-1B, (Poskanzer et al., 2003)]. We next carry out our repetitive stimulation protocol as shown in Figure 4-1. First, we stimulate the neuron (50Hz, 2s) at the permissive temperature and measure the peak n-Syb-pH fluorescence intensity. We do this for two trials, 30 seconds apart, and observe reproducible changes in peak fluorescence intensity, as is observed at wild type synapses (Figure 4-3C). We then raise the preparation to the restrictive temperature, and continued the same stimulation protocol (50Hz, 2s stimuli, 30s inter-trial interval) for 12 more trials. For each trial, fluorescence is quantified as indicated previously (Figure 4-3C).

We find that following the shift to the restrictive temperature, the peak n-Syb-pH fluorescence reached on each of the first seven trials is not significantly different from that reached on each of the preceding trials (Figure 4-3C). Since endocytosis is blocked, an equivalent number of new SVs are released from the total SV pool on each trial. On trials 8–12, the peak n-Syb-pH fluorescence gradually decreases and appears to plateau. Again, since endocytosis is blocked, this indicates that we have severely depleted the SV pool. We then apply NH_4Cl to the preparation to assay whether any SVs or acidified n-Syb-pH containing compartments persist in the pre-synaptic terminal. Application of NH_4Cl does not further increase n-Syb-pH fluorescence (Figure 4-3C'). This can also be appreciated by examination of representative images of the NMJ in this experiment (Figure 4-4B). This indicates that our stimulus protocol has released the entire SV pool, to the limit of our resolution. Since there is no change in fluorescence upon application

of NH_4Cl, we conclude that the resting pool of SVs that we previously defined by NH_4Cl application can be mobilized and released under conditions of endocytic blockade. These data also argue against the possibility that NH_4Cl defines a non-vesicular compartment that contains n-Syb-pH. As controls for genotype and temperature in these experiments, we have carried out our repetitive stimulation protocol in *shibire*^{ts} animals at the permissive temperature and wild-type animals held at the restrictive temperature. In these controls we see no difference compared to wild-type animals at the permissive temperature (Figure 4-3A, B).

How large is the resting pool of SVs? Since our *shibire*^{ts} experiment assessed the entire pool of SVs (as evidenced by a lack of NH_4Cl-dependent change), and the Baf experiment revealed only the releasable pool of SVs, a comparison of these two traces can give an estimate of the relative number of SVs in each of the SV pools. In Figure 4-5A, the amount of cumulative fluorescence change in the Baf curve corresponds to a recycling SV pool. This amount, subtracted from the cumulative *shibire*^{ts} fluorescence change (which corresponds to the entire SV pool), gives a description of the resting pool of SVs. These data, then, describe a resting pool of non-recycling SVs that includes at least 30% of the entire SV pool. This estimation of the resting pool size is a lower limit because we observe that Baf application causes a slow increase in fluorescence intensity over time at a resting synapse. This drift is caused by the slow alkalinization of the entire SV pool when the vesicular proton pump is poisoned by Baf (Sankaranarayanan and Ryan, 2001). Our measurements indicate that this drift can account for a maximum of 11% of the fluorescence change observed over the 12 stimulus trials in our experiments (data not shown). Thus, we can reasonably conclude that the resting pool of SV

encompasses 30-41% of the entire SV pool at the Drosophila NMJ. This is a large fraction of the entire SV pool, in agreement with estimation of a non-recycling SV pool at other synapses (Schikorski and Stevens, 2001).

There is some debate as to whether SV pools are spatially segregated within a nerve terminal (Kuromi and Kidokoro, 1998; Rizzoli and Betz, 2004; Schikorski and Stevens, 2001). At the Drosophila NMJ, experiments using FM-dyes to label SVs have argued for a discrete pool of SVs that resides at the center of a synaptic bouton (Kuromi and Kidokoro, 1998). We examined our data to determine whether our non-recycling, resting pool of SV might correspond to this centrally located pool of SVs. However, when we apply NH_4Cl to a wild type synapse in order to reveal the entire SV pool, we do not generally see evidence of labeling at the center of synaptic boutons (Figure 4A). Since we can completely deplete the NH_4Cl sensitive pool in the *shibire*^{ts} animal, we are confident that the n-Syb-pH allows us to visualize the SV pool, and excludes visualization of other cellular compartments. Our data agree with light and ultrastructural studies where SVs are generally not observed at the very center of synaptic boutons (Eaton et al., 2002; Gramates and Budnik, 1999; Marek and Davis, 2002; Marek et al., 2000; Roos et al., 2000). Thus, our data do not agree with the hypothesis that the resting pool (or any pool of SVs) resides exclusively at the center of the synaptic bouton. This discrepancy may be due to the different imaging techniques used. FM dyes, since they are lipophilic may not get washed off completely and become inserted in membranes in a non-specific manner, whereas synapto-pHluorin fluorescence is confined to a particular protein in the SV.

Finally, the expression of n-Syb-pH in the *shibire*^{ts} animal allows us to visualize the distribution of n-Syb-pH that is trapped at the plasma membrane for prolonged periods of time when endocytosis is blocked (Figure 4-4B). When we examine *shibire*^{ts}; n-Syb-pH synapses that have been held at the non-permissive temperature for six minutes, and have been depleted of SVs during this time, we find that n-Syb-pH fluorescence does not equilibrate across the synaptic plasma membrane. We observe n-Syb-pH fluorescence that remains highly concentrated at the plasma membrane of individual synaptic boutons, with relatively little fluorescence at membranes between boutons. Even within single synaptic boutons we can observe discrete hotspots of fluorescence at this time point. These data suggest that n-Syb-pH is not freely diffusible upon insertion into the synaptic plasma membrane.

Discussion

Here we demonstrate the presence of two pools of SVs at the Drosophila NMJ; a recycling pool of SVs and a non-recycling, resting pool of SVs (Figure 4-5A). We estimate that the size of the resting pool of SVs is 30–41% of the total SV pool. The presence of a resting pool of SVs is consistent with observations at vertebrate central synapses, *in vitro*. We further demonstrate that the SVs within the resting pool can be mobilized and fuse with the plasma membrane under conditions of endocytic blockade. Thus, the resting pool consists of fusion competent SVs that do not normally participate in SV recycling.

In Figure 4-5B, we show a model of the accessibility of the different SV pools. At wild-type synapses, SVs in the recycling pool go through exocytosis and endocytosis, but SVs in the resting pool do not participate. At *shibire*^{ts} synapses, exocytosis of the releasable pool is not balanced by endocytosis, and SVs from the resting pool are mobilized to the active zone and released until all SVs are depleted. At synapses treated with Baf, SVs in the recycling pool are exocytosed and endocytosed, and recycling of these SVs persists during repeated nerve stimulation. However, there is little, if any, mobilization of SVs from the resting pool into the recycling pool in this condition. Since Baf has been shown to not affect normal SV recycling in other systems (Cousin and Nicholls, 1997; Zhou et al., 2000), this condition allows us to measure the recycling SV pool. Subtracting the size of the recycling pool from the total SV pool allows us to estimate the size of the non-recycling, resting pool of SVs.

We present a model that can account for the presence of a large resting SV pool without having to invoke molecular difference between the SVs that reside in different pools. This model is based on the privileged position of recycling SVs relative to the active zone (Sudhof, 2000). In this model, all SVs are considered to be equivalent. SVs that are at sites distant from the active zone are prevented from approaching the release apparatus by the presence of a large number of recycling SVs. This model suggests that the resting pool simply represents a pool of SVs that are prevented from moving into a position that allows them to be released and recycled. We hypothesize, therefore, that the recycling and resting SV pools are simply a consequence of maintaining more SVs at a synapse than are necessary to normally sustain neurotransmission. This model also predicts that the resting pool of SVs resides at a more distant position relative to the active zone, a parameter that has yet to be measured at this synapse. However, our images of the total SV pool are not consistent with the hypothesis that the resting pool resides at the center of the synaptic bouton.

Our data also touch upon the topic of what happens to SV proteins once SVs are fused with the plasma membrane. At central synapses, n-Syb-pH has been shown to diffuse into axonal segments following stimulation (Sankaranarayanan and Ryan, 2000). These data suggest that n-Syb-pH is highly mobile within the synaptic plasma membrane. We have examined the distribution of large amounts of n-Syb-pH deposited at the plasma membrane for prolonged time periods during endocytic blockade. It is somewhat surprising that n-Syb-pH fluorescence remains highly concentrated within sub-regions of individual synaptic boutons. Although some increase in fluorescence may occur at inter-bouton regions, the n-Syb-pH fluorescence clearly does not equilibrate

across the nerve terminal during the time course of our experiment. This suggests that there are restrictions to n-Syb-pH mobility in the plasma membrane. Our results, however, do not necessarily contradict prior data at vertebrate central synapses since we have not assayed mobility of n-Syb-pH in the absence of endocytic blockade. There is an obvious advantage to restricting SV protein mobility, since this could allow efficient sorting of these proteins into newly formed SVs. It remains to be determined whether other SV proteins will show similarly restricted mobility. The genetic tractability of the Drosophila NMJ may allow future experiments to define the molecular mechanisms that restrict n-Syb-pH mobility within individual synaptic boutons.

Figures

Figure 4-1. Assaying SV release and recycling using n-Syb-pH at the Drosophila NMJ.

(A) The change in the mean fluorescence of n-Syb-pH in response to a 50Hz, 2s stimulus train (n = 6). Fluorescence is normalized to the mean of the first ten time-points, prior to stimulation. The arrow indicates the peak fluorescence reached in response to the stimulus. The time of stimulation is indicated (horizontal bar). All stimulation trains given in this study are 50Hz, 2s.

(B) n-Syb-pH fluorescence intensity levels in response to stimulation at a *shibire*^{ts} mutant synapse. The peak fluorescence level is similar at the permissive (open circles, 22°C) and restrictive temperatures (closed circles, 30°C). At the restrictive temperature, n-Syb-pH fluorescence does not decay after the stimulus, indicating that endocytosis is blocked.

(C) Comparison of peak fluorescence values in response to stimulation at the permissive and restrictive temperatures at *shibire*^{ts} synapses (n = 4). Measurements are from the same synapse, before and after the temperature shift. Values at the two temperatures are not significantly different from each other ($p > 0.98$).

(D) Peak n-Syb-pH fluorescence values are plotted for 15 consecutive stimulation trials, 30 seconds apart, at a wild-type synapse. The peak fluorescence value for each trial is calculated by normalizing the observed increase in fluorescence intensity to the baseline fluorescence (ten time points) prior to each stimulus trial (n = 4).

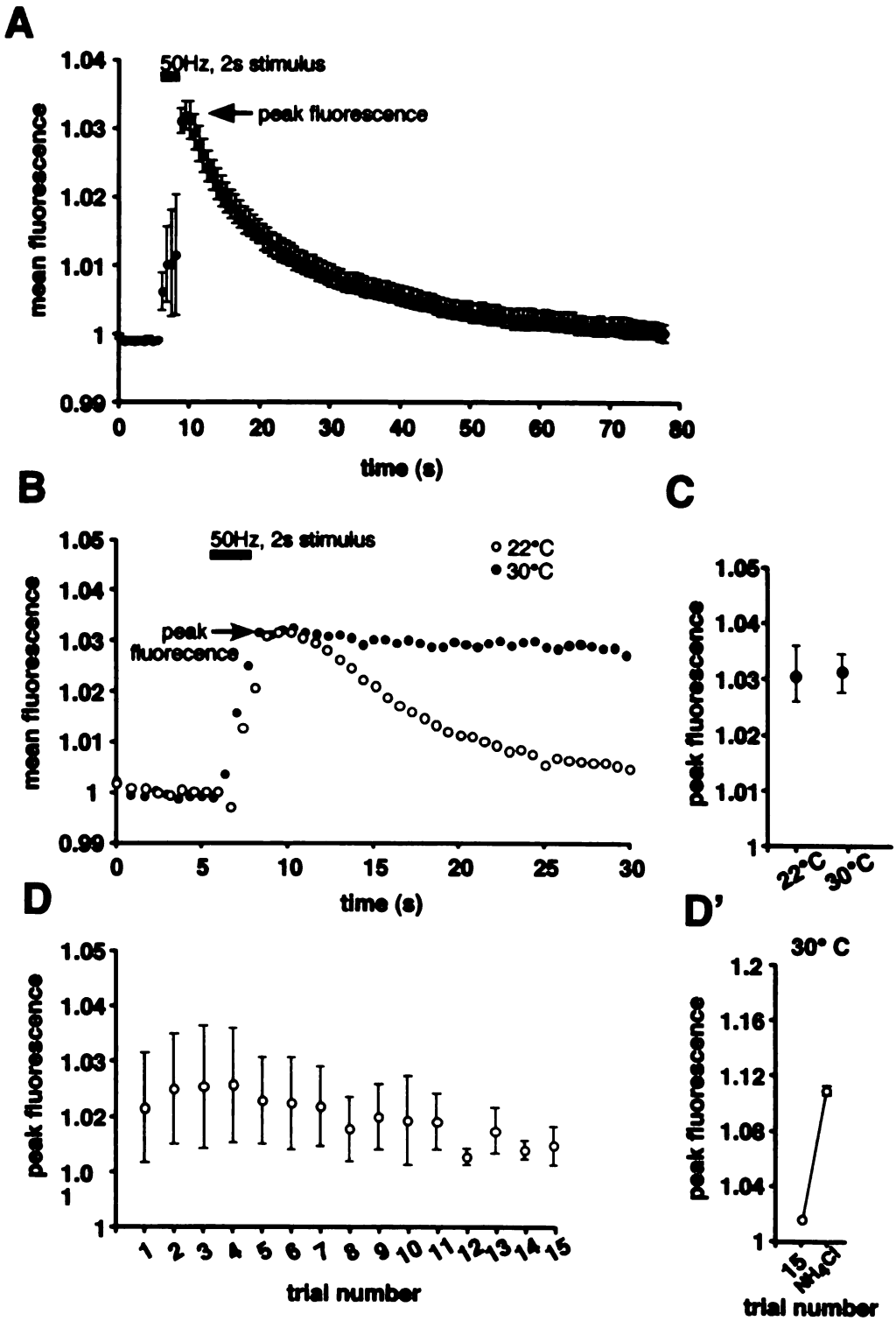
A
50Hz, 2s stimulus
peak fluorescence
mean fluorescence
time (s)
B
50Hz, 2s stimulus
22°C
30°C
peak fluorescence
mean fluorescence
time (s)
C
peak fluorescence
22°C
30°C
D
peak fluorescence
trial number
D'
30° C
peak fluorescence
15 NH4Cl
trial number

Figure 4-2. Stimulation in the presence of bafilomycin provides evidence for a non-recycling, resting pool of SVs.

(A) Example of n-Syb-pH fluorescence intensity changes in response to a stimulus in the absence (open circles) and presence (closed circles) of bafilomycin (Baf). In the presence of Baf, n-Syb-pH fluorescence does not decay following the stimulus train. Peak fluorescence is indicated (arrow).

(B) The peak n-Syb-pH fluorescence change following each stimulus trial is plotted. In the first three trials, the preparation is bathed in HL3 saline without Baf to establish a baseline (trials -3 to -1). The synapse is incubated in Baf for 5 minutes before stimulation trials are resumed (trial 1). Each trial represents the fluorescence increase over and above the prior trial. Note that no further increase in n-Syb-pH fluorescence is observed upon stimulation following trial 5 (n = 5). The addition of Baf is indicated above the graph.

(B') NH_4Cl is added to the preparation following stimulus trial 12. The change in n-Syb-pH fluorescence intensity change upon addition of NH_4Cl is plotted compared to the fluorescence intensity of trial 15 from (B) (n = 5). NH_4Cl application causes a significant increase in fluorescence intensity beyond that which can be achieved during repetitive stimulus trials in the presence of Baf.

A

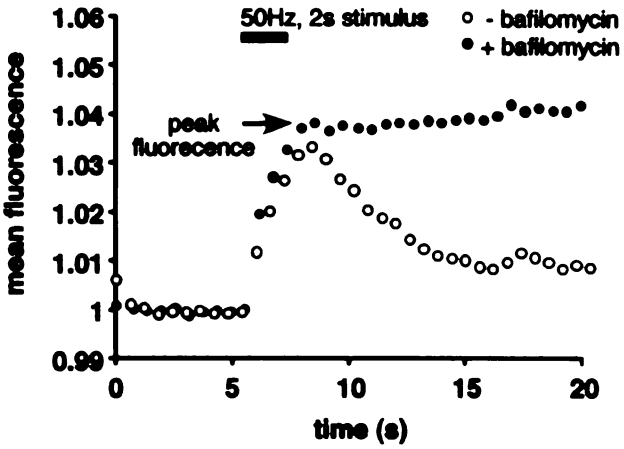
50Hz, 2s stimulus
- bafilomycin
+ bafilomycin
peak fluorescence
mean fluorescence
1.06
1.05
1.04
1.03
1.02
1.01
1
0.99
0
5
10
15
20
time (s)

B

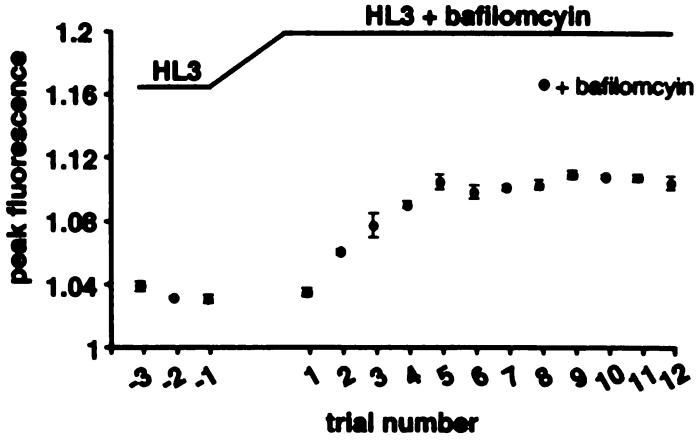
HL3 + bafilomcyin
HL3
+ bafilomcyin
peak fluorescence
1.2
1.16
1.12
1.08
1.04
1
-3 -2 -1 1 2 3 4 5 6 7 8 9 10 11 12
trial number

B'

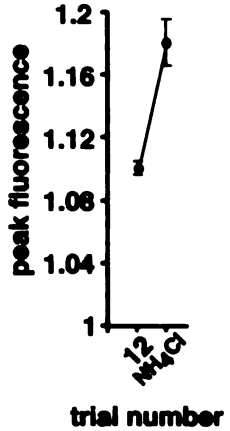
peak fluorescence
1.2
1.16
1.12
1.08
1.04
1
12 NH4Cl
trial number

Figure 4-3. The resting pool of SVs can be mobilized and released under conditions of endocytic blockade.

(A) Peak n-Syb-pH fluorescence levels from 15 consecutive stimulation trials, 30 seconds apart, for wild type (open circles, n = 4) and *shibire^{ts}* (closed circles, n = 2) synapses at 22°C. There is no significant different between peak fluorescence values in any trial.

(A') NH_4Cl is added following stimulus trial 15 (shown in A). NH_4Cl application causes an identical increase in fluorescence intensity in the wild type and *shibire^{ts}* at the permissive temperature.

(B) Peak n-Syb-pH fluorescence levels for wild type synapses held at 22°C (trials -2 and -1) and following a temperature shift to 30°C (trials 1–12). The peak fluorescence value following each trial at 30°C does not change over time (n = 2). The temperature shift is indicated above the graph.

(B') NH_4Cl is added following stimulus trial 12 (shown in B). NH_4Cl application causes a large increase in fluorescence intensity.

(C) Fluorescence intensity at *shibire^{ts}* mutant synapses during repeated stimulus trials. A baseline is established at the permissive temperature (22°C, trials -2 and -1). The shift to the restrictive temperature occurs prior to trial 1. Each trial represents the fluorescence increase over and above the prior trial. Stimulus-dependent increases in fluorescence intensity gradually diminish following trial 7, until trial 12 (n = 4).

(C') NH_4Cl is added following trial 12 and the preparation is held at the restrictive temperature. NH_4Cl application does not cause a further increase in n-Syb-pH

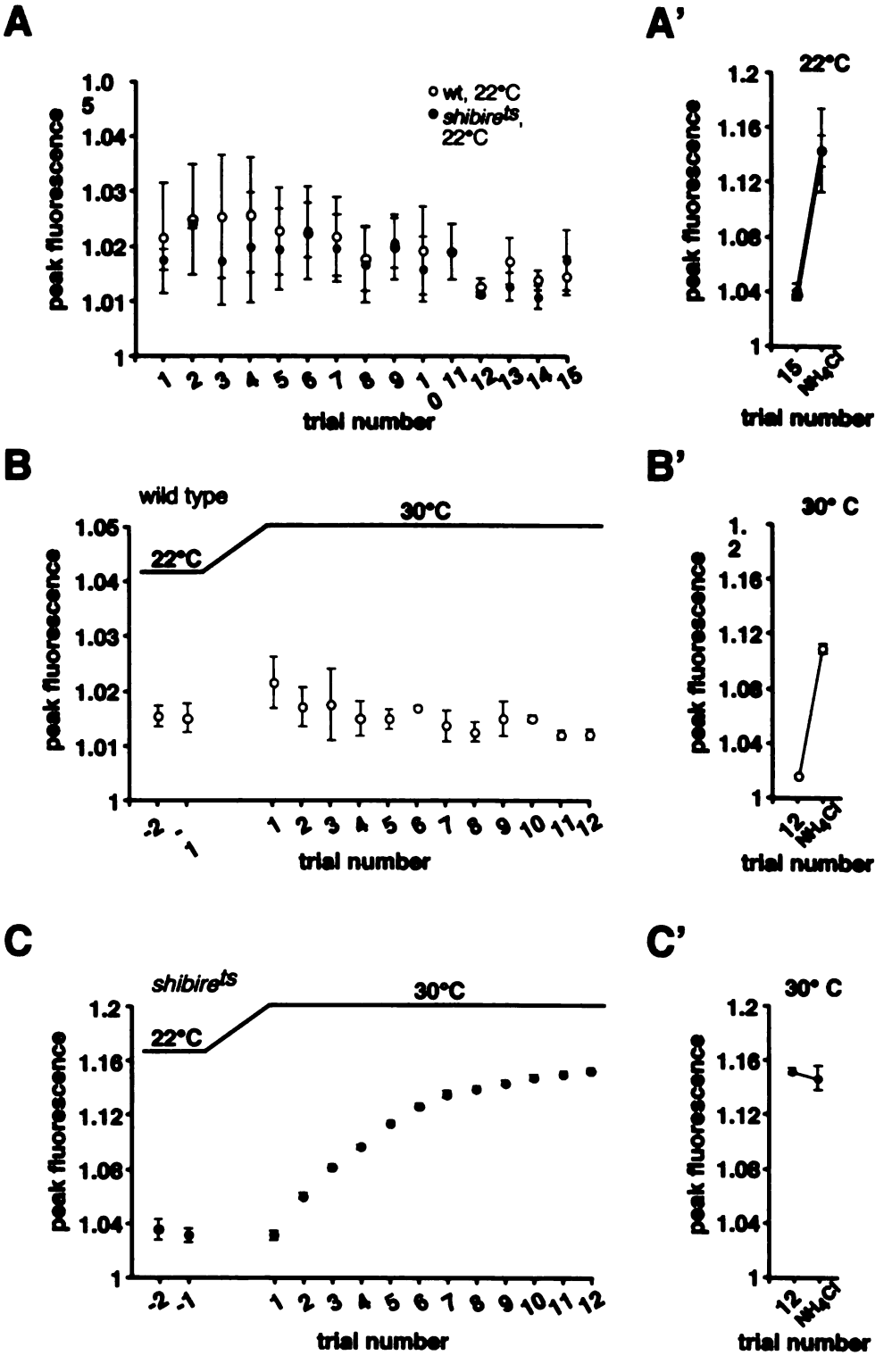
A
A'
B
B'
C
C'
wt, 22°C
shibirets, 22°C
peak fluorescence
trial number
22°C
30°C
wild type
shibirets
NH4Cl

Figure 4-4. Restricted localization of n-Syb-pH at the plasma membrane following endocytic blockade.

(A) Left panel shows baseline n-Syb-pH fluorescence localized to all regions of the presynaptic terminal, with relatively higher fluorescence intensity at the perimeter of synaptic boutons. Right panel shows the same synapse after addition of NH_4Cl. N-Syb-pH fluorescence intensity greatly increases (quantified in Figure 1C'), but is largely absent in the center of synaptic boutons.

(B) Images of *shibire*^{ts} synapses expressing n-Syb-pH. Left panel shows baseline n-Syb-pH fluorescence. Center panel shows the same synaptic terminal after 12 stimulation trials at the restrictive temperature (30°C). Note the higher fluorescence intensity and localization at individual synaptic boutons, but not at inter-bouton regions. Right panel shows same synapse after application of NH_4Cl. Neither n-Syb-pH fluorescence intensity nor localization appears different from the center panel, before NH_4Cl addition.

A wild type

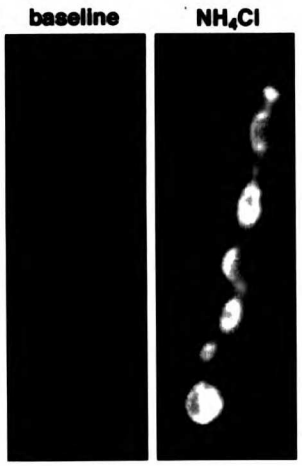

B *shibire^{ts}*

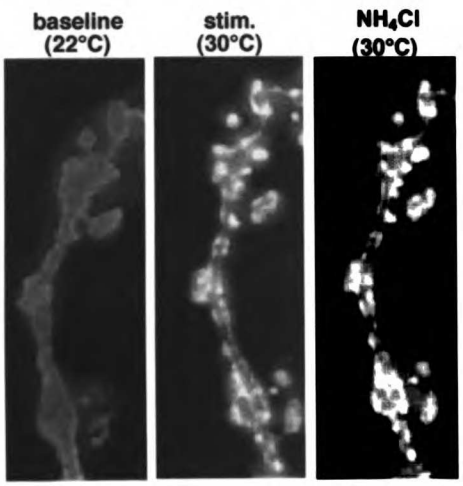

Figure 4-5. Summary and model of synaptic vesicle pools.

(A) Peak fluorescence values from figures 4-2B and 4-3C are replotted on the same graph as indicated. The plateau of fluorescence intensity observed in the presence of Baf (dark grey shading) indicates that we have accessed the entire recycling SV pool in five sequential stimulus trials. The recycling pool of SVs cannot account for the total SV pool since application of NH_4Cl reveals a further fluorescence increase following trial 12 (Figure 2B'). Stimulation under conditions of endocytic blockade (*shibire*^{ts} at the restrictive temperature, light grey) reveals the size of the entire SV pool (total pool). The difference between total pool size and the recycling pool size represents the size of the resting pool of SVs.

(B) Model of SV mobilization from different SV pools. At wild type synapses (left), the recycling pool undergoes active exo- and endocytosis, while the resting pool is not released or recycled. At *shibire*^{ts} synapses (middle), SV exocytosis occurs and endocytosis is blocked. In this case, SVs from the resting pool are mobilized to the active zone and are released. At synapses treated with Baf (right), exo- and endocytosis of SVs in the recycling pool proceeds, even though the SVs are not refilled with neurotransmitter. No resting pool SVs are mobilized or released.

A

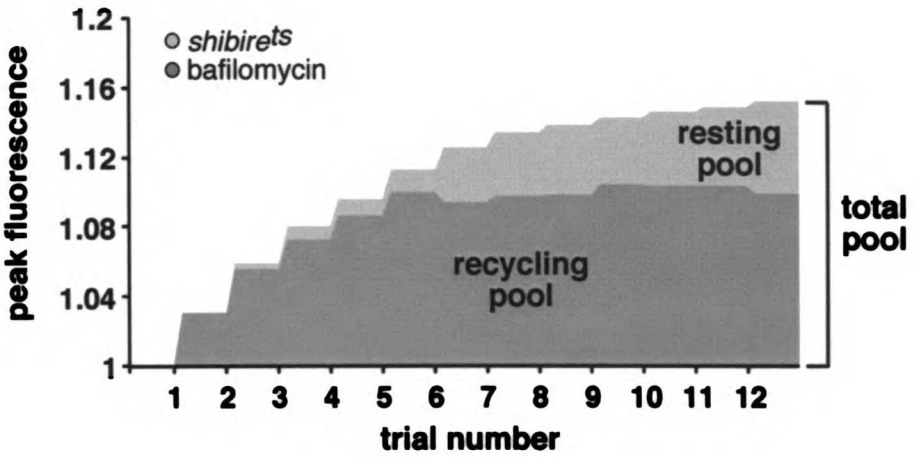
shibire^ts
bafilomycin
peak fluorescence
1.2
1.16
1.12
1.08
1.04
1
resting pool
recycling pool
total pool
1 2 3 4 5 6 7 8 9 10 11 12
trial number

B

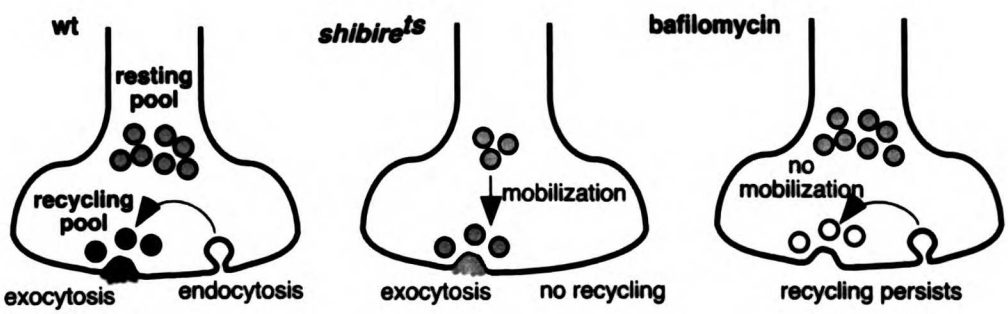
wt
resting pool
recycling pool
exocytosis
endocytosis
shibire^ts
mobilization
exocytosis
no recycling
bafilomycin
no mobilization
recycling persists

Chapter Five:

General Conclusions

Compensatory synaptic vesicle endocytosis is a complex process that enables neurons to communicate quickly (vesicles don't have to be re-synthesized at the cell body), faithfully (constant neuronal size and alignment are maintained), and dynamically (endocytosis compensates for a wide variety of exocytosis events under different conditions). Thus, both the short- and long-term stability of neural circuits are dependent on synaptic vesicle recycling in the pre-synaptic terminal. Although synaptic vesicle endocytosis is much less understood than exocytosis, recent experimental techniques have allowed us to begin to unravel the molecular and phenomenological details of the endocytic process. New techniques are necessary to study endocytosis since it cannot be stimulated—and therefore assayed—independently from exocytosis. In addition, the two phases of the synaptic vesicle cycle involve vastly different cell biological events that are accessible to different experimental methods. On a basic level, exocytosis regulates the fusion of a small, spherical membrane with that of a larger and molecularly distinct sheet of membrane. In contrast, endocytosis directs the process of forming a small, free, spherical membrane with distinct components from a vast expanse of membrane. From this description, it makes sense that each process involves the action of different molecular machines.

Detection and Dissection of Endocytosis with Fluorescence

Syaptotagmin I (Syt I) was originally identified as a 65 kD synaptic antigen that was labeled by an antibody raised against synaptic junctional complexes (Matthew et al., 1981). Most of the functional work that followed its initial description has focused on the role that Syt I plays in exocytosis, since synchronous, calcium-dependent neurotransmitter release is dramatically impaired in Syt I mutants in *Drosophila* and mouse (Geppert et al., 1994; Littleton et al., 1993). Endocytosis in Syt I mutants, as well as in wild type animals, has been much more difficult to describe, for two main reasons. First, by definition, compensatory synaptic vesicle endocytosis is not thought to occur without prior exocytosis. Thus, if exocytosis is inhibited, the investigation of endocytosis is problematic. Secondly, until recently, methods to directly study endocytosis at a genetically altered synapse did not exist. Conclusions about the function of Syt I presented in this thesis—that it *is* necessary for endocytosis, and that it can independently regulate different aspects of the endocytic process—were reached through the application of new technologies to address both of these problems. We have experimentally uncoupled exo- and endocytosis using the *shibire*^{ts} mutant, and have disrupted protein function specifically during endocytosis with FlAsH photoinactivation. Further, the synapto-pHluorins (spH) have allowed us to monitor endocytosis in real time during perturbations in the Syt I protein.

Application of this combination of techniques could next be applied to other synaptic molecules to help form a greater understanding of synaptic vesicle endocytosis. The endocytosis kinetics measured with n-Syb-pH in the Syt I mutant (Chapter 2 and 3) represent the first time that endocytic rate has been directly assayed in a genetic mutant,

in vivo. Mutations exist in other *Drosophila* endocytic proteins, such as endophilin, DAP160, and synaptojanin (Marie et al., 2004; Verstreken et al., 2002; Verstreken et al., 2003). Expressing n-Syb-pH in these backgrounds and tracking its fluorescence dynamics in response to various stimulation conditions could reveal precise, and additional, functions of these proteins. Double mutant combinations may also permit epistasis experiments that probe which molecular interactions are upstream of others in the course of endocytosis. In addition to genetic perturbations, stimulus conditions could be varied to observe how endocytosis can dynamically respond. For example, it will be intriguing to investigate the effect of changing calcium concentration on endocytosis at both wild type and mutant synapses.

In combination with the spH technology, protein photoinactivation holds much promise in this field of study. Some particular proteins especially clamor for acute inhibition of function only during endocytosis. One is stoned, which interacts genetically and biochemically with Syt I, as well as other components of the endocytic machinery (Martina et al., 2001; Phillips et al., 2000; Stimson et al., 1998; Walther et al., 2001). Stoned has been implicated in multiple steps of the synaptic vesicle cycle, including exocytosis and clathrin-uncoating, but endocytosis has not yet been assayed in real time at stoned mutant synapses. Its biochemical association with Syt I suggests that stoned has the potential to function in exocytosis and/or endocytosis. Assaying n-Syb-pH fluorescence in stoned mutants, and during acute inactivation of stoned at different time points in the vesicle cycle, may help to clear up the controversy.

Since the earliest descriptions of endocytosis at the synapse, there have been disagreements about the role of clathrin in this process. Now that methods exist to

temporally and spatially inactivate proteins while assaying real time endocytosis, many questions about the role of clathrin can be addressed. First, to test how much of endocytosis is clathrin-dependent, clathrin could be inactivated so that the clathrin lattice cannot form. By testing whether residual endocytosis takes place after this perturbation, these experiments may reveal if a clathrin-independent, kiss-and-run mode of endocytosis occurs at this synapse. Next, some of the hypotheses about the role of clathrin in synaptic vesicle endocytosis are based on the localization of clathrin coat and accessory proteins at the synaptic peri-active zone (Estes et al., 1996; Gonzalez-Gaitan and Jackle, 1997; Marie et al., 2004). However, it remains possible that these proteins are localized to the peri-active zone to facilitate *other* forms of clathrin-mediated endocytosis, such as receptor-mediated endocytosis. Acutely inactivating clathrin and assaying endocytosis of synaptic vesicles, specifically, could help distinguish whether the clathrin coat, accessory, and scaffolding proteins at the synapse are truly necessary for compensatory synaptic vesicle endocytosis. Finally, spatial information about the nature of clathrin-dependent synaptic vesicle endocytosis may be obtained by using the ReAsH ligand, an analogue of FlAsH that fluoresces in the red spectrum and can be photoconverted to form an electro-dense marker for EM visualization (Gaietta et al., 2002). At the *Drosophila* NMJ, clathrin coats are difficult to discern with EM, so a ReAsH-bound clathrin molecule could be very useful to visualize and pinpoint the localization of clathrin lattice formation during different stages of endocytosis. This would be useful in wild-type animals to describe normal synaptic vesicle endocytosis. It could also be particularly informative in other endocytic mutant backgrounds, to observe the formation and mis-formation of the clathrin lattice during specific perturbations in

the endocytic process. This sort of experimental approach could expand our understanding of the precise order of the protein-protein interactions important for rapid synaptic vesicle endocytosis.

In addition to inactivating stoned and clathrin, it could also be advantageous to try to inactivate only certain domains of other endocytic proteins. Until now, the endocytosis field has been working to identify which molecules are important for endocytosis, and where they might function within the process. Our structure-function experiments with point mutations in Syt I revealed that this protein not only has more than one function within the vesicle cycle, but also that it coordinates more that one aspect of endocytosis (Chapter 3). Certainly, the potential multiple functions of other endocytic proteins could be more specifically described through elimination—either through acute inactivation or genetically—of individual protein domains or interaction residues.

While investigating the endocytic function of Syt I, we were able to say something profound about the process of synaptic vesicle endocytosis itself. Endocytosis has previously been described as a multi-step process, made up of different phases of membrane bending and fission. However, the rate with which some of these steps occur hasn't been described as separate from any other characteristics of the process. For instance, it has been assumed that if the mechanisms that control the size of newly re-formed synaptic vesicles are inhibited, the entire process of endocytosis will be slowed. We have shown that this is not necessarily the case, because the mutation of different residues in Syt I can specifically alter either the rate of endocytosis or the size of newly recycled synaptic vesicles. These findings raise questions about what mechanisms may

control other aspects of endocytosis—such as synaptic vesicle protein composition and the localization—so that they all are coordinated synchronously. Indeed, in specifically studying different aspects of endocytosis, we may come to discover that these characteristics of synaptic vesicle endocytosis are more independent from each other than is currently believed.

Linking Exocytosis and Endocytosis

It has been demonstrated in many systems—with capacitance, ultrastructural, and imaging methods—that endocytosis occurs following synaptic vesicle exocytosis, and is therefore coupled to vesicle release. However, the process of endocytosis can be uncoupled from exocytosis, as demonstrated by the *shibire*^{ts} mutant, which selectively blocks only vesicle endocytosis (Koenig et al., 1983). Since endocytosis is a very different biological problem than exocytosis, it makes sense that these processes *would* function somewhat independently. A key to further understanding endocytosis is to determine just how dependent it is on exocytosis, and what mechanisms control this coordination. Thus, it would be interesting to determine if endocytosis can ever be stimulated to occur in the absence of exocytosis. This is theoretically possible if both exo- and endocytosis are triggered separately, for example, by an increase in calcium concentration. This hypothesis could be tested experimentally by expressing n-Syb-pH in a *syntaxin*^{ts} mutant background. Nerve stimulation would cause an influx of calcium through voltage-gated calcium channels, but all synaptic vesicle exocytosis is blocked in

this mutant at the restrictive temperature (Littleton et al., 1998). A decay in n-Syb-pH fluorescence following stimulation would then indicate if any synaptic vesicle protein normally resident on the plasma membrane is internalized, and therefore if calcium influx could trigger the start of endocytosis. Ultrastructural analysis in this experiment could also reveal whether any steps prior of endocytosis to vesicle re-acidification occurred.

If calcium does not independently trigger exo- and endocytosis on its own, it seems likely that there are protein or lipid molecules involved in both processes that act couple them. However, it remains an open question whether a molecule (such as Syt I) shown to be involved in both processes can truly be said to couple them. In other words, Syt I may have a role in both exo- and endocytosis without necessarily linking one with the other. Exocytosis/endocytosis coupling can be considered to regulate three features of synaptic vesicle recycling: timing the start of endocytosis immediately after exocytosis, matching the extent and composition of protein and membrane internalized with that released, and recycling synaptic vesicles into the same active zone vesicle pool from which they were released. Before a protein can be said to couple exo- and endocytosis, it must be shown that it regulates one of these features. Evidence presented here (Chapter 3) suggests that the calcium-coordinating residues in the C_2B domain of Syt I could potentially initiate synaptic vesicle endocytosis. If shown to be true, this would strengthen the argument that Syt I can couple endocytosis to exocytosis. However, this would not rule out another molecular mechanism at work in regulating other aspects of exocytosis/endocytosis coupling. As a first step toward determining what these may be, it is necessary to figure out what molecules other than Syt I have functions in both exo- and endocytosis. Investigating the function and interacting

partners of these putative "couplers" should provide clues as to how the processes are linked.

One way that exo- and endocytosis coupling might impact neural function is through the partitioning of recycling vesicles into different pools. Data presented in Chapter 4 describe a new assay for the quantification of the proportion of vesicles residing in either an active recycling pool or an inactive reserve pool. The segregation of vesicles into distinct functional pools may be regulated by the neuron in response to—or in order to respond to—various neural stimuli. Assaying the percentage of synaptic vesicles within these two pools in different mutant backgrounds may allow us to determine how important this partitioning is to dynamic neural function. For example, when there is a decrease in post-synaptic responsiveness to neurotransmitter release, the pre-synaptic cell can compensate by increasing the number of vesicles released per action potential (Paradis et al., 2001; Petersen et al., 1997). In cases like this, where pre-synaptic function is altered, it will be interesting to know whether and how the ratio of recycling to non-recycling vesicles is modulated.

Experimental Procedures

Chapter Two: Synaptotagmin I is Necessary for Synaptic Vesicle Endocytosis

Construction of UAS-n-syb-pHluorin

Superecliptic pHluorin GFP was obtained from Dino DeAngelis and Jim Rothman (Sloan-Kettering). To fuse the pHluorin GFP to the C-terminal of n-syb, a BsrB1 site was added to the 3' end of an n-syb cDNA (from Tom Schwarz, Harvard) using the oligos 5'n-syb (ACAGCCGAATTCGCTGAGGC) and 3'n-sybBsrB1 (CCAATTAGATCTCCGCTCACGCCGCCGTGATCGCC). An Xba1 site was added to the 3'end and a BsrB1 site was added to the 5' end of the pHluorin GFP using the oligos 5'GFPBsrB1 (CACGGCGGCGTGGAGCGGCGGAAGCGGCGGG) and 3'GFPXba (TAGCTTCTAGATTAACCGGTTTTGTATAG). PCR fragments were then digested with BsrB1 and ligated together. The appropriate fragment was purified and used as a template for a second round of PCR using the oligos 5'n-syb and 3'GFPXba. The resulting product was then digested with EcoR1 and Xba1 and ligated into pUAST. The resulting clone was sequenced before injecting into *yw* embryos.

Flies

The *UAS-n-Syb-pH* transgene was recombined with *elaV^{3E1}-GAL4*, and balanced with a TM6b chromosome. For the *shibire^{ts}* experiments, *w,shi^{ts2}* was crossed to *UAS-n-Syb-pH, elaV^{3E1}/TM6b* and male larvae were selected against *TM6b*. The *syt^{null}* flies were made by crossing *syt^{AD4}/CyO-GFP;UAS-n-Syb-pH/TM6b* to *syt^{D27}/Cyo-GFP;elaV^{3E1}/TM6b* and selecting against TM6b and Cyo-GFP expression. For the FlAsH-FALI experiments,

syt^{AD4},*UAS-syt4C/CyO-GFP;UAS-n-Syb-pH/TM6b* was crossed to *syt*^{D27}/*CyO-GFP;elaV*^{3E1}/*TM6b* and larvae were selected against CyO-GFP expression. The FlAsH-FALI-*shibire*^{ts} experiments were performed by crossing *w*, *shi*^{ts2};*syt*^{D27}/*CyO-GFP;elaV*^{3E1}/*TM6b* to *syt*^{AD4},*UAS-syt4C/CyO-GFP;UAS-n-Syb-pH/TM6b* and selecting males against CyO-GFP and TM6b expression.

Solutions

Third instar Drosophila larvae were dissected in Ca^{2+}-free HL3 saline, supplemented with calcium and adjusted to pH 7.0 (Marek and Davis, 2002). All experiments were performed in 0.5 mM calcium with the exception of experiments in Figure 2-2E–G, which were performed in 2.0 mM calcium. For FlAsH experiments, dissected animals were either incubated in FlAsH solution (Invitrogen), or in a mock-FlAsH solution then rinsed to remove unbound FlAsH (Marek and Davis, 2002). Larvae were transferred back to HL3 saline before imaging. HL3 saline was adjusted to pH 5.5 in the acid-wash experiments. Ammonium chloride (NH_4Cl) HL3 saline was made by replacing 50 mM NaCl with NH_4Cl and adjusting to pH 7.4.

Imaging and analysis

Images were captured on a Zeiss Axioskop 2 microscope with a water-immersion objective (100x, 0.97 N.A.) using SlideBook software (Intelligent Imaging Innovations). Images were acquired with a Quantix cooled CCD camera including a back-thinned EEV57 chip (Roper Scientific). Illumination was provided by a 175W xenon arc lamp and GFP or CY3 filter sets. Time-lapse imaging (500 ms exposures) was used to

measure the fast time-course of fluorescence changes (Figures 2-2–3,6). Data were quantified by defining a region of interest including multiple synaptic boutons (each bouton contains multiple active zones) using the threshold function of SlideBook. The mean fluorescence intensity of this region was calculated for each time-point. FlAsH-FALI was performed by illuminating the preparations as for fluorescence imaging. The NMJ at muscles 6 and 7 in segments A2–A4 were selected in all experiments. In all experiments, scale represents arbitrary fluorescence units. Data are expressed as average ± SEM.

Acid-wash experiments

Synapses were stimulated at the segmental nerve for 5 seconds at 50 Hz in 2.0 mM Ca^{2+} and imaged for 3 minutes before the HL3 saline (pH 7.0) in the bath was replaced with low pH acid-wash (pH 5.5).

FM4-64 experiments

10 μM FM4-64 (Molecular Probes) was made in HL3 + 0.5 mM Ca^{2+} saline and added to the bath. The nerve was stimulated for 1 minute at 30 Hz. The synapse was then illuminated for 2 minutes. The preparation was washed repeatedly in Ca^{2+}-free HL3 for 5 minutes, and an image of the synapse was captured. To analyze FM4-64 uptake, the fluorescence in the green channel was used to define the region of interest and the mean intensity of the fluorescence in the red channel defined by this region was calculated. We selected a small region of interest over the muscle background and the mean intensity of

this region was subtracted from the synapse intensity to correct for variability in background FM4-64 levels.

shibire^{ts} experiments

Temperature was controlled by a heating/cooling stage with a Peltier module (Brook Industries) and monitored with a temperature probe in the imaging chamber. In Figure 2-2d, the nerve was stimulated identically (2 s, 50 Hz) at the permissive (22°C) and restrictive temperatures (30°C). In the FlAsH experiments (Figure 2-4–5), we stimulated at the restrictive temperature (2 s, 50 Hz, in HL3) every 10 seconds for 200 seconds to deplete synaptic vesicles. Following stimulation, the synapse was illuminated for 2 minutes. The chamber was then brought down to the permissive temperature. Images of the synapse were taken at ~2 minute intervals following return to the permissive temperature, and the mean intensity of the synapse was measured at each time-point.

Chapter Three: Discrete Residues in the C_2B Domain of Synaptotagmin I Independently Specify Endocytic Rate and Synaptic Vesicle Size

Flies

The synapto-pHluorin transgene (*UAS-n-Syb-pH*) was expressed pre-synaptically using the *elaV^{3E1}-GAL4* driver in all synapto-pHluorin experiments. The various *syt* flies harboring mutant alleles (*AD1*, *AD3*, *AD4*, *D27*, *N13*, *T7*, and *T41*) were made by crossing *syt^{X}/CyO-GFP;UAS-n-Syb-pH/TM6b* to *syt^{X}/Cyo-GFP;elaV^{3E1}/TM6b* (where *X=syt* allele) and selecting against TM6b and Cyo-GFP expression. For the FlAsH experiment, *w,shi^{ts2};syt^{D27}/CyO-GFP;elaV^{3E1}/TM6b* flies were crossed to *syt^{AD4},UAS-syt4C/CyO-GFP;UAS-n-Syb-pH/TM6b* flies, and males were selected against CyO-GFP and TM6b expression. For rescue experiments, *syt^{N13}/CyO[tubgal80];elaV^{3E1},UAS-n-Syb-pH/TM6b* flies were crossed to *syt^{AD4}/CyO-GFP;UAS-syt$^{(wt.\ or\ D3,4N,\ or\ KQ,\ or\ D229N)}$/TM6b* flies and non-CyO, non-TM6b flies expressing n-Syb-pH were selected. To promote survival of mutant flies, eggs were laid on apple plates with yeast paste. The appropriate larvae were chosen and transferred to another apple plate in a large petri dish lined with wet Kimwipes for humidity. Small drops of liquid containing water and dissolved yeast were placed on the apple plates each day for the larvae to feed on.

Solutions

Third instar Drosophila larvae were dissected in Ca^{2+}-free haemolymph-like (HL3) saline (Stewart et al., 1994). All live imaging and electrophysiology experiments were

performed in HL3, supplemented with indicated calcium levels. Imaging experiments were done in the presence of 100 μM 1-napthylacetyl spermine trihydrochloride (Sigma) to block post-synaptic glutamate receptor activation and muscle contraction, and enable accurate fluorescence imaging at all time-points. Application of this drug does not alter presynaptic function or n-Syb-pH fluorescence intensity (data not shown). For FlAsH experiments, dissected animals were either incubated for five minutes in FlAsH solution (now called Lumio, Invitrogen), or in a mock-FlAsH solution, then rinsed in an EDT_2 solution for five minutes to remove unbound FlAsH (see (Poskanzer et al., 2003)). Larvae were transferred back to HL3 saline before imaging.

Light microscopy and analysis

Live imaging was done on a Zeiss Axioskop 2 microscope with a water-immersion objective (63x, 0.90 N.A.) using SlideBook software (Intelligent Imaging Innovations). Images were acquired with a cooled CCD camera including a back-thinned EEV57 chip (Roper Scientific), or using the Cascade 512b (Roper Scientific). Illumination was provided by a 175 W xenon arc lamp, liquid light guide and GFP filter set. Time-lapse imaging was carried out using continuous 500 ms exposure times. Data were quantified by defining a region of interest that included multiple synaptic boutons, using the threshold function of SlideBook. The $\Delta F/F$ of this entire region was calculated for each time-point. τ values for n-Syb-pH kinetics were calculated by fitting the fluorescence decay following stimulation to a single exponential function, using Igor Pro software (WaveMetrics, Inc.). Fluorescent data were fit to each experimental curve prior to averaging or normalization. FlAsH-FALI was performed by illuminating the

preparations as for fluorescence imaging. Immunostained synapses were imaged on a Zeiss Axiovert 200 using a cooled CCD camera (Kodak 1401E chip, Roper Scientific). Samples were illuminated with a 175 W xenon arc lamp and an oil immersion objection (100x, 1.4 N.A.). Synapses were optically sectioned at 0.2 μm (15–30 sections/synapse) using a piezo-electric z-drive. Projection images showing the maximum fluorescence levels through the z-stack are shown. The NMJ at muscles 6 and 7 were selected in all experiments.

Electron microscopy

Larvae were prepared for electron microscopy following stimulation by conventional procedures. HL3 saline bathing the filleted larvae was exchanged for 2% glutaraldehyde in 0.12 M Na-cacodylate buffer (pH 7.4) and larvae were allowed to fix for 10 minutes. Larvae were then transferred to vials containing fresh fixative for a total aldehyde fixation of 2 hours. The fixed larvae were rinsed 3 x 15 minutes with 0.12 M Na-cacodylate buffer and post-fixed with 1% osmium tetroxide in 0.12 M Na-cacodylate buffer. After post-fixation, larvae were rinsed 2 x 15 minutes with 0.12 M Na-cacodylate buffer and 2 x 15 minutes with water, then stained *en bloc* with 1% aqueous uranyl acetate for 1 hour. Larvae were rinsed with water, dehydrated with an ethanol series, passed through propylene oxide, and infiltrated and embedded with Eponate 12 resin. All processing steps were done at room temperature with rotation except the initial 10 minute fixation of the filleted preparations, for which rotation was impractical. Thin sections were cut with a Leica Ultracut T ultramicrotome, collected on Formvar-coated slot grids, and stained with 5% uranyl acetate for 10 minutes followed by Sato's lead for 3

minutes (Sato, 1968). Sections were photographed with a JEOL 1200 EX/II using film or an FEI T12 EM with a digital camera, both operated at 80 kV. For quantification, the diameter of vesicular structures within 200 nm of each pre-synaptic active zone was measured. Multiple synaptic boutons from at least two animals from each genotype were analyzed.

Immunostaining

Third instar larvae were dissected in Ca^{2+}-free HL3 saline and fixed in Bouin's fixative for two minutes (Syt, 1:500, gift of Troy Littleton) or in 4% paraformaldehyde for 20 minutes (α-adaptin, 1:50, gift of Marcos González-Gaitán). Immunocytochemistry with each antibody was performed with all of the larval fillets in the same reaction tube for accurate comparison of fluorescence intensity levels across genotypes.

Electrophysiology

Recordings were made from muscle 6 in abdominal segment A3 of third instar larvae with sharp electrodes (15–20 MΩ). Preparations were bathed in HL3 at the indicated Ca^{2+} concentration. Recordings were accepted for analysis with resting membrane potentials more hyperpolarized than -60 mV and with input resistances greater than 5 MΩ. Motoneuron stimulation was achieved with a polished suction electrode, at the rate and frequencies indicated. Preparations were visualized during recording with an Olympus fixed stage microscope and 40x water immersion lens. Data were recorded with PCLAMP software and an axoclamp 2B amplifier with additional 10x amplification

Chapter Four: Mobilization and Fusion of a Non-Recycling Pool of Synaptic Vesicles

Flies

The *UAS-n-Syb-pH* transgene was recombined with *elaV*$^{3L.1}$*-GAL4*, and balanced with a *TM6b* chromosome. For control and bafilomycin experiments, these flies were crossed to *yw* flies, and non-*TM6b* larvae were selected. For *shibire*^{ts} experiments, w,*shi*^{ts2} females were crossed to *UAS-n-Syb-pH*, *elaV*$^{3L.1}$*/TM6b* males and male larvae were selected against *TM6b*. Flies were raised on standard food at room temperature. The NMJ at muscles 6 and 7 in segments A2–A4, in third instar larvae, were selected in all experiments.

Solutions

Third instar Drosophila larvae were dissected in Ca^{2+}-free HL3 saline (70mM NaCl, 5 mM KCl, 70mM $MgCl_2$, 10 mM $NaHCO_3$, 115mM sucrose, 5mM trehalose, 5mM HEPES), supplemented with calcium for a final concentration of 0.5 mM Ca^{2+}, and adjusted to pH 7.0. Bafilomycin A1 (Sigma) solution (1 μM) was made up in HL3 + 0.5 mM Ca^{2+}. Ammonium chloride (NH_4Cl) HL3 saline was made by replacing 50 mM NaCl with NH_4Cl and adjusting the pH to 7.4.

Imaging and analysis

Images were captured on a Zeiss Axioskop 2 microscope with a water-immersion objective (100x, 0.97 N.A.) using SlideBook software (Intelligent Imaging Innovations).

Images were acquired with a Quantix cooled CCD camera including a back-thinned EEV57 chip (Roper Scientific). Illumination was provided by a 175W xenon arc lamp and GFP filter set. 500 ms time-lapse exposures were captured in all experiments. Data were quantified by defining a region of interest using the threshold function of SlideBook software that included the synapse area. The mean fluorescence intensity of this region was calculated for each time-point. Data are expressed as average ± SEM.

shibire^{ts} experiments

The temperature of the microscope stage was controlled by a heating/cooling stage with a Peltier module (Brook Industries) and monitored with a probe in the imaging chamber. The chamber saline temperature was held at 22°C for trials at the permissive temperature, then raised to the restrictive temperature (30°C) for the rest of the trials. The shift between temperatures requires approximately five minutes.

Bafilomycin experiments

As in the *shibire*^{ts} experiments, motoneurons were stimulated and the synapse was imaged before bafilomycin addition. Bafilomycin was added to the preparation and allowed to incubate for five minutes before stimulation. We have previously shown that this amount of incubation time is sufficient to block SV re-acidification at this synapse (Poskanzer et al., 2003).

Appendix:

Synapto-pHluorin Imaging at the *Drosophila* NMJ

A wide field fluorescent microscope is used to optically record fluorescence dynamics of the pre-synaptically expressed synapto-pHluorins. First, a standard recording pipette is pulled from a glass capillary tube; this will serve as the stimulating pipette. The recording pipette has a long, thin tip that is necessary to fit under the high power objectives (100x and 63x) with small working distances used for fluorescence imaging. The first few millimeters of the tip should be broken off using forceps. This broken tip is then polished so the opening is as large as a standard suction stimulating pipette for NMJ electrophysiology. The pipette is bent by about 30–40 degrees by holding it over a narrow flame. An aluminum foil "hat" on a Bunsen burner can be used to decrease the diameter of the normal flame; a large flame will easily melt the tip of pipette. The pipette needs to be bent so that the tip fits under the objective, but the rest of the pipette does not touch the imaging chamber during the experiment; this is especially important for imaging under a 100x water-immersion objective (working distance = 1 mm).

Once the suction electrode is set up in a micromanipulator, the larva should be dissected in a chamber similar to that used for *Drosophila* NMJ electrophysiology, except with only one layer of magnetic tape, again to maximize working distance between the chamber and the objective. The HL3 saline used for standard synapto-pHluorin imaging should be at pH 7.0. The synapse (muscle 6/7) can be identified under bright-field illumination, and then the synapto-pHluorins can be imaged under a GFP filter set. A flat section of the synapse should be imaged to maximize the amount of the terminal that is in focus. Often, the section most proximal to the end-terminal bouton of a branch is

the flattest, rather than the part of the pre-synaptic terminal closest to the axon. Using an *elaV'-GAL4* to drive the *UAS-syb-pH* transgene, the 1s boutons often have a higher basal fluorescence level than 1b boutons. Images are captured continuously under "rapid capture" mode so that there are no breaks between exposures and the camera shutter remains open for the course of the experiment. For high frequency, long stimulation experiments, imaging is carried out in 100μM naphthylacetyl spermine, a glutamate receptor antagonist that blocks muscle contraction. This can be re-used multiple times throughout experiments carried out over the course of a day.

For bafilomycin experiments, a 10 μM bafilomycin stock is made up in DMSO and kept at -20° C. For synapto-pHluorin imaging experiments, bafilomycin is diluted to 0.1 μM in HL3 saline. When added to a preparation, the bafilomycin will cause a gradual increase in synapto-pHluorin fluorescence intensity, as the pH in internal compartments becomes more neutral. Different concentrations of bafilomycin will block vesicle re-acidification with varying time courses. A 0.1 μM bafilomycin solution will successfully block re-acidification of synaptic vesicles after a 1.5 minute incubation. After this time, the nerve can be stimulated and fluorescence dynamics recorded. Again, for high frequency, long duration stimulus trains, 100 μM naphthylacetyl spermine should be added to the solution with the bafilomycin. Although previous studies have reported that bafilomycin can be washed off from the neuron to restore normal synaptic function, it has been difficult to do so at the *Drosophila* NMJ. However, the bafilomycin can be reused for multiple imaging experiments.

References

Aravanis, A. M., Pyle, J. L., and Tsien, R. W. (2003). Single synaptic vesicles fusing transiently and successively without loss of identity. Nature *423*, 643-647.

Bauerfeind, R., Takei, K., and De Camilli, P. (1997). Amphiphysin I is associated with coated endocytic intermediates and undergoes stimulation-dependent dephosphorylation in nerve terminals. J Biol Chem *272*, 30984-30992.

Betz, W. J., Mao, F., and Bewick, G. S. (1992). Activity-dependent fluorescent staining and destaining of living vertebrate motor nerve terminals. J Neurosci *12*, 363-375.

Beutner, D., Voets, T., Neher, E., and Moser, T. (2001). Calcium dependence of exocytosis and endocytosis at the cochlear inner hair cell afferent synapse. Neuron *29*, 681-690.

Brodin, L., Low, P., and Shupliakov, O. (2000). Sequential steps in clathrin-mediated synaptic vesicle endocytosis. Curr Opin Neurobiol *10*, 312-320.

Brose, N., Petrenko, A. G., Sudhof, T. C., and Jahn, R. (1992). Synaptotagmin: a calcium sensor on the synaptic vesicle surface. Science *256*, 1021-1025.

Ceccarelli, B., Hurlbut, W. P., and Mauro, A. (1973). Turnover of transmitter and synaptic vesicles at the frog neuromuscular junction. J Cell Biol *57*, 499-524.

Chapman, E. R., An, S., Edwardson, J. M., and Jahn, R. (1996). A novel function for the second C2 domain of synaptotagmin. Ca2+-triggered dimerization. J Biol Chem *271*, 5844-5849.

Chapman, E. R., Desai, R. C., Davis, A. F., and Tornehl, C. K. (1998). Delineation of the oligomerization, AP-2 binding, and synprint binding region of the C2B domain of synaptotagmin. J Biol Chem *273*, 32966-32972.

Chen, H., Fre, S., Slepnev, V. I., Capua, M. R., Takei, K., Butler, M. H., Di Fiore, P. P., and De Camilli, P. (1998). Epsin is an EH-domain-binding protein implicated in clathrin-mediated endocytosis. Nature *394*, 793-797.

Chen, H., Slepnev, V. I., Di Fiore, P. P., and De Camilli, P. (1999). The interaction of epsin and Eps15 with the clathrin adaptor AP-2 is inhibited by mitotic phosphorylation and enhanced by stimulation-dependent dephosphorylation in nerve terminals. J Biol Chem *274*, 3257-3260.

Chen, Y., Deng, L., Maeno-Hikichi, Y., Lai, M., Chang, S., Chen, G., and Zhang, J. F. (2003). Formation of an endophilin-Ca2+ channel complex is critical for clathrin-mediated synaptic vesicle endocytosis. Cell *115*, 37-48.

Cousin, M. A., and Nicholls, D. G. (1997). Synaptic vesicle recycling in cultured cerebellar granule cells: role of vesicular acidification and refilling. J Neurochem *69*, 1927-1935.

Cousin, M. A., Tan, T. C., and Robinson, P. J. (2001). Protein phosphorylation is required for endocytosis in nerve terminals: potential role for the dephosphins dynamin I and synaptojanin, but not AP180 or amphiphysin. J Neurochem *76*, 105-116.

Daly, C., Sugimori, M., Moreira, J. E., Ziff, E. B., and Llinas, R. (2000). Synaptophysin regulates clathrin-independent endocytosis of synaptic vesicles. Proc Natl Acad Sci U S A *97*, 6120-6125.

Damke, H., Baba, T., Warnock, D. E., and Schmid, S. L. (1994). Induction of mutant dynamin specifically blocks endocytic coated vesicle formation. J Cell Biol *127*, 915-934.

David, C., McPherson, P. S., Mundigl, O., and de Camilli, P. (1996). A role of amphiphysin in synaptic vesicle endocytosis suggested by its binding to dynamin in nerve terminals. Proc Natl Acad Sci U S A *93*, 331-335.

Deak, F., Schoch, S., Liu, X., Sudhof, T. C., and Kavalali, E. T. (2004). Synaptobrevin is essential for fast synaptic-vesicle endocytosis. Nat Cell Biol *6*, 1102-1108.

Del Castillo, J., and Katz, B. (1954). Quantal components of the end-plate potential. J Physiol *124*, 560-573.

Delgado, R., Maureira, C., Oliva, C., Kidokoro, Y., and Labarca, P. (2000). Size of vesicle pools, rates of mobilization, and recycling at neuromuscular synapses of a Drosophila mutant, shibire. Neuron *28*, 941-953.

Di Paolo, G., Moskowitz, H. S., Gipson, K., Wenk, M. R., Voronov, S., Obayashi, M., Flavell, R., Fitzsimonds, R. M., Ryan, T. A., and De Camilli, P. (2004). Impaired PtdIns(4,5)P2 synthesis in nerve terminals produces defects in synaptic vesicle trafficking. Nature *431*, 415-422.

DiAntonio, A., and Schwarz, T. L. (1994). The effect on synaptic physiology of synaptotagmin mutations in Drosophila. Neuron *12*, 909-920.

Eaton, B. A., Fetter, R. D., and Davis, G. W. (2002). Dynactin is necessary for synapse stabilization. Neuron *34*, 729-741.

Estes, P. S., Roos, J., van der Bliek, A., Kelly, R. B., Krishnan, K. S., and Ramaswami, M. (1996). Traffic of dynamin within individual Drosophila synaptic boutons relative to compartment-specific markers. J Neurosci *16*, 5443-5456.

Fergestad, T., and Broadie, K. (2001). Interaction of stoned and synaptotagmin in synaptic vesicle endocytosis. J Neurosci *21*, 1218-1227.

Fernandez, I., Arac, D., Ubach, J., Gerber, S. H., Shin, O., Gao, Y., Anderson, R. G., Sudhof, T. C., and Rizo, J. (2001). Three-dimensional structure of the synaptotagmin 1 C2B-domain: synaptotagmin 1 as a phospholipid binding machine. Neuron *32*, 1057-1069.

Fernandez-Alfonso, T., and Ryan, T. A. (2004). The kinetics of synaptic vesicle pool depletion at CNS synaptic terminals. Neuron *41*, 943-953.

Fernandez-Chacon, R., Konigstorfer, A., Gerber, S. H., Garcia, J., Matos, M. F., Stevens, C. F., Brose, N., Rizo, J., Rosenmund, C., and Sudhof, T. C. (2001). Synaptotagmin I functions as a calcium regulator of release probability. Nature *410*, 41-49.

Fesce, R., Grohovaz, F., Valtorta, F., and Meldolesi, J. (1994). Neurotransmitter release: fusion or 'kiss-and-run'? Trends Cell Biol *4*, 1-4.

Fukuda, M., Kabayama, H., and Mikoshiba, K. (2000). Drosophila AD3 mutation of synaptotagmin impairs calcium-dependent self-oligomerization activity. FEBS Lett *482*, 269-272.

Fukuda, M., Kojima, T., Aruga, J., Niinobe, M., and Mikoshiba, K. (1995a). Functional diversity of C2 domains of synaptotagmin family. Mutational analysis of inositol high polyphosphate binding domain. J Biol Chem *270*, 26523-26527.

Fukuda, M., Moreira, J. E., Lewis, F. M., Sugimori, M., Niinobe, M., Mikoshiba, K., and Llinas, R. (1995b). Role of the C2B domain of synaptotagmin in vesicular release and recycling as determined by specific antibody injection into the squid giant synapse preterminal. Proc Natl Acad Sci U S A *92*, 10708-10712.

Gad, H., Low, P., Zotova, E., Brodin, L., and Shupliakov, O. (1998). Dissociation between Ca2+-triggered synaptic vesicle exocytosis and clathrin-mediated endocytosis at a central synapse. Neuron *21*, 607-616.

Gad, H., Ringstad, N., Low, P., Kjaerulff, O., Gustafsson, J., Wenk, M., Di Paolo, G., Nemoto, Y., Crun, J., Ellisman, M. H., *et al.* (2000). Fission and uncoating of synaptic clathrin-coated vesicles are perturbed by disruption of interactions with the SH3 domain of endophilin. Neuron *27*, 301-312.

Gaidarov, I., Santini, F., Warren, R. A., and Keen, J. H. (1999). Spatial control of coated-pit dynamics in living cells. Nat Cell Biol *1*, 1-7.

Gaietta, G., Deerinck, T. J., Adams, S. R., Bouwer, J., Tour, O., Laird, D. W., Sosinsky, G. E., Tsien, R. Y., and Ellisman, M. H. (2002). Multicolor and electron microscopic imaging of connexin trafficking. Science *296*, 503-507.

Gandhi, S. P., and Stevens, C. F. (2003). Three modes of synaptic vesicular recycling revealed by single-vesicle imaging. Nature *423*, 607-613.

Geppert, M., Goda, Y., Hammer, R. E., Li, C., Rosahl, T. W., Stevens, C. F., and Sudhof, T. C. (1994). Synaptotagmin I: a major Ca2+ sensor for transmitter release at a central synapse. Cell *79*, 717-727.

Gonzalez-Gaitan, M., and Jackle, H. (1997). Role of Drosophila alpha-adaptin in presynaptic vesicle recycling. Cell *88*, 767-776.

Gramates, L. S., and Budnik, V. (1999). Assembly and maturation of the Drosophila larval neuromuscular junction. Int Rev Neurobiol *43*, 93-117.

Griffin, B. A., Adams, S. R., and Tsien, R. Y. (1998). Specific covalent labeling of recombinant protein molecules inside live cells. Science *281*, 269-272.

Guichet, A., Wucherpfennig, T., Dudu, V., Etter, S., Wilsch-Brauniger, M., Hellwig, A., Gonzalez-Gaitan, M., Huttner, W. B., and Schmidt, A. A. (2002). Essential role of endophilin A in synaptic vesicle budding at the Drosophila neuromuscular junction. Embo J *21*, 1661-1672.

Harata, N., Ryan, T. A., Smith, S. J., Buchanan, J., and Tsien, R. W. (2001). Visualizing recycling synaptic vesicles in hippocampal neurons by FM 1-43 photoconversion. Proc Natl Acad Sci U S A *98*, 12748-12753.

Haucke, V., and De Camilli, P. (1999). AP-2 recruitment to synaptotagmin stimulated by tyrosine-based endocytic motifs. Science *285*, 1268-1271.

Haucke, V., Wenk, M. R., Chapman, E. R., Farsad, K., and De Camilli, P. (2000). Dual interaction of synaptotagmin with mu2- and alpha-adaptin facilitates clathrin-coated pit nucleation. Embo J *19*, 6011-6019.

Heuser, J. E., and Reese, T. S. (1973). Evidence for recycling of synaptic vesicle membrane during transmitter release at the frog neuromuscular junction. J Cell Biol *57*, 315-344.

Heuser, J. E., Reese, T. S., Dennis, M. J., Jan, Y., Jan, L., and Evans, L. (1979). Synaptic vesicle exocytosis captured by quick freezing and correlated with quantal transmitter release. J Cell Biol *81*, 275-300.

Hinshaw, J. E. (2000). Dynamin and its role in membrane fission. Annu Rev Cell Dev Biol *16*, 483-519.

Jarousse, N., and Kelly, R. B. (2001a). The AP2 binding site of synaptotagmin 1 is not an internalization signal but a regulator of endocytosis. J Cell Biol *154*, 857-866.

Jarousse, N., and Kelly, R. B. (2001b). Endocytotic mechanisms in synapses. Curr Opin Cell Biol *13*, 461-469.

Jockusch, W. J., Praefcke, G. J., McMahon, H. T., and Lagnado, L. (2005). Clathrin-dependent and clathrin-independent retrieval of synaptic vesicles in retinal bipolar cells. Neuron *46*, 869-878.

Jorgensen, E. M., Hartwieg, E., Schuske, K., Nonet, M. L., Jin, Y., and Horvitz, H. R. (1995). Defective recycling of synaptic vesicles in synaptotagmin mutants of Caenorhabditis elegans. Nature *378*, 196-199.

Kadota, K., and Kaneseki, T. (1969). Isolation of a synaptic vesicle fraction from guinea pig brain with the use of DEAE-sephadex column chromatography and some of its properties. J Biochem (Tokyo) *65*, 839-842.

Kee, Y., and Scheller, R. H. (1996). Localization of synaptotagmin-binding domains on syntaxin. J Neurosci *16*, 1975-1981.

Klingauf, J., Kavalali, E. T., and Tsien, R. W. (1998). Kinetics and regulation of fast endocytosis at hippocampal synapses. Nature *394*, 581-585.

Koenig, J. H., and Ikeda, K. (1989). Disappearance and reformation of synaptic vesicle membrane upon transmitter release observed under reversible blockage of membrane retrieval. J Neurosci *9*, 3844-3860.

Koenig, J. H., and Ikeda, K. (1996). Synaptic vesicles have two distinct recycling pathways. J Cell Biol *135*, 797-808.

Koenig, J. H., Saito, K., and Ikeda, K. (1983). Reversible control of synaptic transmission in a single gene mutant of Drosophila melanogaster. J Cell Biol *96*, 1517-1522.

Koh, T. W., Verstreken, P., and Bellen, H. J. (2004). Dap160/intersectin acts as a stabilizing scaffold required for synaptic development and vesicle endocytosis. Neuron *43*, 193-205.

Kosaka, T., and Ikeda, K. (1983). Possible temperature-dependent blockage of synaptic vesicle recycling induced by a single gene mutation in Drosophila. J Neurobiol *14*, 207-225.

Kuromi, H., and Kidokoro, Y. (1998). Two distinct pools of synaptic vesicles in single presynaptic boutons in a temperature-sensitive Drosophila mutant, shibire. Neuron *20*, 917-925.

Kuromi, H., and Kidokoro, Y. (1999). The optically determined size of exo/endo cycling vesicle pool correlates with the quantal content at the neuromuscular junction of Drosophila larvae. J Neurosci *19*, 1557-1565.

Kuromi, H., and Kidokoro, Y. (2000). Tetanic stimulation recruits vesicles from reserve pool via a cAMP-mediated process in Drosophila synapses. Neuron *27*, 133-143.

Kuromi, H., and Kidokoro, Y. (2002). Selective replenishment of two vesicle pools depends on the source of Ca2+ at the Drosophila synapse. Neuron *35*, 333-343.

Li, C., Ullrich, B., Zhang, J. Z., Anderson, R. G., Brose, N., and Sudhof, T. C. (1995). Ca(2+)-dependent and -independent activities of neural and non-neural synaptotagmins. Nature *375*, 594-599.

Li, Z., Burrone, J., Tyler, W. J., Hartman, K. N., Albeanu, D. F., and Murthy, V. N. (2005). Synaptic vesicle recycling studied in transgenic mice expressing synaptopHluorin. Proc Natl Acad Sci U S A *102*, 6131-6136.

Littleton, J. T., Bai, J., Vyas, B., Desai, R., Baltus, A. E., Garment, M. B., Carlson, S. D., Ganetzky, B., and Chapman, E. R. (2001). synaptotagmin mutants reveal essential functions for the C2B domain in Ca2+-triggered fusion and recycling of synaptic vesicles in vivo. J Neurosci *21*, 1421-1433.

Littleton, J. T., Chapman, E. R., Kreber, R., Garment, M. B., Carlson, S. D., and Ganetzky, B. (1998). Temperature-sensitive paralytic mutations demonstrate that synaptic exocytosis requires SNARE complex assembly and disassembly. Neuron *21*, 401-413.

Littleton, J. T., Stern, M., Perin, M., and Bellen, H. J. (1994). Calcium dependence of neurotransmitter release and rate of spontaneous vesicle fusions are altered in Drosophila synaptotagmin mutants. Proc Natl Acad Sci U S A *91*, 10888-10892.

Littleton, J. T., Stern, M., Schulze, K., Perin, M., and Bellen, H. J. (1993). Mutational analysis of Drosophila synaptotagmin demonstrates its essential role in Ca(2+)-activated neurotransmitter release. Cell *74*, 1125-1134.

Liu, J. P., Sim, A. T., and Robinson, P. J. (1994). Calcineurin inhibition of dynamin I GTPase activity coupled to nerve terminal depolarization. Science *265*, 970-973.

Llinas, R. R., Sugimori, M., Moran, K. A., Moreira, J. E., and Fukuda, M. (2004). Vesicular reuptake inhibition by a synaptotagmin I C2B domain antibody at the squid giant synapse. Proc Natl Acad Sci U S A *101*, 17855-17860.

Loewen, C. A., Mackler, J. M., and Reist, N. E. (2001). Drosophila synaptotagmin I null mutants survive to early adulthood. Genesis *31*, 30-36.

Mackler, J. M., Drummond, J. A., Loewen, C. A., Robinson, I. M., and Reist, N. E. (2002). The C(2)B Ca(2+)-binding motif of synaptotagmin is required for synaptic transmission in vivo. Nature *418*, 340-344.

Mackler, J. M., and Reist, N. E. (2001). Mutations in the second C2 domain of synaptotagmin disrupt synaptic transmission at Drosophila neuromuscular junctions. J Comp Neurol *436*, 4-16.

Marek, K. W., and Davis, G. W. (2002). Transgenically encoded protein photoinactivation (FlAsH-FALI): acute inactivation of synaptotagmin I. Neuron *36*, 805-813.

Marek, K. W., Ng, N., Fetter, R., Smolik, S., Goodman, C. S., and Davis, G. W. (2000). A genetic analysis of synaptic development: pre- and postsynaptic dCBP control transmitter release at the Drosophila NMJ. Neuron *25*, 537-547.

Marie, B., Sweeney, S. T., Poskanzer, K. E., Roos, J., Kelly, R. B., and Davis, G. W. (2004). Dap160/intersectin scaffolds the periactive zone to achieve high-fidelity endocytosis and normal synaptic growth. Neuron *43*, 207-219.

Marks, B., and McMahon, H. T. (1998). Calcium triggers calcineurin-dependent synaptic vesicle recycling in mammalian nerve terminals. Curr Biol *8*, 740-749.

Marks, B., Stowell, M. H., Vallis, Y., Mills, I. G., Gibson, A., Hopkins, C. R., and McMahon, H. T. (2001). GTPase activity of dynamin and resulting conformation change are essential for endocytosis. Nature *410*, 231-235.

Martina, J. A., Bonangelino, C. J., Aguilar, R. C., and Bonifacino, J. S. (2001). Stonin 2: an adaptor-like protein that interacts with components of the endocytic machinery. J Cell Biol *153*, 1111-1120.

Matthew, W. D., Tsavaler, L., and Reichardt, L. F. (1981). Identification of a synaptic vesicle-specific membrane protein with a wide distribution in neuronal and neurosecretory tissue. J Cell Biol *91*, 257-269.

McPherson, P. S., Garcia, E. P., Slepnev, V. I., David, C., Zhang, X., Grabs, D., Sossin, W. S., Bauerfeind, R., Nemoto, Y., and De Camilli, P. (1996). A presynaptic inositol-5-phosphatase. Nature *379*, 353-357.

Meshul, C. K., and Pappas, G. D. (1984). The relationship of pinocytosis and synaptic vesicles at the frog neuromuscular junction. Brain Res *290*, 1-18.

Micheva, K. D., Buchanan, J., Holz, R. W., and Smith, S. J. (2003). Retrograde regulation of synaptic vesicle endocytosis and recycling. Nat Neurosci *6*, 925-932.

Miesenbock, G., De Angelis, D. A., and Rothman, J. E. (1998). Visualizing secretion and synaptic transmission with pH-sensitive green fluorescent proteins. Nature *394*, 192-195.

Murthy, V. N., and Stevens, C. F. (1999). Reversal of synaptic vesicle docking at central synapses. Nat Neurosci *2*, 503-507.

Neves, G., and Lagnado, L. (1999). The kinetics of exocytosis and endocytosis in the synaptic terminal of goldfish retinal bipolar cells. J Physiol *515 (Pt 1)*, 181-202.

Nicholson-Tomishima, K., and Ryan, T. A. (2004). Kinetic efficiency of endocytosis at mammalian CNS synapses requires synaptotagmin I. Proc Natl Acad Sci U S A *101*, 16648-16652.

Paillart, C., Li, J., Matthews, G., and Sterling, P. (2003). Endocytosis and vesicle recycling at a ribbon synapse. J Neurosci *23*, 4092-4099.

Paradis, S., Sweeney, S. T., and Davis, G. W. (2001). Homeostatic control of presynaptic release is triggered by postsynaptic membrane depolarization. Neuron *30*, 737-749.

Perin, M. S., Brose, N., Jahn, R., and Sudhof, T. C. (1991). Domain structure of synaptotagmin (p65). J Biol Chem *266*, 623-629.

Perin, M. S., Fried, V. A., Mignery, G. A., Jahn, R., and Sudhof, T. C. (1990). Phospholipid binding by a synaptic vesicle protein homologous to the regulatory region of protein kinase C. Nature *345*, 260-263.

Petersen, S. A., Fetter, R. D., Noordermeer, J. N., Goodman, C. S., and DiAntonio, A. (1997). Genetic analysis of glutamate receptors in Drosophila reveals a retrograde signal regulating presynaptic transmitter release. Neuron *19*, 1237-1248.

Phillips, A. M., Smith, M., Ramaswami, M., and Kelly, L. E. (2000). The products of the Drosophila stoned locus interact with synaptic vesicles via synaptotagmin. J Neurosci *20*, 8254-8261.

Poskanzer, K. E., and Davis, G. W. (2004). Mobilization and fusion of a non-recycling pool of synaptic vesicles under conditions of endocytic blockade. Neuropharmacology *47*, 714-723.

Poskanzer, K. E., Marek, K. W., Sweeney, S. T., and Davis, G. W. (2003). Synaptotagmin I is necessary for compensatory synaptic vesicle endocytosis in vivo. Nature *426*, 559-563.

Pyle, J. L., Kavalali, E. T., Piedras-Renteria, E. S., and Tsien, R. W. (2000). Rapid reuse of readily releasable pool vesicles at hippocampal synapses. Neuron *28*, 221-231.

Qualmann, B., Roos, J., DiGregorio, P. J., and Kelly, R. B. (1999). Syndapin I, a synaptic dynamin-binding protein that associates with the neural Wiskott-Aldrich syndrome protein. Mol Biol Cell *10*, 501-513.

Reist, N. E., Buchanan, J., Li, J., DiAntonio, A., Buxton, E. M., and Schwarz, T. L. (1998). Morphologically docked synaptic vesicles are reduced in synaptotagmin mutants of Drosophila. J Neurosci *18*, 7662-7673.

Richards, D. A., Guatimosim, C., and Betz, W. J. (2000). Two endocytic recycling routes selectively fill two vesicle pools in frog motor nerve terminals. Neuron *27*, 551-559.

Richards, D. A., Guatimosim, C., Rizzoli, S. O., and Betz, W. J. (2003). Synaptic vesicle pools at the frog neuromuscular junction. Neuron *39*, 529-541.

Ringstad, N., Gad, H., Low, P., Di Paolo, G., Brodin, L., Shupliakov, O., and De Camilli, P. (1999). Endophilin/SH3p4 is required for the transition from early to late stages in clathrin-mediated synaptic vesicle endocytosis. Neuron *24*, 143-154.

Rizzoli, S. O., and Betz, W. J. (2004). The structural organization of the readily releasable pool of synaptic vesicles. Science *303*, 2037-2039.

Rizzoli, S. O., and Betz, W. J. (2005). Synaptic vesicle pools. Nat Rev Neurosci *6*, 57-69.

Rizzoli, S. O., Richards, D. A., and Betz, W. J. (2003). Monitoring synaptic vesicle recycling in frog motor nerve terminals with FM dyes. J Neurocytol *32*, 539-549.

Robinson, I. M., Ranjan, R., and Schwarz, T. L. (2002). Synaptotagmins I and IV promote transmitter release independently of Ca(2+) binding in the C(2)A domain. Nature *418*, 336-340.

Roos, J., Hummel, T., Ng, N., Klambt, C., and Davis, G. W. (2000). Drosophila Futsch regulates synaptic microtubule organization and is necessary for synaptic growth. Neuron *26*, 371-382.

Roos, J., and Kelly, R. B. (1998). Dap160, a neural-specific Eps15 homology and multiple SH3 domain-containing protein that interacts with Drosophila dynamin. J Biol Chem *273*, 19108-19119.

Rosenmund, C., and Stevens, C. F. (1996). Definition of the readily releasable pool of vesicles at hippocampal synapses. Neuron *16*, 1197-1207.

Ryan, T. A., Reuter, H., Wendland, B., Schweizer, F. E., Tsien, R. W., and Smith, S. J. (1993). The kinetics of synaptic vesicle recycling measured at single presynaptic boutons. Neuron *11*, 713-724.

Ryan, T. A., Smith, S. J., and Reuter, H. (1996). The timing of synaptic vesicle endocytosis. Proc Natl Acad Sci U S A *93*, 5567-5571.

Sankaranarayanan, S., and Ryan, T. A. (2000). Real-time measurements of vesicle-SNARE recycling in synapses of the central nervous system. Nat Cell Biol *2*, 197-204.

Sankaranarayanan, S., and Ryan, T. A. (2001). Calcium accelerates endocytosis of vSNAREs at hippocampal synapses. Nat Neurosci *4*, 129-136.

Sara, Y., Mozhayeva, M. G., Liu, X., and Kavalali, E. T. (2002). Fast vesicle recycling supports neurotransmission during sustained stimulation at hippocampal synapses. J Neurosci *22*, 1608-1617.

Sato, T. (1968). A modified method for lead staining of thin sections. J Electron Microsc (Tokyo) *17*, 158-159.

Schiavo, G., Gu, Q. M., Prestwich, G. D., Sollner, T. H., and Rothman, J. E. (1996). Calcium-dependent switching of the specificity of phosphoinositide binding to synaptotagmin. Proc Natl Acad Sci U S A *93*, 13327-13332.

Schikorski, T., and Stevens, C. F. (2001). Morphological correlates of functionally defined synaptic vesicle populations. Nat Neurosci *4*, 391-395.

Schmid, S. L. (1997). Clathrin-coated vesicle formation and protein sorting: an integrated process. Annu Rev Biochem *66*, 511-548.

Sheng, Z. H., Yokoyama, C. T., and Catterall, W. A. (1997). Interaction of the synprint site of N-type Ca2+ channels with the C2B domain of synaptotagmin I. Proc Natl Acad Sci U S A *94*, 5405-5410.

Shupliakov, O., Low, P., Grabs, D., Gad, H., Chen, H., David, C., Takei, K., De Camilli, P., and Brodin, L. (1997). Synaptic vesicle endocytosis impaired by disruption of dynamin-SH3 domain interactions. Science *276*, 259-263.

Slepnev, V. I., Ochoa, G. C., Butler, M. H., Grabs, D., and De Camilli, P. (1998). Role of phosphorylation in regulation of the assembly of endocytic coat complexes. Science *281*, 821-824.

Smith, J. E., and Smith, D. O. (1984). Coated vesicle morphology and sub-populations at the neuromuscular junction. Brain Res *299*, 383-388.

Stevens, C. F., and Sullivan, J. M. (2003). The synaptotagmin C2A domain is part of the calcium sensor controlling fast synaptic transmission. Neuron *39*, 299-308.

Stevens, C. F., and Williams, J. H. (2000). "Kiss and run" exocytosis at hippocampal synapses. Proc Natl Acad Sci U S A *97*, 12828-12833.

Stewart, B. A., Atwood, H. L., Renger, J. J., Wang, J., and Wu, C. F. (1994). Improved stability of Drosophila larval neuromuscular preparations in haemolymph-like physiological solutions. J Comp Physiol [A] *175*, 179-191.

Stimson, D. T., Estes, P. S., Smith, M., Kelly, L. E., and Ramaswami, M. (1998). A product of the Drosophila stoned locus regulates neurotransmitter release. J Neurosci *18*, 9638-9649.

Stoorvogel, W., Oorschot, V., and Geuze, H. J. (1996). A novel class of clathrin-coated vesicles budding from endosomes. J Cell Biol *132*, 21-33.

Sudhof, T. C. (2000). The synaptic vesicle cycle revisited. Neuron *28*, 317-320.

Sugita, S., Hata, Y., and Sudhof, T. C. (1996). Distinct Ca(2+)-dependent properties of the first and second C2-domains of synaptotagmin I. J Biol Chem *271*, 1262-1265.

Sun, J. Y., Wu, X. S., and Wu, L. G. (2002). Single and multiple vesicle fusion induce different rates of endocytosis at a central synapse. Nature *417*, 555-559.

Teng, H., and Wilkinson, R. S. (2000). Clathrin-mediated endocytosis near active zones in snake motor boutons. J Neurosci *20*, 7986-7993.

Teng, H., and Wilkinson, R. S. (2005). Clathrin-mediated endocytosis in snake motor terminals is directly facilitated by intracellular Ca2+. J Physiol *565*, 743-750.

Torri-Tarelli, F., Villa, A., Valtorta, F., De Camilli, P., Greengard, P., and Ceccarelli, B. (1990). Redistribution of synaptophysin and synapsin I during alpha-latrotoxin-induced release of neurotransmitter at the neuromuscular junction. J Cell Biol *110*, 449-459.

Tour, O., Meijer, R. M., Zacharias, D. A., Adams, S. R., and Tsien, R. Y. (2003). Genetically targeted chromophore-assisted light inactivation. Nat Biotechnol *21*, 1505-1508.

Turner, P. T., and Harris, A. B. (1973). Ultrastructure of synaptic vesicle formation in cerebral cortex. Nature *242*, 57-59.

Ubach, J., Zhang, X., Shao, X., Sudhof, T. C., and Rizo, J. (1998). Ca2+ binding to synaptotagmin: how many Ca2+ ions bind to the tip of a C2-domain? Embo J *17*, 3921-3930.

Verstreken, P., Kjaerulff, O., Lloyd, T. E., Atkinson, R., Zhou, Y., Meinertzhagen, I. A., and Bellen, H. J. (2002). Endophilin mutations block clathrin-mediated endocytosis but not neurotransmitter release. Cell *109*, 101-112.

Verstreken, P., Koh, T. W., Schulze, K. L., Zhai, R. G., Hiesinger, P. R., Zhou, Y., Mehta, S. Q., Cao, Y., Roos, J., and Bellen, H. J. (2003). Synaptojanin is recruited by endophilin to promote synaptic vesicle uncoating. Neuron *40*, 733-748.

von Gersdorff, H., and Matthews, G. (1994). Dynamics of synaptic vesicle fusion and membrane retrieval in synaptic terminals. Nature *367*, 735-739.

von Poser, C., Zhang, J. Z., Mineo, C., Ding, W., Ying, Y., Sudhof, T. C., and Anderson, R. G. (2000). Synaptotagmin regulation of coated pit assembly. J Biol Chem *275*, 30916-30924.

Walther, K., Krauss, M., Diril, M. K., Lemke, S., Ricotta, D., Honing, S., Kaiser, S., and Haucke, V. (2001). Human stoned B interacts with AP-2 and synaptotagmin and facilitates clathrin-coated vesicle uncoating. EMBO Rep *2*, 634-640.

Whitney, J. A., Gomez, M., Sheff, D., Kreis, T. E., and Mellman, I. (1995). Cytoplasmic coat proteins involved in endosome function. Cell *83*, 703-713.

Wu, L. G. (2004). Kinetic regulation of vesicle endocytosis at synapses. Trends Neurosci *27*, 548-554.

Wu, L. G., and Betz, W. J. (1996). Nerve activity but not intracellular calcium determines the time course of endocytosis at the frog neuromuscular junction. Neuron *17*, 769-779.

Yoshihara, M., and Littleton, J. T. (2002). Synaptotagmin I functions as a calcium sensor to synchronize neurotransmitter release. Neuron *36*, 897-908.

Zenisek, D., Steyer, J. A., and Almers, W. (2000). Transport, capture and exocytosis of single synaptic vesicles at active zones. Nature *406*, 849-854.

Zhang, B., Koh, Y. H., Beckstead, R. B., Budnik, V., Ganetzky, B., and Bellen, H. J. (1998). Synaptic vesicle size and number are regulated by a clathrin adaptor protein required for endocytosis. Neuron *21*, 1465-1475.

Zhang, J. Z., Davletov, B. A., Sudhof, T. C., and Anderson, R. G. (1994). Synaptotagmin I is a high affinity receptor for clathrin AP-2: implications for membrane recycling. Cell *78*, 751-760.

Zhou, Q., Petersen, C. C., and Nicoll, R. A. (2000). Effects of reduced vesicular filling on synaptic transmission in rat hippocampal neurones. J Physiol *525 Pt 1*, 195-206.

7537627
3 1378 00753 7627
UC San Francisco LIBRARY
UNIVERSITY OF CALIFORNIA

For reference
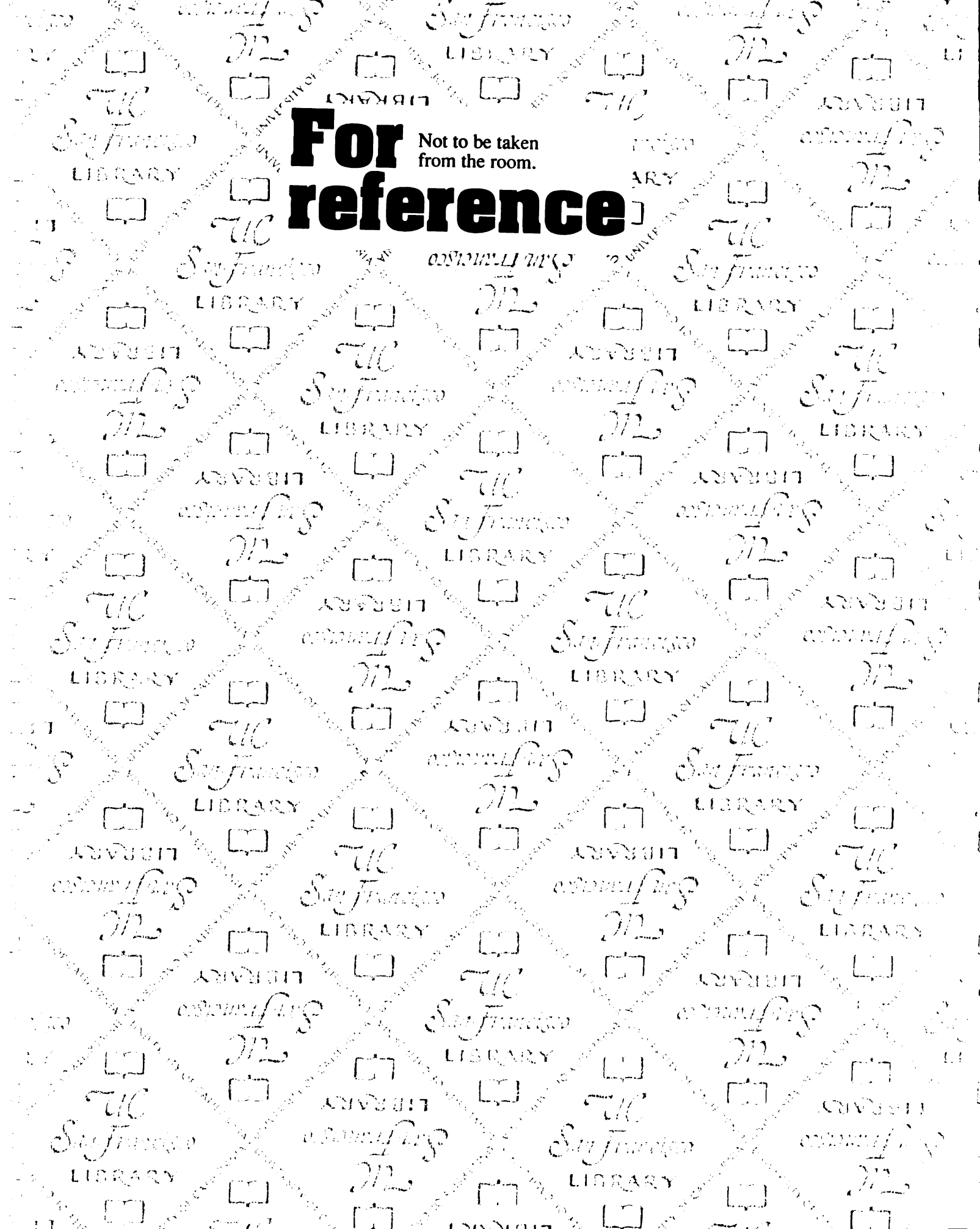
Not to be taken from the room.